REPORT DOCUMENTATION PAGE

Form Approved
OMB No. 0704-0188

1. REPORT DATE *(DD-MM-YYYY)*	2. REPORT TYPE	3. DATES COVERED *(From - To)*
27-02-2017	Final	01-06-2015 to 30-11-2016

4. TITLE AND SUBTITLE
HYPERVELOCITY EXPANSION FACILITY FOR FUNDAMENTAL HIGH-ENTHALPY RESEARCH

5a. CONTRACT NUMBER

5b. GRANT NUMBER
N00014-15-1-2260

5c. PROGRAM ELEMENT NUMBER

6. AUTHOR(S)
PI: Bowersox, Rodney D.W.
Co-PI's White, Edward, B. and North, Simon, W.
Major Students: Marcotte, Evan, K., Aguilar, Gabe, J. and Pages, Alex, E.,

5d. PROJECT NUMBER

5e. TASK NUMBER

5f. WORK UNIT NUMBER

7. PERFORMING ORGANIZATION NAME(S) AND ADDRESS(ES)
Aerospace Engineering and Chemistry Departments
710 HRBB, 3141-TAMU
Texas A&M University
College Station, TX 77843

8. PERFORMING ORGANIZATION REPORT NUMBER
M1503074 (504122)

9. SPONSORING/MONITORING AGENCY NAME(S) AND ADDRESS(ES)
Dr. Knox T. Millsaps, Director, Code 35
Office of Naval Research (ONR)
875 N. Randolph Street, Suite 1425
Arlington, VA 22203-1995

10. SPONSOR/MONITOR'S ACRONYM(S)
ONR

11. SPONSOR/MONITOR'S REPORT NUMBER(S)

12. DISTRIBUTION/AVAILABILITY STATEMENT
Approved for public release; distribution is unlimited

13. SUPPLEMENTARY NOTES
None

14. ABSTRACT
The objective for this project is to provide a clean air venue for basic research in high enthalpy, high Reynolds number transitional and turbulent boundary layer flow, which aligns with Navy interests in hypersonic vehicle systems. A 20-inch diameter hypervelocity expansion tunnel into the National Aerothermochemistry and Hypersonics Laboratory at Texas A&M University. In this document, we report on the progress over the 18-month period of performance. The project progressed as planned, where the expansion tube was designed (flow path and mechanical), constructed, installed, instrumented for shock speed, and a preliminary shake-down test was performed.

15. SUBJECT TERMS
Hypervelocity flow, expansion tunnel, hypersonics

16. SECURITY CLASSIFICATION OF:			17. LIMITATION OF ABSTRACT	18. NUMBER OF PAGES	19a. NAME OF RESPONSIBLE PERSON
a. REPORT	b. ABSTRACT	c. THIS PAGE			Rodney D. W. Bowersox
U	U	U	UU	87	19b. TELEPHONE NUMBER *(Include area code)* (979) 845-4184

INSTRUCTIONS FOR COMPLETING SF 298

1. REPORT DATE. Full publication date, including day, month, if available. Must cite at least the year and be Year 2000 compliant, e.g. 30-06-1998; xx-06-1998; xx-xx-1998.

2. REPORT TYPE. State the type of report, such as final, technical, interim, memorandum, master's thesis, progress, quarterly, research, special, group study, etc.

3. DATE COVERED. Indicate the time during which the work was performed and the report was written, e.g., Jun 1997 - Jun 1998; 1-10 Jun 1996; May - Nov 1998; Nov 1998.

4. TITLE. Enter title and subtitle with volume number and part number, if applicable. On classified documents, enter the title classification in parentheses.

5a. CONTRACT NUMBER. Enter all contract numbers as they appear in the report, e.g. F33315-86-C-5169.

5b. GRANT NUMBER. Enter all grant numbers as they appear in the report. e.g. AFOSR-82-1234.

5c. PROGRAM ELEMENT NUMBER. Enter all program element numbers as they appear in the report, e.g. 61101A.

5e. TASK NUMBER. Enter all task numbers as they appear in the report, e.g. 05; RF0330201; T4112.

5f. WORK UNIT NUMBER. Enter all work unit numbers as they appear in the report, e.g. 001; AFAPL30480105.

6. AUTHOR(S). Enter name(s) of person(s) responsible for writing the report, performing the research, or credited with the content of the report. The form of entry is the last name, first name, middle initial, and additional qualifiers separated by commas, e.g. Smith, Richard, J, Jr.

7. PERFORMING ORGANIZATION NAME(S) AND ADDRESS(ES). Self-explanatory.

8. PERFORMING ORGANIZATION REPORT NUMBER. Enter all unique alphanumeric report numbers assigned by the performing organization, e.g. BRL-1234; AFWL-TR-85-4017-Vol-21-PT-2.

9. SPONSORING/MONITORING AGENCY NAME(S) AND ADDRESS(ES). Enter the name and address of the organization(s) financially responsible for and monitoring the work.

10. SPONSOR/MONITOR'S ACRONYM(S). Enter, if available, e.g. BRL, ARDEC, NADC.

11. SPONSOR/MONITOR'S REPORT NUMBER(S). Enter report number as assigned by the sponsoring/ monitoring agency, if available, e.g. BRL-TR-829; -215.

12. DISTRIBUTION/AVAILABILITY STATEMENT. Use agency-mandated availability statements to indicate the public availability or distribution limitations of the report. If additional limitations/ restrictions or special markings are indicated, follow agency authorization procedures, e.g. RD/FRD, PROPIN, ITAR, etc. Include copyright information.

13. SUPPLEMENTARY NOTES. Enter information not included elsewhere such as: prepared in cooperation with; translation of; report supersedes; old edition number, etc.

14. ABSTRACT. A brief (approximately 200 words) factual summary of the most significant information.

15. SUBJECT TERMS. Key words or phrases identifying major concepts in the report.

16. SECURITY CLASSIFICATION. Enter security classification in accordance with security classification regulations, e.g. U, C, S, etc. If this form contains classified information, stamp classification level on the top and bottom of this page.

17. LIMITATION OF ABSTRACT. This block must be completed to assign a distribution limitation to the abstract. Enter UU (Unclassified Unlimited) or SAR (Same as Report). An entry in this block is necessary if the abstract is to be limited.

Standard Form 298 Back (Rev. 8/98)

Final Technical Report of Contract ONR N00014-15-1-2260

Entitled:

HYPERVELOCITY EXPANSION FACILITY FOR FUNDAMENTAL HIGH-ENTHALPY RESEARCH

Submitted by

Drs. R. Bowersox,[1] E. White[1] and S. North[2]
E. Marcotte,[1] G. Aguilar,[1] A. Pages[1]
[1]Aerospace Engineering and [2]Chemistry

bowersox@tamu.edu
(979) 845-4184

710 HRBB, 3141-TAMU
Texas A&M University
College Station, TX 77843

To

Dr. Knox T. Millsaps
Director, Division of Aerospace Sciences Air Warfare and Weapons Department
Code 35, Air Warfare and Weapons
knox.millsaps@navy.mil
(703) 588-2962

Office of Naval Research (ONR)
875 N. Randolph Street, Suite 1425
Arlington, VA 22203-1995

Feb 27, 2017

ABSTRACT

The objective for this project is to provide a clean air venue for basic research in high enthalpy, high Reynolds number transitional and turbulent boundary layer flow, which aligns with Navy interests in hypersonic vehicle systems. To meet this goal, we developed and installed a relatively large-scale hypervelocity expansion tunnel (HXT) into the National Aerothermochemistry and Hypersonics Laboratory (NAL) at Texas A&M University. This venue leverages previous DoD investments in high-energy pulsed laser diagnostics for instantaneous planar velocimetry and thermometry to perform scientific studies of high temperature hypersonic boundary layers. The combination of the expansion tunnel facility with our signature laser diagnostics will provide a capability for fundamental and applied studies of hypervelocity high enthalpy flows. In this document, we report on the progress over the 18-month period of performance. The project progressed as planned, where the expansion tube was designed (flow path and mechanical), constructed, installed, instrumented for shock speed, and a preliminary shake-down test was performed.

Three important facility changes occurred to improve the design with respect to the original proposal. First, the tube diameter was increased from the proposed 12-in to 20-in. This change helped minimize viscous loss effects on the tube performance. This was a major change, as the cost of the facility was significantly increased. Hence, the nozzle construction was postponed. Second, provisions were included to allow operation as either an expansion tunnel or a shock tunnel to expand the utility of the facility. Third, a new method of characteristic nozzle design tool was developed and was used to design 36-in exit diameter nozzle, which, when constructed, will significantly increase the diameter and length of the stream tube, thus allowing for larger test articles. At the time of this writing, two steps remain in order to enable full operation of the facility. These include (1) installation of a diaphragm breech and (2) installation of mechanical shock absorbers.

TABLE OF CONTENTS

1. LONG-TERM GOALS

1.1 MOTIVATION

The Office of Naval Research emphasizes basic and applied research in hypersonic flow (Smith 2016). Extreme thermos-mechanical loads are main obstacles. Thus, understanding turbulent and transitional boundary layers under these harsh conditions is essential for vehicle design.

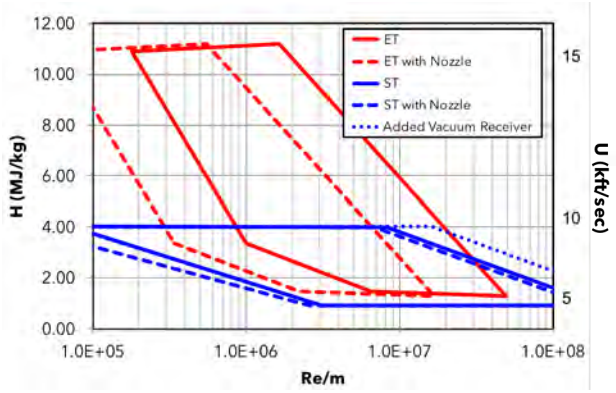

Fig. 1 TAMU Hypervelocity Expansion Tunnel operating conditions, with and without the exit nozzle

The Texas A&M University National Aerothermochemistry and Hypersonics Laboratory (NAL) was founded, by Drs. Bowersox and North, to provide a venue for modern research of non-equilibrium gaseous flows and their surface interactions. Defining features of the NAL are national resource quality facilities, advanced laser instrumentation, and modern numerical methods. The purpose of this project is to add a high-enthalpy capability to enable realistic enthalpy flows. The expansion tunnel is an efficient way to produce high enthalpy gaseous flows with the correct freestream composition and internal energy states. Adding this facility to the NAL will leverage major DoD investments in our signature laser based vibrationally excited nitric oxide monitoring (VENOM) diagnostic to provide never before achieved measurements in hypersonic turbulent and transitional flows.

1.2. OBJECTIVE

The central objective for this project is to develop a relatively large-scale (36-in exit diameter) hypervelocity expansion tunnel. This facility will be incorporated into the TAMU NAL to take advantage of the available suite advanced high-energy pulsed laser flow field diagnostics and fast response surface sensors. The planned operating map is shown in Fig. 1.

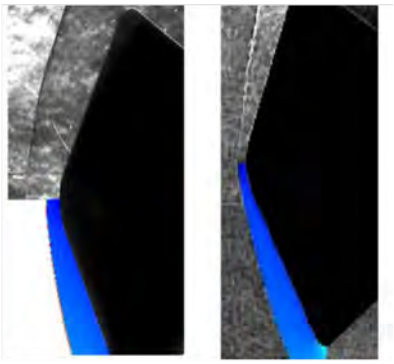

Fig. 2 Shock stand-off in a shock tunnel (left) and expansion tunnel (right) (Holden 2010).

2. APPROACH

2.1 Background Review of Impulse Hypersonic Facilities

Impulse facilities, reflected mode shock tunnels and expansion tunnels, are effective means to produce high stagnation enthalpies representative of hypersonic flight (Hornung, 1993; Dufrene et al 2007).

Reflected mode shock tunnels such as the CUBRC LENS I and II tunnels (Albrechcinski et al 1995) and the Caltech T5 (Hornung 1992) provide high-enthalpy flow up to about 15 MJ/kg for test times of 2-10 msec. The principal drawback of these facilities is related to the chemical and thermal non-equilibrium present in the tunnel freestream for enthalpies greater than 5 MJ/kg (Holden et al 2013). This non-equilibrium results from stagnating the flow just upstream of a converging-diverging nozzle. In this stagnation region, the gas achieves extreme temperatures with a highly excited and dissociated composition. As the flow expands through the nozzle, the gases begin to recombine and relax. However, a substantial portion of the chemical composition and thermal states "freeze" out at unrealistic values. The impact of this is clearly shown in Fig. 2, which compares the shock stand off for a blunt body in reflected mode shock tunnel (LENS 1) and an expansion tunnel (LENS X), with a comparison to a computational fluid dynamics (CFD) simulation. The expansion tunnel (described in the next paragraph) does not suffer the unrealistic chemical and thermal affects, and hence is in much better agreement with the expected shock stand off as predicted by the simulation. The minimization of the freestream composition problem is the primary advantage of expansion tunnel facilities over reflected shock tunnels. The drawback is shorter test times. The available pulsed laser diagnostics and high frequency response sensors within our laboratory mitigate this drawback. Hence, we proposed an expansion tunnel to produce an aerodynamically "clean" freestream (correct gas composition and internal state distribution) for fundamental high enthalpy studies of turbulent and transitional boundary layers.

Expansion tube facilities have been the subject of considerable study, e.g., Trimpi (1962, 1966), Miller (1975), Shinn and Miller (1978), Durfrene et al (2007) and Holden (2010). The operating principle builds on that of the shock tunnel. The primary difference is the inclusion of an unsteady "expansion section." The geometry and wave diagram are shown schematically in Fig. 3, where the numbering scheme for the flow regions on the x-t plot follows Dufrene et al (2010). As indicated, the expansion tube consists of three sections, a driver section, a driven sec-

tion and an expansion section. A diverging nozzle can be included at the end of the expansion section to further increase the Mach number. When a nozzle is included on the expansion tube, the facility is typically called an "expansion tunnel." Existing large-scale hypervelocity expansion tunnel facilities include the 26-in exit diameter HYPULSE facility at GASL (Erdos et al 1997) and 96-in LENS XX facility at CUBRC (Holden 2010). Smaller expansion tube facilities include the 3.4-in and 7.0-in free piston expansion tube facilities at the University of Queensland (Neely and Morgan 1994), the 6-in tube at UIUC capable of Mach 7 enthalpy (Dufrene et al 2007, now at Caltech), and the 3.5-in diameter Mach 8-12 facility at Stanford (Ben-Yakar and Hanson 1992).

The driver-driven pair operates as an open-ended (on the right side of the driven tube) shock tube. The driver section is charged to a high-pressure, where the pressure, gas composition and temperature of the driver are used to control the speed of the shock that traverses into the driven section once the diaphragm between the driver and driven section ruptures. When the initial shock moves to the right in Fig. 3, it heats the test gas in the driven section. When the shock wave reaches the end of the driven tube, the high pressure ruptures a second diaphragm, and the driven flow accelerates into the expansion section. The pressure and gas composition in the expansion section are used to control the acceleration. The test gas is then accelerated to higher Mach numbers within the diverging nozzle expansion.

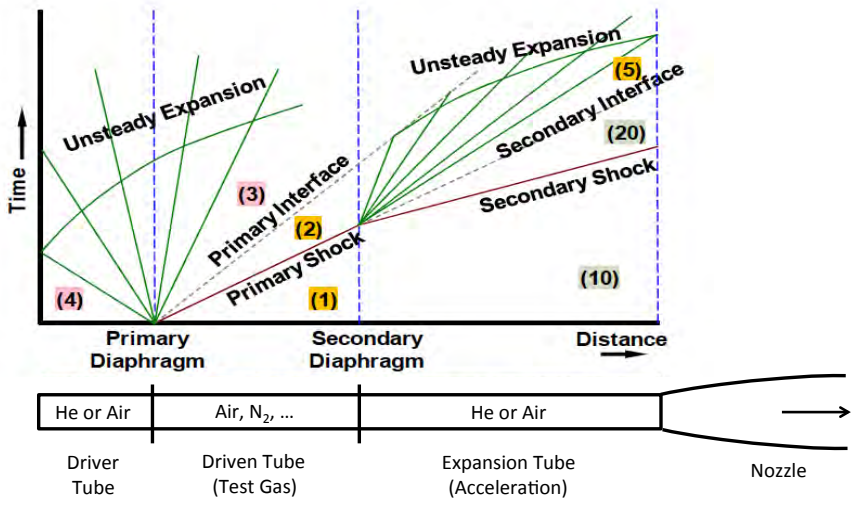

Fig. 3 Expansion tunnel schematic and x-t wave diagram (adapted from Dufrene et al 2010)

2.2 PROJECT OVERVIEW

The flowpath design for the Texas A&M University Hypervelocity Expansion Tunnel (HXT) was performed using classical 1-D, perfect gas, gasdynamics following Dufrene et al (2007) and Dufrene et al (2010).† This model is reasonable for initial design, as the driver-driven conditions were tailored such that the maximum static temperature downstream of the shock was always less than 5000°F. As described with respect to Fig. 3, extreme enthalpies are achieved through acceleration of the test gas to high velocities during the unsteady expansion. Maintaining the peak static temperature to be less than 4000°F (2500K) helps ensure an aerodynamically representative freestream. However, higher temperatures are readily achieved for cases where dissociation is acceptable.

The planned driver pressure range is 20 – 2000 psia. The driven tube contains the test gas. The design calculations were performed assuming air as the test gas. The driven tube will have a pressure range of 1 – 50 psia. The expansion tube will contain helium at low-pressure and room temperature. The driver, driven and expansion flow conditions enable flexible control of the tube exit conditions in terms of total enthalpy and Mach number. Two modes of operation are proposed, with and without an exit nozzle. For the design (and present) calculations, the tube Mach number was set to 9.5. This is the inlet to the nozzle, which will have a 3.6 area ratio. The peak enthalpy for the room temperature driver was greater than 11 MJ/kg. Higher enthalpies are possible by either heating the driver or lowering the driven tube pressure. The facility run times were estimated following Trimpi (1966). Based on these data, the length of the test gas streamtube (L_{ST}) exiting the expansion tube, just before the nozzle in Fig. 3, will be greater than six feet for all test conditions, which allows for model lengths up to ~20 in (0.5 m). This length will double with the installation of the nozzle (Scott 2006).

A CAD drawing of the facility layout is given in Fig. 4. As indicated, the facility will have available two modes of operation. The originally planned HXT mode and a non-reflected shock tunnel mode. The expansion tunnel freestream chemistry limits were placed on shock tunnel mode as well, which led to the predicted operating map in Fig. 1. The reasons for the dual mode operation are as follows. Shock tunnels have the advantage of producing a wide range of en-

† This design was performed using software provided by Dr. MacLean from CUBRC.

thalpies (~25-50 MJ/kg), with relatively long run times. However, realistic freestream gas composition limits the operation to enthalpies < 5 MJ/kg. Expansion tunnels are well suited for very high enthalpies (80 MJ/kg), but not low enthalpies (<5 MJ/kg) due to the Paull and Stalker acoustic disturbance (Paull and Stalker 1992). Realistic freestream gas composition with minimal emission for enthalpies limits the enthalpy to <10 MJ/kg. Collectively, these constraints result in the operating envelope shown in Fig. 1.

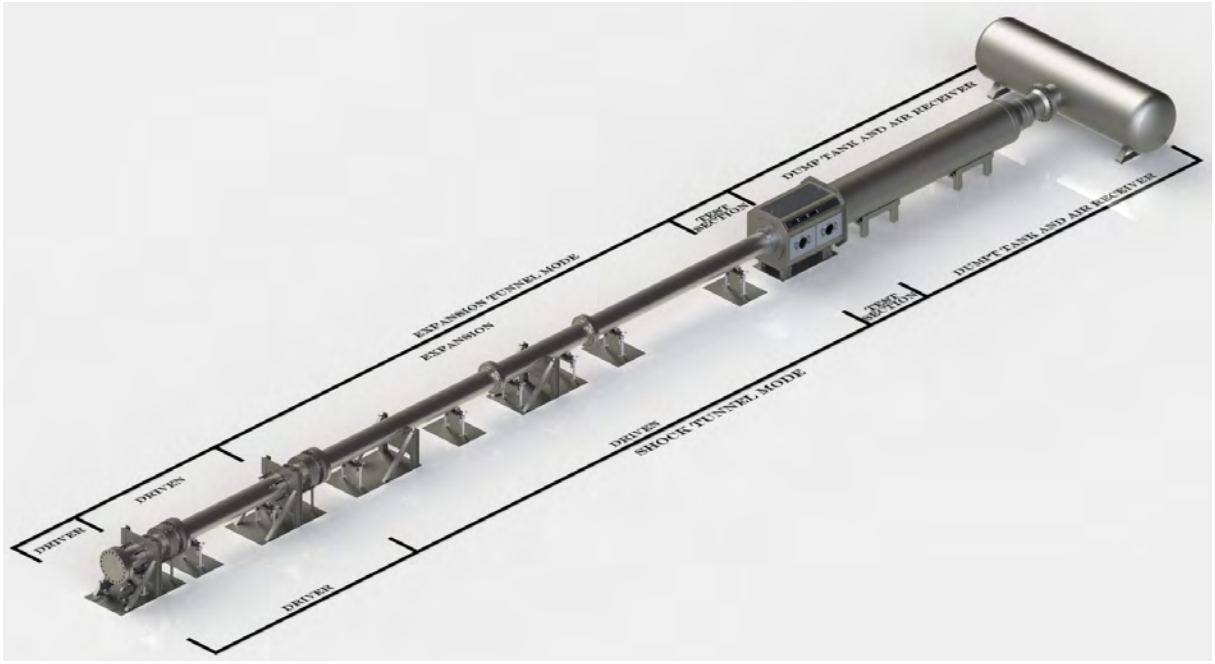

Fig. 4 Three-Dimensional CAD Sketch of TAMU Hypersonic Expansion Tunnel (HXT)

The hypersonic expansion tunnel (HXT) facility is integrated into the Texas A&M University National Aerothermochemistry and Hypersonics Laboratory (NAL) as shown in Fig. 5. The NAL currently houses the NASA Langley Mach 6 Quiet Tunnel, the Actively Controlled Expansion (ACE) Tunnel, a suite of specialized test cells, and an array of advanced laser and conventional diagnostics. The laser diagnostics include particle image velocimetry, planar laser induced fluorescence, coherent anti-Stokes spectroscopy, and molecular tagging velocimetry. The conventional diagnostics include IR thermometry, pressure/temperature sensitive paint, schlieren photography, high-frequency response pressure (Kulite and PCB), and thermometry.

Vibrationally excited nitric oxide monitoring (VENOM) for combined molecular tagging velocimetry and 2-line planar laser induced fluorescence is a signature diagnostic capability developed by our group (Sanchez-Gonzalez et al 2011/2014, Hsu et al 2009) to study hypersonic non-equilibrium flow. The principal advantage of this method is the ability to acquire planar velocity

and temperature simultaneously and instantaneously (~0.5 μs). The planned position of the expansion tunnel is shown in Fig. 5. As shown in Fig. 5, the HXT is strategically located between the two VENOM legs to take full advantage of this diagnostic capability. It is our goal to utilize the combination of the HXT facility and VENOM to provide never before achieved measurements of the flow structure under true high-enthalpy hypersonic flow conditions. In addition, the PIs (through University support) are installing two 1MHz pulse burst laser PLIF systems to allow for statistical measurements with in 1 msec. The data acquisition system is installed in the control room shown in Fig. 5.

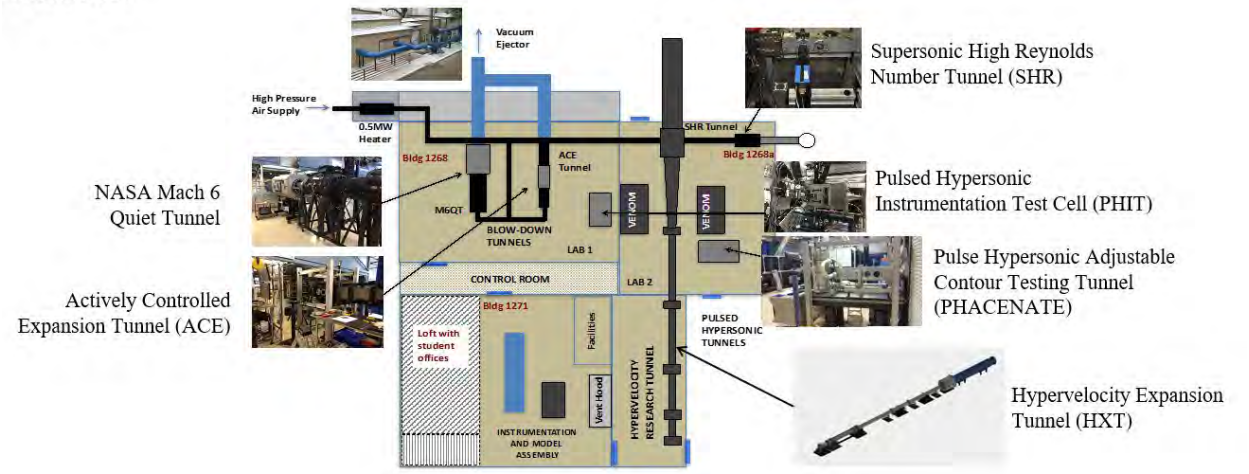

Fig. 5 Lab Layout within the NAL

3. WORK COMPLETED

3.1 TUBE DESIGNS

Originally, the proposed diameter of the HXT was 12-ines. However, under similar conditions, the boundary layer at the expansion tube exit for the CUBRC LENS XX facility, as generalized in Fig. 6, was estimated at approximately 2.7 inches for both laminar and turbulent boundary layers by Dufrene *et al* 2010 following Mirels (Mirels, 1964). Dufrene and Holden subsequently verified this estimate experimentally in the

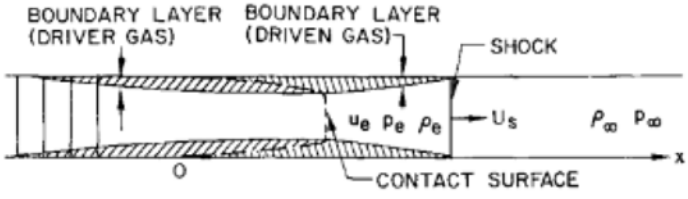

Fig. 6 Representative illustration of shock or expansion tunnel boundary layer (Mirels 1964).

LENS XX tunnel. Since the overall length of HXT is approximately half the length of LENS XX, the boundary layer thickness is expected to be about 2.0-in under the highest Mach number condition. Numerical confirmation of the viscous effects is underway, and the tube exit flow will be characterized following Dufrene and Holden. The estimated core flow for the 12-in and 20-in options are listed in Table 1. The 20-in pipe presented the cost-benefit relationship. This diameter offers a huge advantage to the one presented in the proposal, with an exit diameter (19") almost 80% of that proposed to ONR with a nozzle. This also allows for a larger nozzle to be incorporated in the facility as well, or, at the very least, a smaller inlet-to-exit ratio.

TABLE 1. Driven pipe size comparison (304l welded stainless steel)

NPS Size	Schedule	Inner Diameter (in)	Core Flow Diameter (in)
12-in	XS	11.75	7.75
20-in	XS	19.00	15.00

A classical 1-D unsteady gas dynamics code was written for flow path design. With this code, optimal lengths for the driver, driven, and accelerators were calculated at multiple conditions using helium and air as a driver gas. Given in Fig. 7a-b are example results from this flow solver. Shown in Fig. 7c are the trends in lengths vs run time for these various conditions. Based on these simulations, a 5-15-50 configuration was chosen.

The driver sections are constructed from 20-in diameter Schedule 160 Stainless Steel welded pipe (domestic, ASTM A358, with x-ray and ASME pressure ratings of 2100 psia at 400 deg F). The driven and expansion sections are constructed from 20-in diameter Schedule 80 Stainless Steel welded pipe (domestic, ASTM A358, with x-ray and ASME pressure ratings of 750 psia at 400 deg F). An in-house designed nozzle, with 3.6:1 area ratio, will be incorporated to increase the Mach number, test area and test gas streamtube length (Scott 2006).

Stainless steel was chosen for the driver and driven sections to prevent corrosion. Listed in Table 2 are calculated the allowable working pressures for 20-in 304 stainless steel pipe. The pressures were calculated using as $p = SEt/D$, where p is the allowable working pressure, E is the weld quality index, t is wall thickness, and D is the outer diameter. The flange ratings were based on ANSI pressure and temperature ratings. The driver/driven sections are constructed from Schedule 160 pipe with 900-lb flanges, and the accelerator section from Schedule XS pipe and 300-lb flanges.

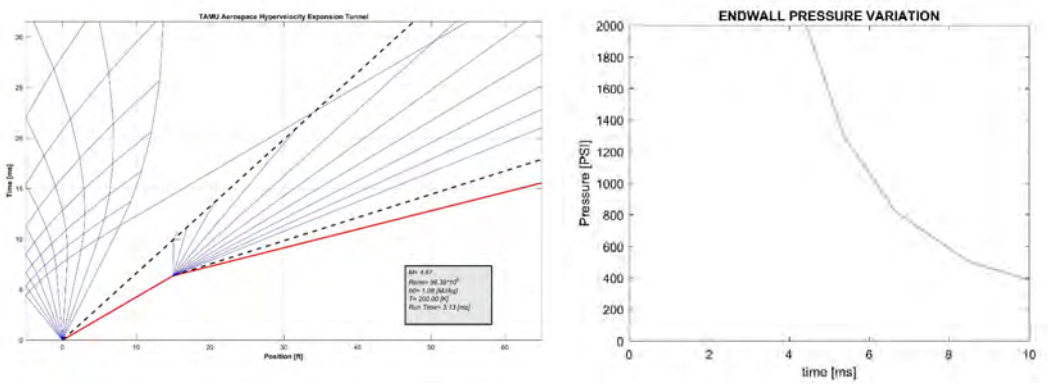

(a) x-t diagram and back-wall pressure (low enthalpy, high pressure case)

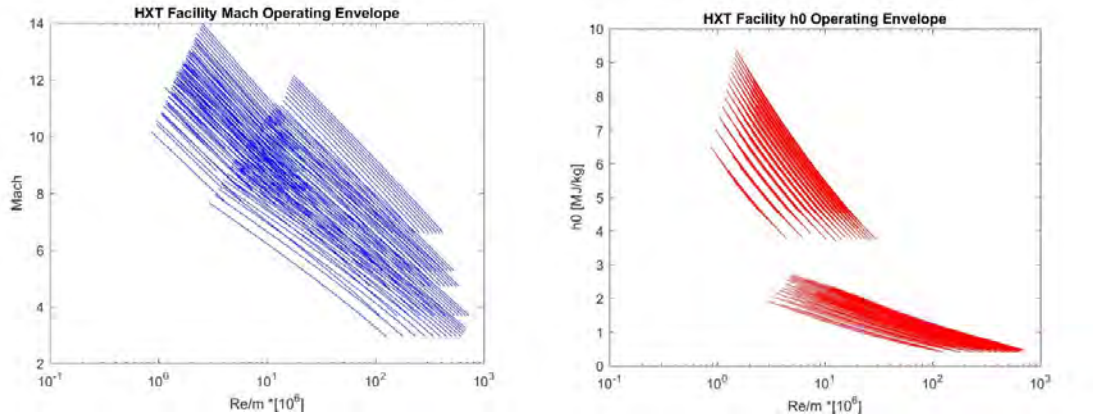

(b) Operating envelops for pure air and pure helium (no heating)

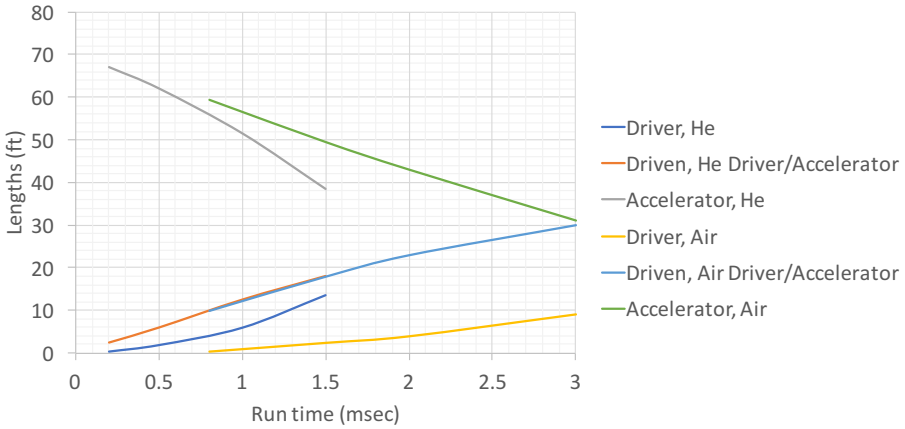

(c) Optimal lengths for maximum run time over the full operating range for both helium and air driver gases

Fig. 7. Example design code results.

TABLE 2. Maximum allowable working pressures of 20-in 304 ss pipe and flanges

Pipe NPS Schedule	Pipe Wall Thick-ness (in)	Pipe Allowable Working Pressure (psi)[1]	Flange	Flange Allowable Working Pressure (psi)[2]
XS	0.500	700/500	300-lb	720/435
160	1.969	2760/1970	900-lb	2160/1435

[1]Allowable stress: 14 ksi (100 deg F)/10 ksi (500 deg F), ASTM A358 weld with a quality index of 1.0.
[2]100 deg F/500 deg F

The second design factor for the driver and driven is how it will interface with the load bearing support stands that transfer the recoil forces to the concrete. This is important when changing diaphragms, as the driver must be moved back from the driven to do this. Stands were designed to transmit the full load to the concrete floor, which is rated for 6000-psi. However, shock absorbers are planned (not installed at the time of this writing) to significantly reduce the load and vibrations transmitted to the floor.

Finally, three breech options were considered. The first is a simple pipe section that uses the flange bolts to seal the diaphragm. This set-up is currently installed. One concern is potential fracture and loss of diaphragm material. A square section is also being designed to help eliminate this potential problem. The third option includes a hydraulic system to move and seal the diaphragm system. This design is described in the appendix. The square concept was under design at the time of this writing. Figure 8 details the resulting lengths of the driver and driven pipe segments needed as 49.375-in and 160.125-in, respectively.

Circle H Manufacturing and Refrigeration Valves and Systems designed, welded, tested, and registered per ASME Section VIII, Division 1 all of the tube sections. The full specifications are stated in Appendix A, with the requirements document for the all of the sections. The drawing contains signature approval from the responsible engineers on the HXT team and is ASME code verified and checked with the National Board of Boiler and Pressure Vessel Inspectors. Drawings for all five sections can be found in Appendix B, having been properly documented since the tube segments represent a significant fraction of the overall budget and pose the biggest safety risk.

A final design point is the plumbing connection interface. Both the driver and driven contain fill lines running into the pipe segments, though most of the primary lines used to fill and vacuum the driver run through the blind flange. One main connection point is located on the driver 16.00-in from the flange opposite the blind. This connection is a 1-in NPT coupling used to immediately divert the high-pressure gas in the driver through a pipe line and outside the lab in case of emergency.

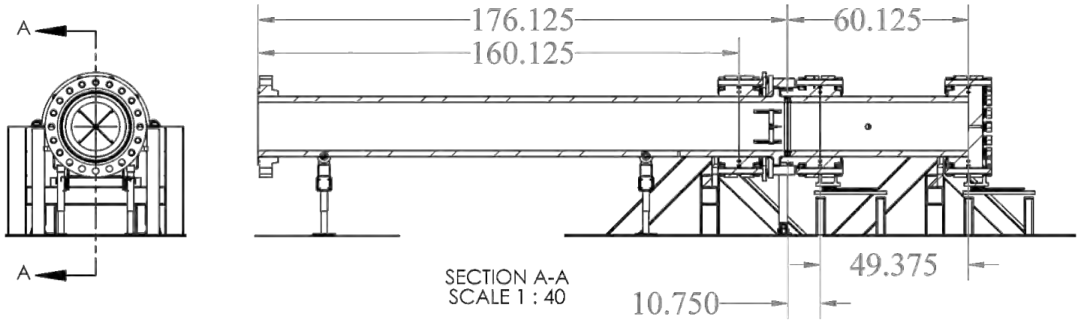

FIG. 8 Dimensional drawing for the driver and driven section with lengths of the pipe sections and effective lengths of each section located within the breech assembly.

The driven contains additional interfaces, though both are ½-in NPT couplings. Because the driven is sandwiched between the driver and accelerator pipes, the only interface point to fill and/or vacuum is through couplings welded into its walls. One of these couplings is used for fill/vent, while the other is a potential port for a hydraulic line to actuate the diaphragm pin assembly. The two ports are located 20-in and 32-in from the flange that connects with the breech/driver and technical drawings can be found in Appendix B.

The accelerator pipe underwent a design process similar to that of the driver and driven sections with consideration to the schedule of the pipe, class of flanges, and interface with the stands. A major advantage of the accelerator pipe, however, is the lower expected pressures. During expansion tunnel mode, the accelerator is always under vacuum and, even when under pressure during shock tunnel mode as discussed in the next section, the pressures never exceeds the 700-psi rating. The first accelerator section contains a 900-lb flange on the end that connects to the driver, as portrayed in Fig. 9, while the third accelerator has no flange located on the end that sits inside the test section. The flange-less end of the third accelerator pipe is intended interface with the test section by use of an inflatable seal that sits around the outer diameter of the pipe. Like the driver and driven, the accelerator pipe sections contain plumbing connections for fill and vacuum, located in the first accelerator pipe 48-in downstream of the 900-lb flange, but also include three coupling points along the third section to allow the installation of time-of-arrival sensors. The use for these sensors are specified in Section 5.3 and are required to be spaced out at large lengths to accurately measure the shock speed. For this reason, three ½-in

NPT couplings are placed at 20-in, 120-in, and 220-in downstream of the 300-lb flange of the third accelerator section, allowing 100 inches between each sensor.

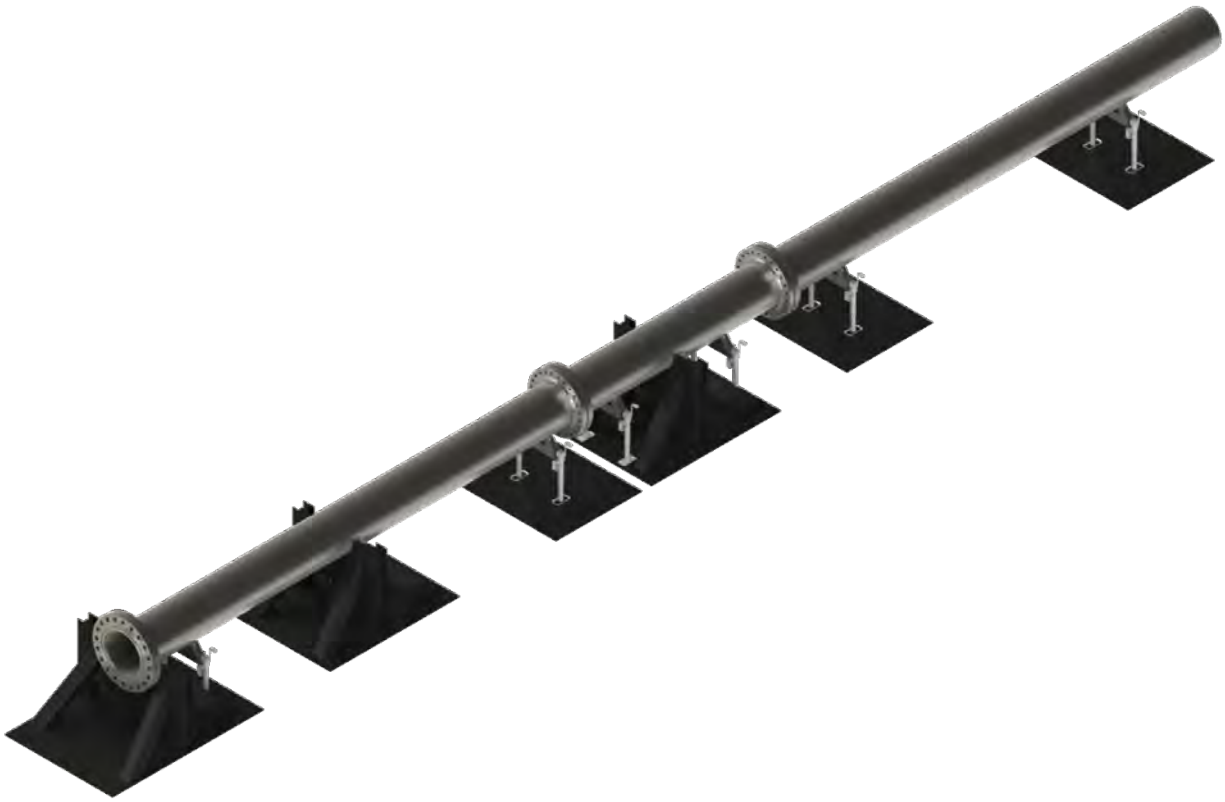

FIG. 9 Computer aided design model for accelerator pipe as it appears with a 900-lb flange on the driven side of the segment, structural stands, and roller supports.

One of the major advantages of HXT is its ability to operate in shock tunnel mode by moving the metal diaphragm location from the driver-driven flanges to the driven-accelerator interface (Fig. 10). This allows the expansion tunnel driver (XT-driver) and expansion tunnel driven (XT-driven) to become the shock tunnel driver (ST-driver). The rest of the facility, including the test section and tailpipe become the shock tunnel driven (ST-driven). This is enabled by manufacturing the driven and driver tube from similar materials with similar pressure ratings. One concern with the ST mode is the increased rest pressure after the run. To overcome this, a vacuum receiver is required.

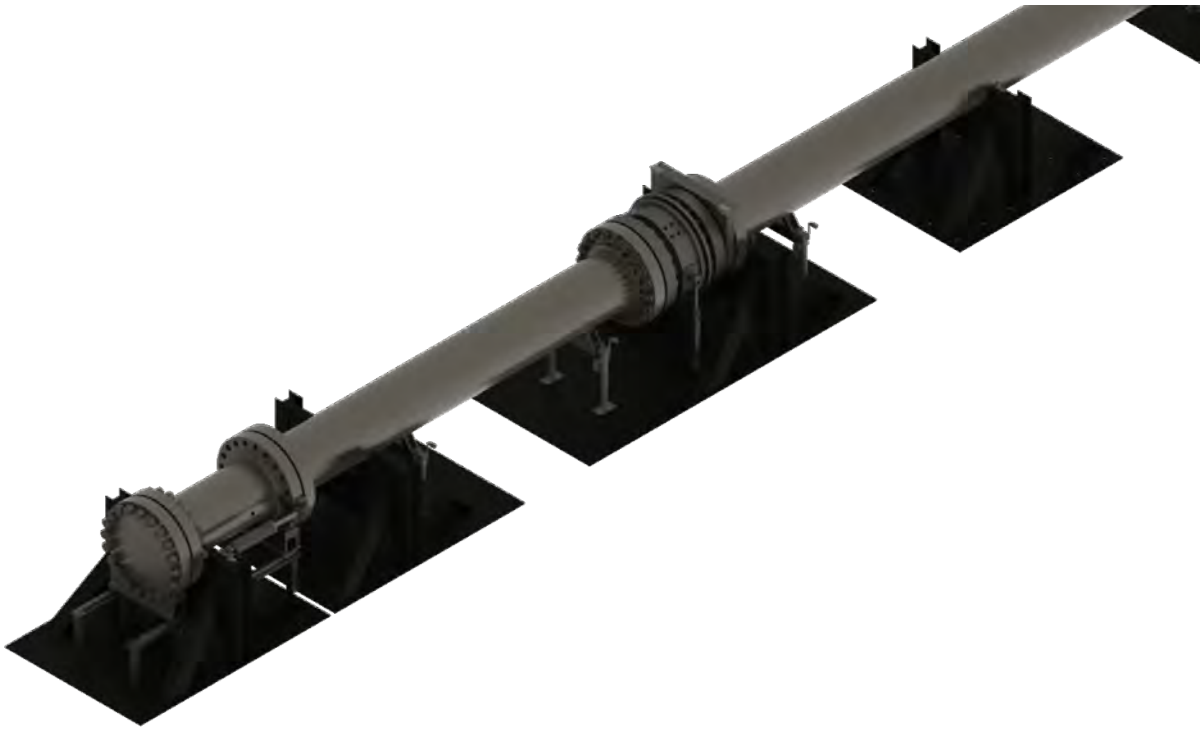

Fig. 10 The Hypervelocity Expansion Tunnel as it would appear in shock tunnel mode with the breech system reinstalled between the ST-driven and accelerator pipes.

3.2 NOZZLE OPTION

The Hypervelocity Expansion Tunnel is designed to ultimately include a diverging nozzle to increase the overall Mach number and core flow for the test section. In the original ONR proposal, the nozzle was to expand the flow from a 12-in pipe inner diameter to a 24-in exit diameter. When the pipe size of the entire facility was increased from 12-in to 20-in it was suggested that the 2:1 nozzle ratio stay roughly the same, with an exit diameter of 36-in.

Design of the nozzle contour was performed using an in-house, viscously corrected method of characteristics code. The characteristic mesh for inlet Mach number of 9 and outlet Mach number of 13 is shown in Fig.11. The overall length of the nozzle is approximately 23.5-ft, but is truncated at 20 feet when accounting for viscous effects.

Manufacturing is the major obstacle in the design of the nozzle. Acquiring steel segments in excess of 24-in in diameter, especially those which gradually increase to the required 36-in, is extremely difficult, even in short sections. For this reason, an innovative solution is proposed in terms of both machining and material fabrication.

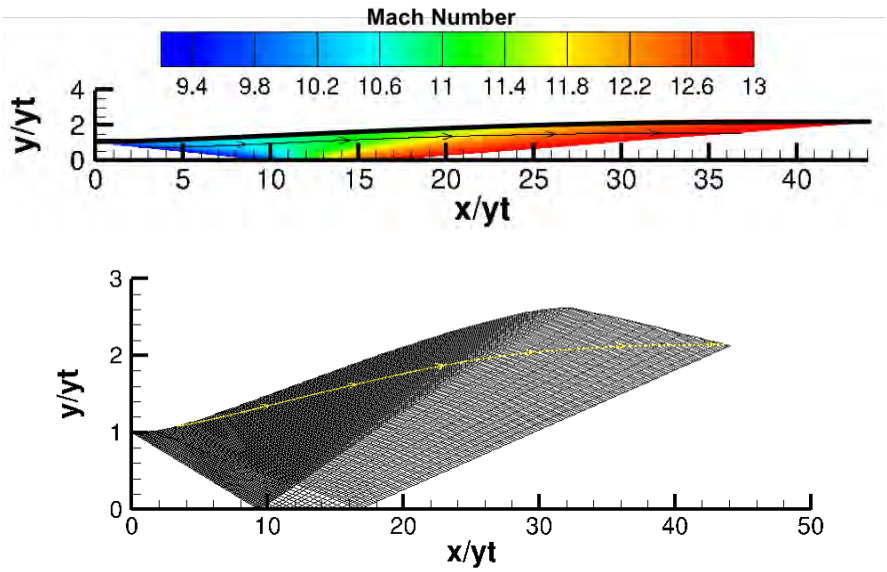

FIG. 11 Method of characteristics diagram used to predict the contour and length of the nozzle.

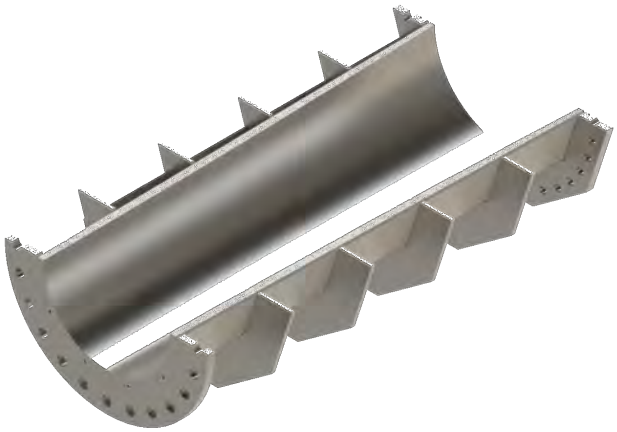

FIG. 12 First segment of the nozzle, cut in half and displayed as it would sit in the CNC mill for machining of the contour.

First, the nozzle is divided into four separate sections 5-ft long. This allows machining of the axisymmetric contour to be done on an accessible machine. Each section is machined in halves to further simplify the machining process and allow it to be performed on a mill rather than requiring a lathe with a 5-ft travel. Ribs are located across the entire nozzle, which serve a dual use during fabrication as alignment jigs. These ribs, as portrayed in Fig. 13, all sit at the same face diameter in order to sit flush on the machining table. The CNC mill can then be pro-

grammed to machine the angle and contour required by the design. The second major challenge to the nozzle is acquiring material capable of being machined in the proposed manner. Forging pieces of stainless steel at the required outer diameters is one solution, and one that would decrease movement of pieces during welding. However, another, cheaper solution is to weld thin bars together to create a polygon that can then be machined, especially since the machining process already requires each segment to be manufactured as a half.

FIG. 13 Nozzle assembly using a decagon shape and ribs that double as alignment jigs.

Using a decagon shape and manufacturing each segment half as a welded assembly of 5 steel bars, the minimum required thickness for each individual bar is approximately 1.25-in, with widths ranging from 7.5-in for the first segment to 12-in for the fourth segment. Each of these bars are manufactured and beveled on the sides in order to weld together using the alignment ribs/jigs. Once five are welded together, they can be machined and combined with their other halves and once again welded. Each segment is fastened together using a custom alignment rib with an o-ring groove placed on the face of one side. Bolt holes are also placed across these joining ribs, allowing each segment to be removed individually if required. Figure 13 shows the nozzle assembly with all four segments. The rib thicknesses are currently designed at ½-in, though this dimension could increase or decrease depending on the finite element analysis that should be performed. It may also be determined that four ribs are either not enough or exceed the number required by structural analysis. Interfacing the nozzle with HXT requires the addition of a new

structural support stand. While it should be designed to carry some recoil, if expected, the support stand primarily carries the weight of the nozzle, estimated at 6,500-lbs. Additionally, since the third accelerator pipe segment is the one designed with time-of-arrival sensor input, the nozzle will also need to accommodate coupling ports for these sensors.

3.4 Preliminary Breech and Diaphragm Holders

For the initial phase of construction, a spacer pipe is used in conjunction with the diaphragm holder (described later in this section) in place of the breech system. This allows for initial operation while the breech is completed. The preliminary configuration uses a 20-in schedule 160 section of pipe 25-in long along with the diaphragm holder with a thickness of 2-in. Fig. 14 shows how the section of pipe and diaphragm holder are held into place with studs that span from 900-lb flange to 900-lb flange. These studs keep a constant, uniform force along the o-rings present on each face of the flanges. Drawings for the preliminary breech can be found in Appendix B.

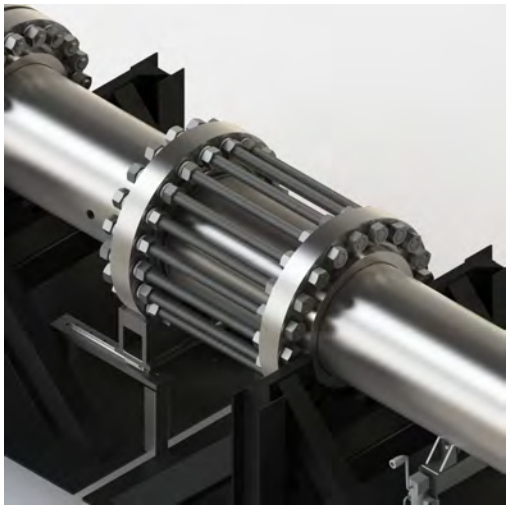

FIG. 14 Preliminary diaphragm holder and a 20-in schedule 160 pipe section.

Technical drawings of the diaphragm holder components can be found in Appendix B. As depicted in Fig. 15a, the circular diaphragm holder consists of two holding rings clasped around the diaphragm to equal a total thickness of 2-in. Both rings are machined out of 20-in schedule 160 pipe for ease of manufacturability. O-ring grooves are placed on both sides of both rings for adequate sealing as illustrated in Fig. 15b. Inner grooves place the o-rings against the diaphragm and are held tight using ¼-in countersunk screws. One ring, called the “female” ring, has thread-

ed holes machined into it while the other ring with through holes is labeled as the "male" ring. Due to the placement of the counter bored hole on the male ring, an o-ring groove is placed to match the inner or-ing grooves to avoid any interference, while the female ring has its dowel pin alignment holes further inside to allow for a notch on the outside. A diaphragm thickness of ¼-in was chosen to be the standard for the diaphragm holder. Although variable thicknesses can be used, this would greatly affect the design and seal of the breech system. This is because the teeth carrying the loads on the breech system have very little tolerance for movement and so the breech must be redesigned to account for any deviation from a ¼-in. This will be better understood after a series of experiments are conducted which will characterize how the diaphragms break and at what pressure differential. If ¼-in diaphragms are too hard or too easy to break, then the correct thickness can be redesigned into the breech system. Because of the 2000-psi (max) pressure, large 400-series o-rings were chosen to ensure maximum squeeze and prevent breaking with softer materials such as silicone. The 400-series groove width and depth ranges, as recommended by the Parker Handbook, are 0.309 to 0.314-in and 0.201 to 0.211-in, respectively (Parker Hannifin Corporation, 2016). A conservative depth of 0.195-in was chosen to abide the 70% rule of thumb for o-ring sizing, which dictates that the groove depth should be 70% of the actual o-ring cross sectional diameter. A square version of this concept is under design. Also, a double diaphragm system is uncer consideration.

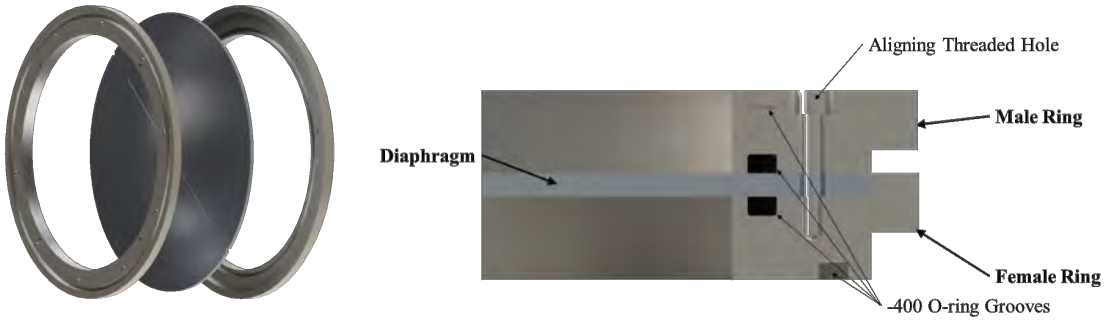

FIG. 15 (a) Diaphragm holder exploded view with (left) male holding ring, (middle) etched diaphragm, and (right) female holding ring. (b) Diaphragm holder cutout with labels and locations of O-ring grooves, dowel pin alignment holes, and threaded holes.

In expansion tunnel mode, the driven and accelerator tube gases are separated by a diaphragm. This diaphragm requires a much lower pressure rating due to the maximum experienced conditions after the driver. The Mylar diaphragm system, hereby referred to by MDS, is designed

using the configuration originally intended for the driver-driven diaphragms, using a slip-in mechanism to quickly replace the Mylar, as shown in Fig. 16a. One of the main reasons this becomes practical for the MDS is the expectation that the Mylar vaporizes when struck by the primary shock. Even if a portion of the plastic is still intact, the flexibility of the Mylar still allows for a short diaphragm housing. In contrast, a slip-in mechanism for the driver-driven interface would need an opening at least 12 inches long to allow removal of the ruptured diaphragm. The Mylar diaphragm assembly must interface with the same 20-in 900-lb flanges present in the breech system, though to avoid excess costs, welding on of additional flanges to the MDS was avoided. An alternative to this is to buy two thick plates that serve as the central body to the assembly and either tap threads or drill clearance holes into them that match the hole configuration of the 20-in 900-lb flanges as portrayed in Fig. 16b. This allows the nuts and studs to press against the flanges located on the driven and accelerator pipe and screw directly into the MDS. Threaded holes are used on the top region since the diaphragm must slip-in from this direction, preventing the studs from passing through. Figure 16c displays some of the mentionable design aspects of the MDS, including the matching RTJ grooves to seal between the 20-in 900-lb flanges. Additionally, the body itself made from two large plate, one welded onto the other by means of an alignment groove.

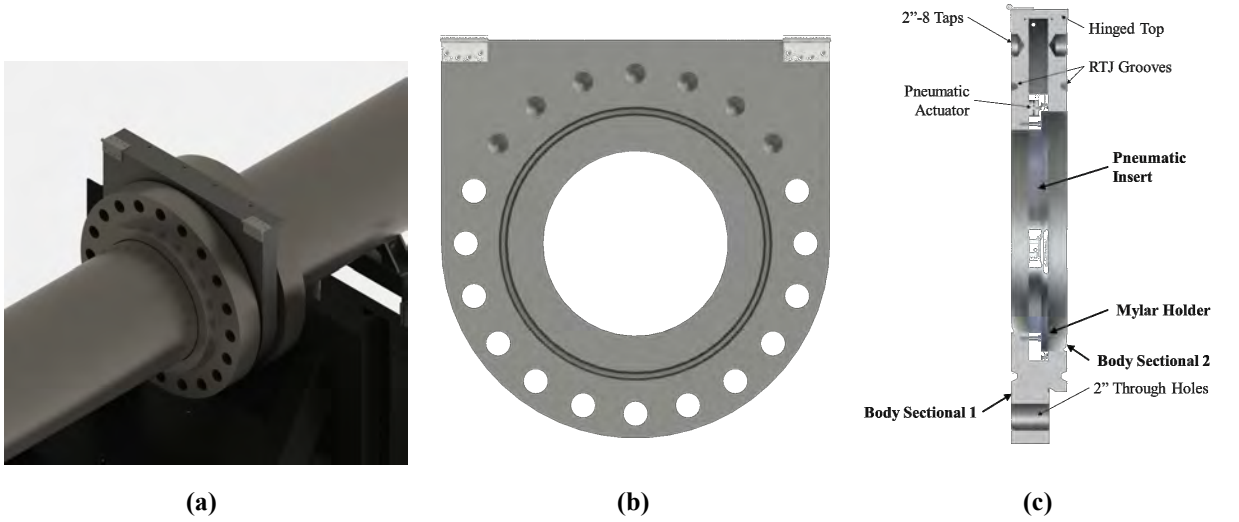

FIG. 16 (a) Mylar diaphragm mechanism at the interface between the driven and accelerator sections of HXT. (b) Threaded holes up top and clearance holes around the mid to bottom holes. (c) Design points for the Mylar diaphragm system assembly with major components in bold.

3.3 Test Section

The design for the test section is shown in Fig. 17. As depicted, the test section consists of a welded skeleton, ten access panels, and a stand to bolt into the floor. Drawings for the test section can be found in Appendix B. Given here is brief review of the development.

The accelerator pipe enters the test section from the bottom left face as shown in the figure while the tailpipe interfaces with the side opposite and out of view of the rendering. Because rectangular prisms have increased stress concentrations on their corners when under pressure, the main skeleton has an octagonal cross-section. The test section measures 70-in long inside from face to face, with two flat-to-flat lengths of the octagon at 60.75-in and 52-in as illustrated in Fig. 18. Each lateral face has a 0.6-in wall thickness. The diagonal faces of the octagon are made shorter to maximize access through the sides and are specifically designed so that the length of one horizontal/vertical face and one diagonal face are equal to just under 48-in. This simplifies manufacturing, as standard plate sizes plateau at 48 inches by 96 inches. Each lateral face of the skeleton, minus the diagonals, also contains two series of ¼-in-28 threaded holes for mounting. In total, each plate has sixteen of these holes in order to mount optics, test models, pitot probes, or any other sensors that may be needed.

the front and back plates of the test section are significantly thicker than the lateral plates, at 1.25-in and 1.9-in respectively. The front plate is machined with a diameter of 37-in to accept the planned nozzle mentioned earlier, which has an exit diameter of 36-in. While a nozzle is not in use the current configuration of the facility, it does include an adapter plate to reduce this opening to 20.5-in and allow the installation of an inflatable seal. The adapter plate mounts to the skeleton using twenty 3/8-in-24 bolts and a 300-series o-ring groove. Mechanical Research and Design, Inc. as described later. The back-plate wall thickness (1.9-in) is calculated by adding the expected wall thickness of 0.50-inc to the minimum threading distance acceptable for a 1½-inc. This bolt hole size is used to secure the tailpipe to the test section and patterned based off the matching 42-in 150-lb flange that it mates with. Because the test section must maintain a seal, the bolts could not go all the way through the back plate. Similarly, the width and height of the back plate was determined by the mating tailpipe flange which possesses a hub diameter of 53-in. Figure 19 depicts how the black plate dimensions rely heavily on the tailpipe flange, increasing its overall size and weight.

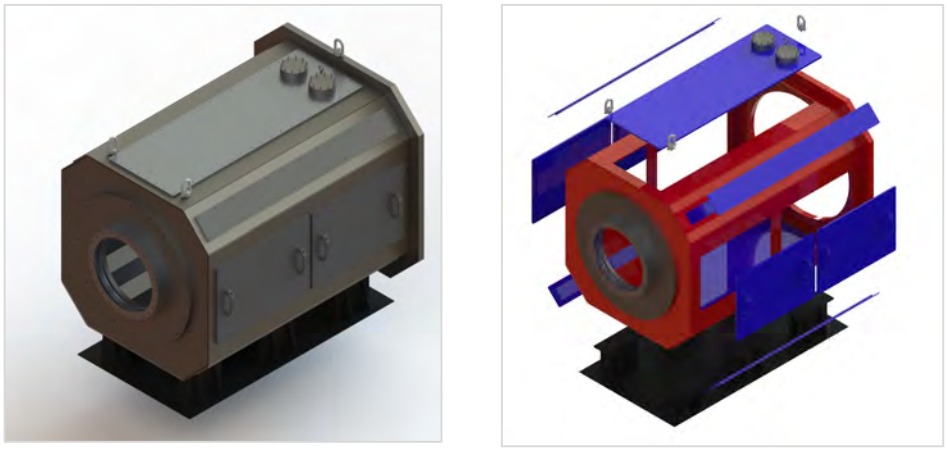

FIG. 17 CAD renderings of the test section with skeleton (red), access panels (blue), and base stand (black).

FIG. 18 The test section as it would appear at the NAL without a nozzle and with the tailpipe protruding through a wall to the outside.

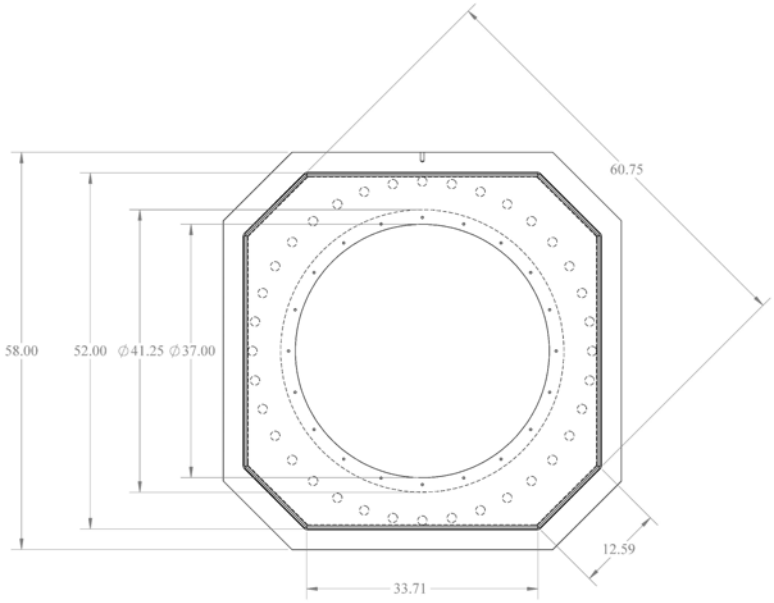

FIG. 19 Dimensions of the test section with flat-to-flat lengths and hole diameters.

Overall there are ten access panels: four general purpose doors along the sides, four slant panels, a roof access panel, and a floor access panel. Because the entire side face need not usually be accessed from run-to-run, typical access through the sides was split into two door access holes measuring 29.5-in wide by 20-in in height, as detailed in Fig. 20. Furthermore, each door is fastened with twenty-four ¼-in -28 socket head cap screws, whereas a single panel would require approximately forty, reducing panel removal time. Two handles, rated for 100lbs each, accompany each door for additional ease of removal, leaving an approximate square area of 24-in x 20-in between the handles and cap screws for the placement of windows or mounting of probes.

The roof access panel is sized to allow test models to be inserted or removed when too large to use the side doors. Additionally, the roof has two pressure relief plates for safety which lift when the test section experiences a slight positive pressure. To avoid mounting holes around the test section stand, the floor access panel was specially designed to be inserted from the inside, whereas all other panels mount into threaded holes on the outside of the skeleton. Because of this, the roof access hole measures at 22-in wide by 64-in long and the floor access hole measures at 18-in wide by 64-in long, allowing the floor access panel to be lowered from above with the use of a crane. The test section bolts into the stand using twenty-four 3/8-in -24 bolts that are machined into the underside of the skeleton.

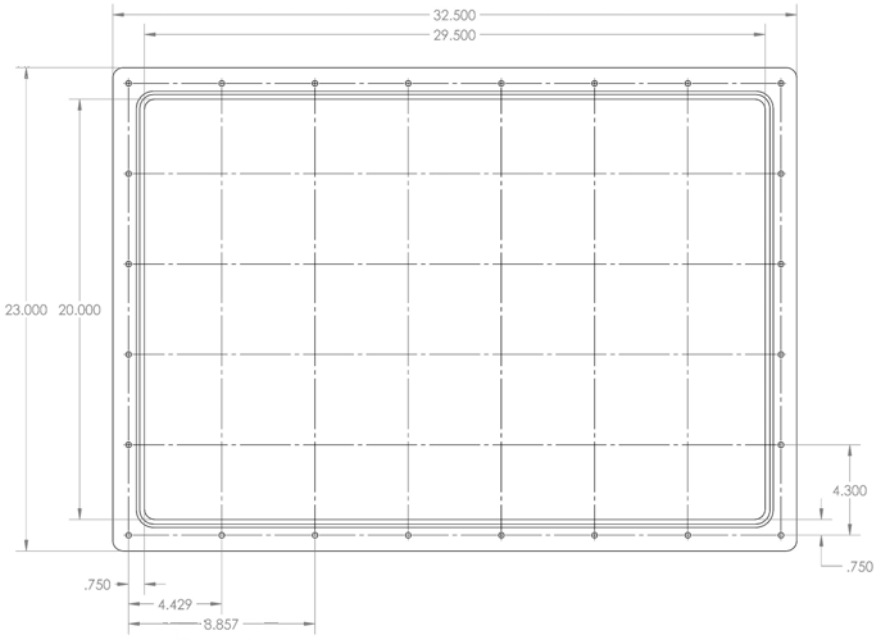

FIG. 20 Test section door with mounting holes and flange. Inside dimensions are associated with the access hole located on the skeleton.

The minimum anticipated text section pressure will be 0.1-torr. The maximum expected pressure is 43-psia (28-psig), which is the maximum rest pressure after a run between expansion tunnel and shock tunnel modes. Finite element analysis was performed on this design using a pressure of 40 psig, a yield strength for A36 steel of 36ksi (AZO Materials, 2012), and a yield strength of aluminum 6061-T651 of 35ksi (low side). Based on the finite element calculations, a rib was added through the middle of the skeleton to prevent bowing. The rib runs between the two door cutouts and spans across the roof access where a series of screws can be fastened from the inside, through the rib, and into the access panel. The rib ends at the floor access plate since the support stands prevent excess bowing along the bottom of the skeleton (Fig. 21a). The final finite element analysis is presented in Fig. 22 with isolated von Mises stresses corresponding to a yield FOS of 2 and 4. A limitation to the finite element analysis performed is that SolidWorks assumes all coincident surfaces to be perfectly bonded, whereas usually the surfaces are welded or fastened. The FEA does not account for variations in the weld, such as addition of weld or locations where weld may still sit underneath the beveled surface. Overall, however, the pressure rating of the test section does not solely depend on FEA, as hydrostatic testing was performed up to 45-psia.

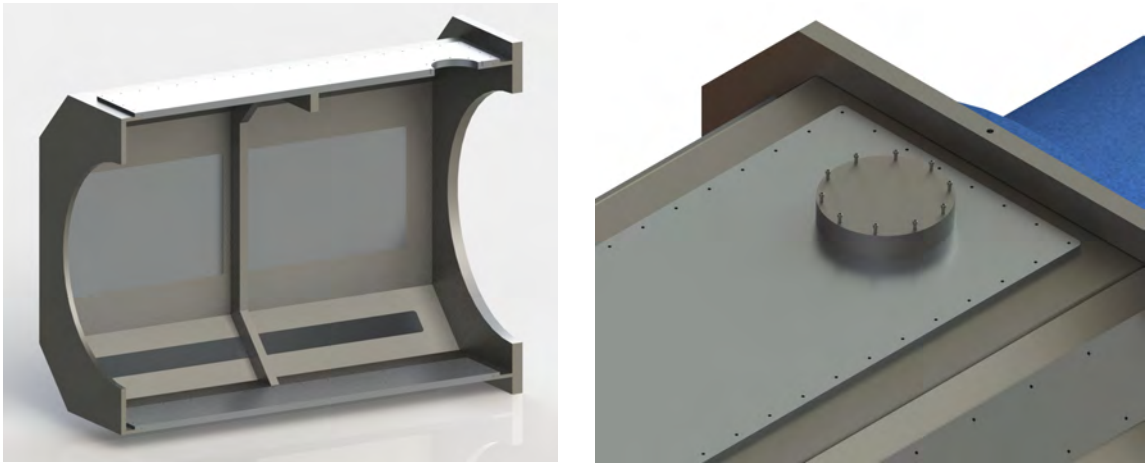

(a) **(b)**

FIG. 21 (a) cross-section of the test section with a rib welded to the inside of the skeleton to increase support. (b) Pressure relief plate set for approximately 1psi differential to assist with avoiding over-pressurization of the back assembly.

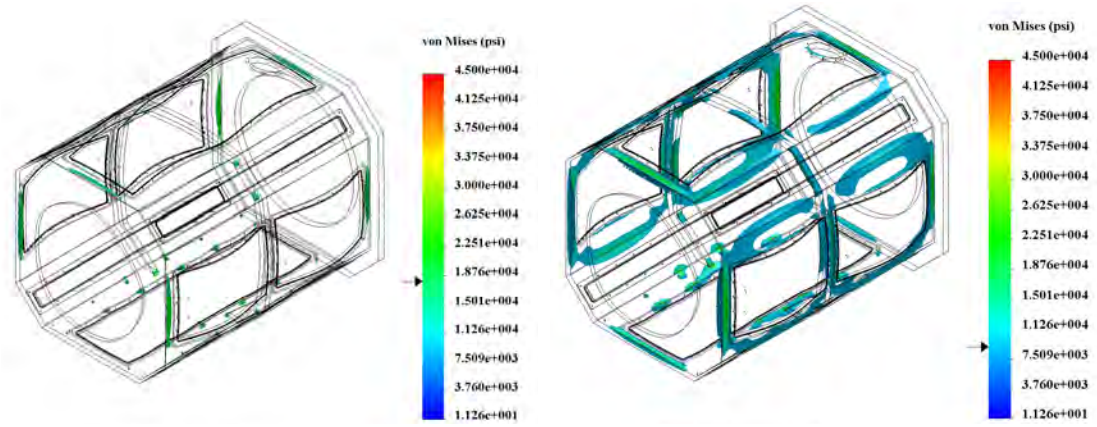

(a) **(b)**

FIG. 22 ISO-clipping of von mises stresses for (a) 18ksi corresponding to a factor of safety of 2, and (b) 9ksi corresponding to a factor of safety of 4.

A further safety measure designed into the test section is the addition of a pressure relief plate. This plate simply seals against the top face of the roof access panel using the force of gravity. When under vacuum, the relief plate has additional force due to atmospheric pressure which assists in sealing, whereas an internal positive gauge pressure begins to act against the weight of the plate. Made out of stainless steel with a diameter of 10.25-in, thickness of 2.00-in, and weight of 46.5-lbs, the relief plate sits above an 8.00-in diameter hole with an area of 50.27 in^2. Using a simple free body diagram with the weight of the plate and the pressure across the hole with a result of 0.925-psig (see Fig. 21b).

Using the maximum end-of-operation pressure of 42.8-psig (28.1-psia), the force exerted on each panel was calculated and is listed in Table 3. The main concern when designing the fastening of the access panels is that the force due to the pressures may overwhelm the proof load ratings of the combined bolts that hold them to the skeleton. Assuming a grade 8 bolt with a minimum tensile strength of 150-ksi, minimum yield of 130-ksi, and minimum proof strength of 120-ksi, the minimum number of bolts for each panel is listed with the maximum force. These values are accompanied by the actual number of bolts used. All calculations correspond to a proof load of a ¼-in -28 bolt of 4,350-lbf (Alma Bolt Company, 2006) as is rated for grade 8 bolts. The number of bolts used to secure each panel for a factor of safety of 3 was 36. Additional fasteners serve a dual purpose since the O-rings require constant, uniform pressure along the groove to maintain proper squeeze and seal.

TABLE 3 Dimensions and resulting forces on each access panel with minimum required bolts

Access Panel	Dimensions	Area [in^2]	Max Force [lb_f]	Min. Bolt	Bolt -lb
Door	29.5-in x 20-in	590	16,571	4	24
Slant	64-in x 4-in	256	7,190	2	24
Roof	64-in x 22-in	1408	39,545	10	36
Floor	64-in x 18-in	1152	32,355	8	36

¼in -28 grade 8 bolts with a proof load of 4,350 lb_f.

All access panels located along the lateral faces of the test section use 200-series O-rings with actual cross-sectional diameters of 0.139±0.004 (Parker Hannifin Corporation, 2016). Besides these lateral seals, the only other O-ring in use is with the pip-to-test section adapter plate, which uses a 300-series O-ring with a cross-sectional area of 0.210±0.005-in (Parker Hannifin Corporation, 2016). All O-rings and gaskets used in the facility are silicone unless otherwise noted. For a 200-series O-ring, the Parker Handbook recommends a gland width of 0.158-in to 0.164-in for vacuum and gases and a gland depth of 0.101-in to 0.107-in (Parker Hannifin Corporation, 2016). Common rule of thumb also usually dictates that the groove depth be roughly 70% of the actual O-ring cross-sectional diameter which would equal 0.0973-in, shallower than what the handbook suggests. Because it would increase squeeze, a final gland width of 0.160-in and gland depth of 0.098-in was used for the panel seals, with the thought that if the O-rings were to slip out or wear too quickly than the grooves could be machined to depths within the range that the Parker Handbook suggests. The 300-series O-ring was designed in a similar fashion, with a suggested groove width of 0.239-in to 0.244-in and depth of 0.152-in to 0.162-in (Parker Hannifin Corporation, 2016). The finalized dimensions using the rule of thumb of 70% are 0.239-in for the width and 0.147-in for the depth. Because all the grooves for the adapter and access panels have linear lengths longer than any commercial O-ring manufactured, stock O-ring had to be used and glued together to make custom sizes. This is not preferred since one-piece O-rings are the strongest and the point that is glued presents a weak joint in the seal.

The test section skeleton was engineered to be welded together as ten individually machined plates as illustrated in Fig. 23a. Each of the plates were waterjet to the appropriate material dimensions. The water jetting included all large access points and the general outline of each plate with a tolerance of +/-0.010-in. Drawings can be found in Appendix B. In order to prepare for welding, the ten plates of the skeleton were machined down to thickness, tapped, and beveled.

With the exception of the front and back plates, which were sent to Machine Works for their final cuts, all plates were machined at the shop located at the Low Speed Wind Tunnel Complex and welded at the Texas A&M University Cyclotron Lab. An alignment groove was engineered into the back plate as seen in Fig. 23a in order to ease assembly before welding while the front plate was designed to slide between the lateral faces. For purposes of alignment, the skeleton is assembled on its back and clamped to reduce bowing as shown in Fig. 23b. This configuration minimizes movement of the plates during welding and creates a more accurate final product. Each access panel is machined out of 1 1/8-in thick 6061-T651 aluminum plates, which was done at the LSWT shop. The access panels and skeleton plates are all too long to have been machined in one pass on the CNC mill located at the LSWT, so each was done using two or more passes and aligning at a common point. All finalized drawings for the access panels, plates, and the support stand for the test section can be found in Appendix B.

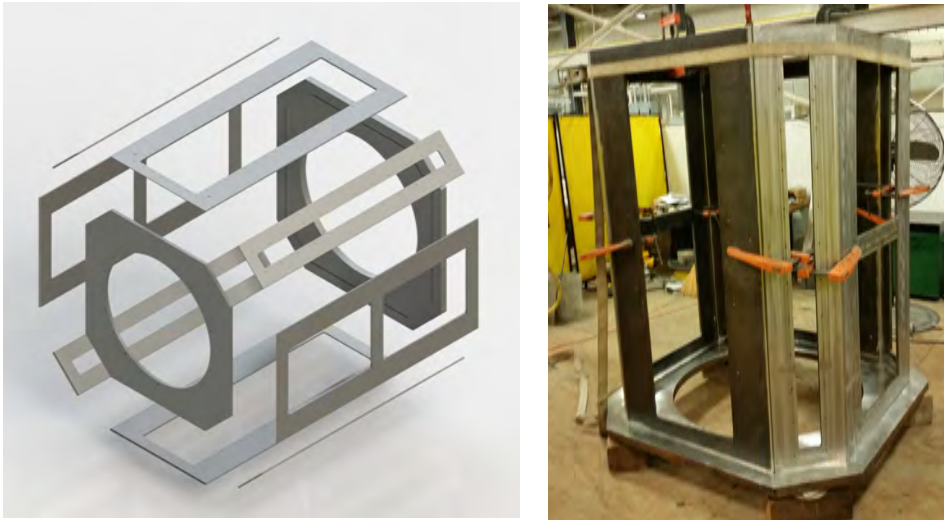

(a) (b)

FIG. 23 Test section skeleton. (a) Exploded view illustrating construction. (b) Photograph of sections clamped together for welding.

3.4 TAIL PIPE

A tailpipe is fastened directly to the back plate of the test section allow the flow to pass over the model uninterrupted. Drawings for the tailpipe can be found in Appendix B. The length tailpipe is 20-ft, provides a vacuum receiver and provides sufficient distance for the shock travel such that the reflected shock does not interfere with the test gas. The diameter is 42-in. A standard schedule (0.375-in w.t.) is used and is rated for 189-psig (Atlas Specialty Metals). Figure 24 shows the tailpipe assembly in its planned initial configuration. The end of the tailpipe which

connects to the test section has a 42-in 150-lb raised face slip-on flange. This flange is rated for 285-psig (The Engineering Toolbox) and bolts directly into the back plate of the test section skeleton using thirty-six 1 ½-in -6 grade 5 bolts at a length of 4-in long each. A 1/8-in thick, full face gasket is used to seal between the raised face of the flange and the flat face of the test section. Silicone was chosen due to its low cost and chemical resistance for the potential use of corrosives such as nitric oxide in diagnostics. Opposite the test section, the tailpipe necks down to a 30-in OD with a 300-lb raised face weld neck flange. This flange then bolts into a 300-lb raised face blind A 30-in 300-lb flange is rated at 750-psig (The Engineering Toolbox). Table 4 lists each component with its pressure rating. Since the 42-in 150-lb flange contains the lowest workable pressure, the tailpipe has a 189-psig pressure rating, which far exceeds that designed into the test section. A photograph of the tailpipe is shown in Fig. 25.

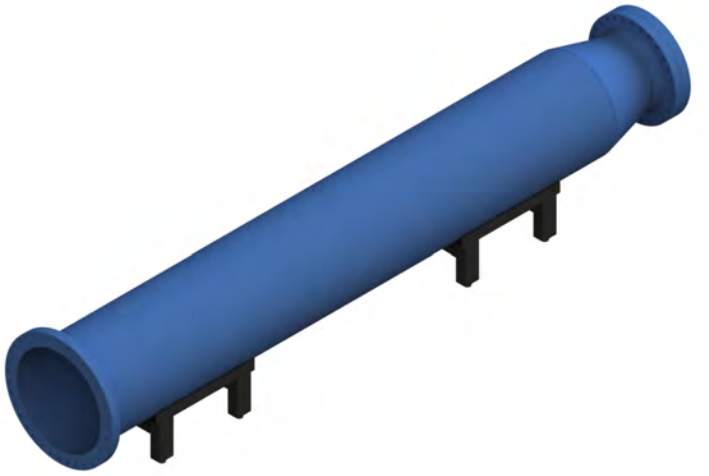

FIG. 24 Full overview of the tailpipe with the 42-in flange of the bottom left and the reducer and 30-in flange on the top right.

TABLE 4 Tailpipe pressure ratings.

TAILPIPE COMPONENT	PRESSURE RATING (PSIG)
42-IN STD SCHEDULE PIPE (0.375-IN W.T.)	189
42-IN 150-LB RF SLIP-ON FLANGE	285
30-IN 300-LB RF WELD-NECK FLANGE	750
30-IN 300-LB RF BLIND	750

FIG. 25 Tailpipe during installation.

3.5 SUPPORT STANDS

The primary purpose of the structural support system is to transmit the horizontal recoil loadings of the facility into the ground. Additionally, the structures serve in the ease of alignment for the entire facility through the inclusion of rails and hydraulics. The support stands are divided into three separate designs: the primary, secondary, and roller stands. Before discussing some of the requirements and the reasoning behind them, it is important to note the assumptions of the load distribution system. The recoil force is calculated using an unbalanced pressure located at the blind end of the driver. This maximum loading due to a conservative pressure differential of 2000-psi acting upon an area of 203 in^2 was computed to be 405,350 lbf. Furthermore, the loading distribution is assumed to be a rigid system, which is true to within tolerance considering the thickness of the pipe, especially along the driver and driven lengths. The thick walls allow one to assume that the overall displacement from one stand to the next remains very minimal. Under this rigid body assumption, the horizontal design load of each support (five total) is set to 81,200 lbf. The safety of factor for each support stand was set at 4 times the design load, resulting in a failure criterion of 324,800 lbf. Failure was defined as the yield point of the material chosen to construct each member. Drawings for all of the stands can be found in Appendix B. Given here is brief review of the support structure development.

Shock absorbers are currently being installed to reduce the loads and vibrations to the building foundation.

In order to manufacture stands capable of handling 324,800 lbs, many structural calculations relied on the ability to weld large steel components into place. This, in turn, limited the

ability to adjust the height of the facility after manufacture. For this, separate roller stands were fabricated to specifically support the weight of each pipe section. These supports were placed two on each section in order to keep the center of mass in between two points of contact. Moreover, the roller stands would not inhibit movement in the horizontal direction, allowing the sliding of pipe sections apart from each other for either cleaning or inspecting. These roller stands, as a pair, were determined to be rated for twice the weight of the heaviest section of pipe: the driven at 9,450 lbs. The final requirement of note is that the stands be able to properly fasten to parts of the facility. The primary stands are designed to bolt through the 20-in 900-lb flanges welded to the ends of the driver and driven while the secondary stands push against two halves of a 150-lb stainless steel flange welded to the middle of the first and second accelerator pipe sections.

There are three primary support stands, as shown in Fig. 26. One attaches to the blind end of the driver, one to the driver end of the driven section, and one to the accelerator end of the driven section. All of these interfaces are with 20-in 900-lb flanges which fasten with the use of four 2-in threaded studs and a nut. The general, design of the primary supports relies on a central 2-in -thick A36 steel plate. Four of the 2-in threaded studs are cut longer than the other sixteen found on the 900-lb flange interfaces. The steel plate sits atop a 6-in square tube (0.5-in wall thickness) and is supported along its sides by two vertical W6x25-lb H beams, all of which are welded together. The square tube is milled down along the edges to fit inside the webbing of the H beam, which, when welded, creates an H-shaped support that the 2-in plate slips into. Gussets are engineered in multiple locations between the H beam webbing and steel plate, as well as between the steel plate and the 6-in square tube. These alleviate stress concentrations along the weld seams from building past the point of yield. For bracing, two S8x23-lb I-beams are located on the back end and welded at a 45-degree angle from the base to the 2-in thick plate. Two additional 6-in square tubes at ½-in thick wall are placed on the front to directly oppose the recoiling force (compression). These square tubes are placed at a 45-degree angle similar to the I-beam except with an additional cant of 15 degrees pointing toward the center of the stand.

FIG. 26 Primary stand with h-shaped central body, hole interfaces, and brace supports on both sides.

The H-shaped central body and bracing members are welded directly to a ½-in thick A36 steel plate. A series of twenty-two ¾-in holes are placed along each stand base in order to bolt into the concrete. The floor strength has a rating of 6-ksi and, while each stand is placed in a location in the lab with a unique floor height. With an extreme load of 81,200 lbs, it was deemed necessary to perform extensive finite element analysis using SolidWorks Simulation on each stand. The baseplate is fixed along the twenty-two holes where the concrete anchors are located and the entire underside of stand is constrained as a roller fixture in order to provide a no penetration condition that simulates the existence of a floor. Additionally, the entire support stand assembly is assumed to have all its components perfectly bonded to each other. The material used in the simulation was conservatively chosen as A36 because it is on the lower end of the yield and ultimate tensile strength rating, at 36-ksi and 58-ksi respectively (AZO Materials, 2012). While most components are, in fact, made of A36, some of the structural members such as the I-beam, H-beam, and square tubing have material properties that are slightly higher in strength. Shown in Fig. 27a shows the von Mises stress distribution on the primary stands. Under the design load of 81,200 lbs, an iso-clipping of these von Mises stresses simulate that no point of the assembly passes the point of yield. Shown in Fig. 26b is a representation of the stand under an experienced load of 324,800 lbs, which is 4 times the expected load for a given stand.

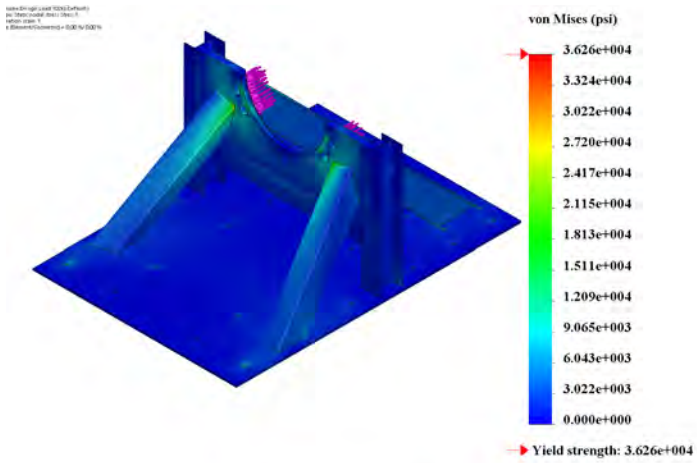

(a)

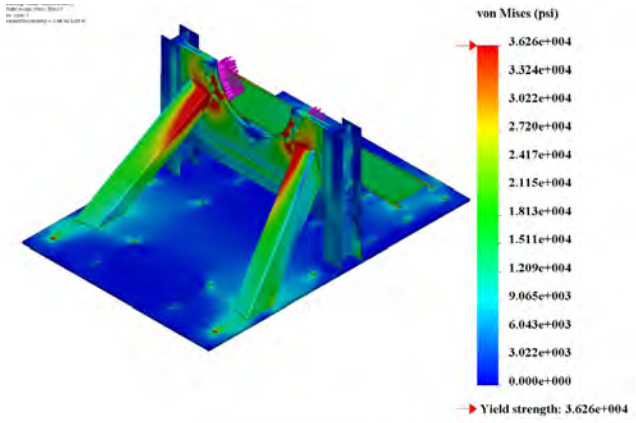

(b)

FIG. 27 Von Mises stress distribution of the primary stand. (a) Total load of 81,200 lbs. (b) Total load of 324,800 lbs to simulate a factor of safety of 4.

The secondary stands are derivatives of the primary stands, with key differences being that they interface with the facility at 150-lb stainless steel half flanges welded to two of the three accelerator pipe segments. Separate finite element analyses were performed on the secondary stands to insure a similar factor of safety of 4 (Fig. 28). All assumptions discussed for the primary stands apply for the second stands, including the use of A36 steel for all components and perfect bonding between all connected faces. The secondary stands, while smaller, are designed to be rated at the same 81,200 lbs of force as the primary stands, with a factor of safety of 4 yielding a load of 324,800 lbs. Like the primary stands, no point of the assembly ever exceeds the yield point for this load, whereas for the load of 324,800lbs, a stress can be seen along the tips of the 6-in square tubes.

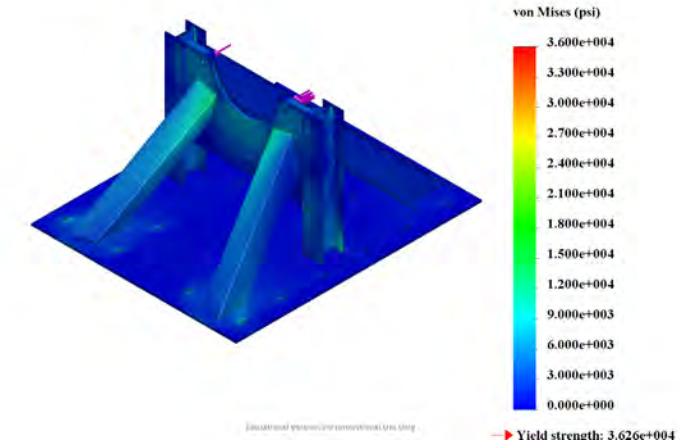

(a)

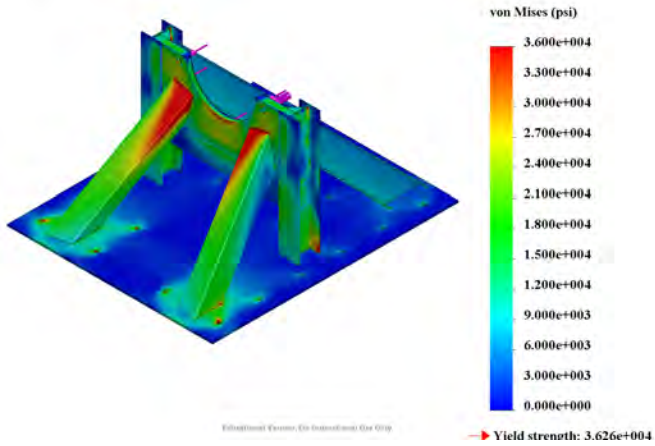

(b)

FIG. 28 Von Mises stress distribution of the secondary stand. (a) Total load of 81,200 lbs. (b) Total load of 324,800 lbs to simulate a factor of safety of 4.

For supporting the weight for the facility, roller stands were incorporated at two points along each pipe segment as can be recalled in Fig. 29a. The roller stand is designed into an adjustable height crank shaft. For convenience, two crank shafts straddle the main body of the roller stand. These leveling jacks have a vertical adjustment of 10-in and a weight capacity of 5,000lbs. At its minimum height, the jack sits at 16 ¾-in with mounting holes located at 9-in and 12-in above the ground. These mounting holes are sized at 3/8-in free clear and are equally spaced at 3-in x3-in at the heights previously listed. For durability, the main body of the roller stand is made from 4-in square tube with 3/8-in thick walls. Two 4-in wide by 8.5-in long steel bars ¾-in thick are welded to each end of the square tub. These bars extend underneath the main body where matching holes are machined to interface with the crank jacks. This additional height is not only required to achieve the proper centerline height of 36-in for the facility but also allow

the bolts to be tightened against the nuts located on the opposite side of the jacks. Sitting atop the central body are two ¾-in thick plates 3-in wide by 4-in tall. These raise the axis that the roller sits on to a position where the roller will avoid hitting the central body. The roller relies on two ball bearings located at each end of the roller as depicted in Fig. 29b. These ball bearings are rated for 5,000lbs each to match the two leveling jacks. Due to this and the overdesign of the central body and roller, each roller stand is appropriately rated for 10,000lbs of vertical force. In order to best accommodate the 20-in outer diameter of the pipe that it supports, the rollers were custom designed for this diameter. The Roller was manufactured by the LSWT machine shop.

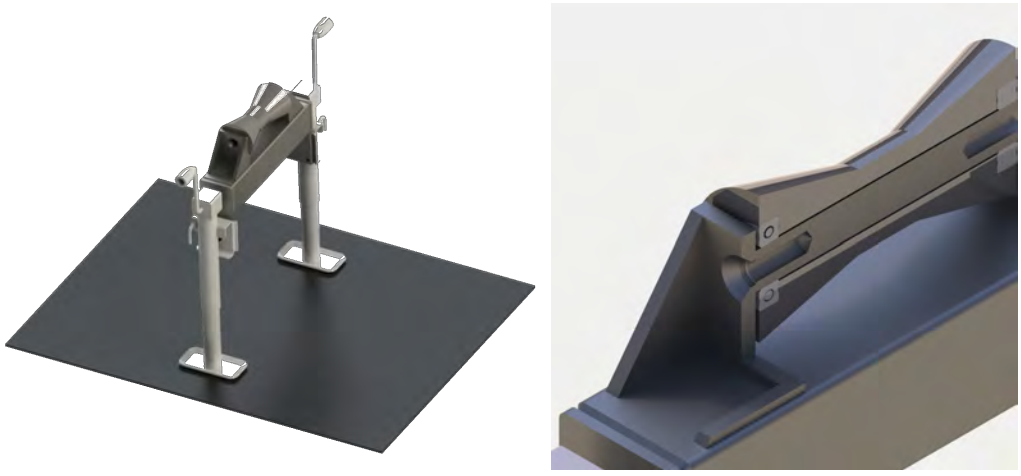

(a) **(b)**

FIG. 29 Roller stand as it is welded to its own plate, independent of the primary or secondary stands.

3.6 TUNNEL FLOW CONTROL AND INSTRUMENTATION

An overall flow diagram of the general locations of the components involved during the operation and monitoring of the facility is given in Fig. 30. The high-pressure air (thin light blue line) is supplied from the compressors and run through a ½-in pipe into the NAL. This line is then split and regulated into two pressures: one line is controlled by the high pressure digital regulator (PRA) that goes to the driver, and the other lines goes to a manual regulator that reduces the pressure to the maximum input for the low pressure digital regulator (QPV1) for the driven. A separate vacuum line for each of the driver and driven sections are installed in order to allow independent control. For shock tunnel mode, the XT-driver and XT-driven combine to become the ST-driver, a three-way ball valve can be used to switch filling from the driven to the accel-

erator, which becomes the ST-driven along with the back assembly. The 3-way ball valve also is designed to accept a custom-built position sensor with two switches: one which closes a circuit when in ST mode and the other which closes when in XT mode. All fill lines run through a minimum size tubing of 3/8-in with a wall thickness of 0.028-in rated to 2,300-psia (McMaster-Carr, n.d.). Along the length of the facility, depending on what obstacles arise, these tubes may alternate to pipe or hose rated for similar pressures. For quick venting, the emergency relief line for the driver flows through a 1-in stainless steel schedule 80 pipe rated for 2,601psi between -20F and 650F (Atlas Specialty Metals). For all locations, except the emergency relief and driver fill valves, a Dynaquip Controls 3/8-in NPT spring return-fail close pneumatic ball valve are used. These valves are rated for 1,000-psi and utilize a pneumatic supply pressure between 80-110psi controlled by a solenoid powered by 120VAC (Grainger, n.d.). Two digital regulators are used: one with a lower, more accurate pressure range, and another with a higher, error-prone pressure range. Both digital regulators are bought from Equilibar and are operated by sending a 0-10V signal to the regulator which scales linearly with its total pressure range. Each regulator also includes a pressure monitor which can feed back directly to the controls computer.

For the driven segments of the facility, a lower pressure digital regulator is used to provide a higher accuracy when filling the test gas. An Equilibar QPV1 High Resolution Pressure Control Valve with a custom upper pressure range of 105-psia is powered by a supply voltage ranging from 15-24VDC and has an accuracy of less than ±0.2% full scale (0.21psi) and resolution up to ±0.005% (0.005psi) (Equilibar, 2016). Due to the maximum pressure of the driver being 2,000-psia, a different digital regulator had to be chosen. The PRA-45-2500-E works similar to the QPV1 since the PRA utilizes a QB2 pneumatic pilot regulator, which then controls the outlet pressure with a 45:1 ratio diaphragm. With a maximum pressure of 2,500-psi and a similar command signal of 0-10V, the overall accuracy of the PRA is 2.5% of full scale (62.5psi).

Safety relief valves are located throughout HXT, with a summary listed in Table 5. An emergency vent line is installed that plumbs directly into the driver volume and connected to an emergency switch in the control room. This switch, when activated, opens a 1-in NPT ball valve that vents high pressures in the driver through a pipe that runs through the roof.

The pressure transducers used for monitoring the fill/vent lines and shock time of arrival are discussed. All pressure transducers are amplified to either a 0-5V or 0-10V scale for signal measurement. Type K thermocouples are also included. The data are acquired with a multi-use

Data Acquisition (cDAQ 9184) (National Instruments, 2014) from National Instruments uses pic-and-choose task modules that conform to the instrumentation needs of the facility.

TABLE 5 Pressure ratings of pipe and tube lines with the pressure relief settings.

Section	Line Pressure Rating (psi)	Relief Valve Setting (psi)
Driver Fill Line	2,300	
Driven Fill Line	2,300	
Vacuum Line	350	50
Supply Line (2500psi)	2,600	N/A
Shop Air Line (130psi)	2,500	N/A

All instruments and relay controls are housed in a single electronics unit called the Control and Instrumentation Hardware Interface (CIHI). The cDAQ system, power supplies, and common wiring for the safety system are all run through this unit. The front and back panels of the box are shown and labeled in Fig. 31. Due to variable needs in power, CIHI runs on 120 VAC, 24VDC, and 12 VDC. Two rows of Type K thermocouple connectors are wired directly into the thermocouple module of the cDAQ. Two analog outputs are provided through use of standard BNC connectors on the front panel. Connecting through the back panel, solenoid interfaces run through and are controlled through the use of solid state relays. Figure 32 displays a circuit diagram of how the solid-state relays control each of the ball valves and the resulting current rating increase by using a second solid state relay not part of the cDAQ module. Warning notifications are designed to be controlled through the CIHI to make the system more integrated when operating. There are two different warning systems: one for facility status during fill/vacuum and the other for hydraulic operation. Facility status employs the use of two warning light colors and a siren. Yellow flashing begins at the onset of operation and indicates the vacuuming down of all sections. Red flashing indicates pressurization of the facility.

Two computers are used to control HXT. One is the tunnel control computer and the other is a high-speed sampling rate data acquisition computer (HSDaq). Both computers share information with each other as laid out in Fig. 33. Before operation, the communication between the computers is terminated, allowing the HSDaq computer to fulling focus on data sampling. Operation of HXT begins with the input of two of three variables: Reynolds number, Mach number, or the driver/driven pressure ratio. These are input into the HSDaq computer, computed for initial pressures for each of the tube sections, and forwarded to the controls LABVIEW virtual instrument (VI). Based on the initial parameters it receives, the controls computer calculates the

required voltage signals needed to be generated through the analog out ports and sent to the digital regulators. Once the controls computer receives this information, the communication pathway collapses and each computer runs individually.

The HSDaq records the time-of-arrival sensors and high-speed pitot probes. The HSDaq system also calculates the 1-dimensional fluid mechanical modelling code that converts desired inputs of Reynolds number, altitude, Mach number, …, using the driver, driven, and accelerator gases into set pressures for the controls computer. Since a minimum of two people are required to operate the facility, one for each computer system, this also reduces the responsibility of the controls operator and allows redundancy for insuring the settings are correct. The VI interfaces are shown in Figs. 34.

4. RESULTS AND FUTURE WORK

The central result for this project was the development of new a relatively large-scale hypervelocity expansion tunnel as described in the previous section. This facility was incorporated into the TAMU NAL to take advantage of the available suite advanced high-energy pulsed laser flow field diagnostics and fast response surface sensors. The planned operating map is shown in Fig. 1. The approach toward developing the expansion tunnel was broken down into four basic tasks. The timeline is summarized in Table 8. In Task 1, we finalized the facility design. In Task 2, we manufactured the facility. Task 3 involved integration of the facility into the NAL infrastructure. The "as-built" sketch of the facility is given in Fig. 35. Modifications and characterization studies are underway. Finally, shake down testing and calibration studies are just underway, where the first diaphragm rupture test within the facility took place in December of 2016.

The future work includes (1) introduction of a double diaphragm breech, (2) inclusions of shock absorbers to reduce loads and vibrations, (3) improved support structure, and (4) characterization of the flow structure.

5. IMPACT/IMPLICATIONS

In terms of impact, this project provides a new capability that targets important high enthalpy aerothermodynamic viscous flow problems of interest to the Navy and DoD. This capability builds on the extensive backgrounds of the PIs in facility development, diagnostic development, fundamental hypersonic flow study, and work force development. We believe this facility will be unique to the University setting and complement existing large-scale facilities such as those at

GASL and CUBRC. In terms of workforce development, the NAL supports graduate, postdoc and undergraduate students annually through participation from faculty in aerospace engineering, chemistry, mechanical engineering and physics.

6. TRANSITIONS AND RELATED PROJECT

None

7. PUBLICATIONS AND PATENTS

None

8. HONORS/AWARDS

None

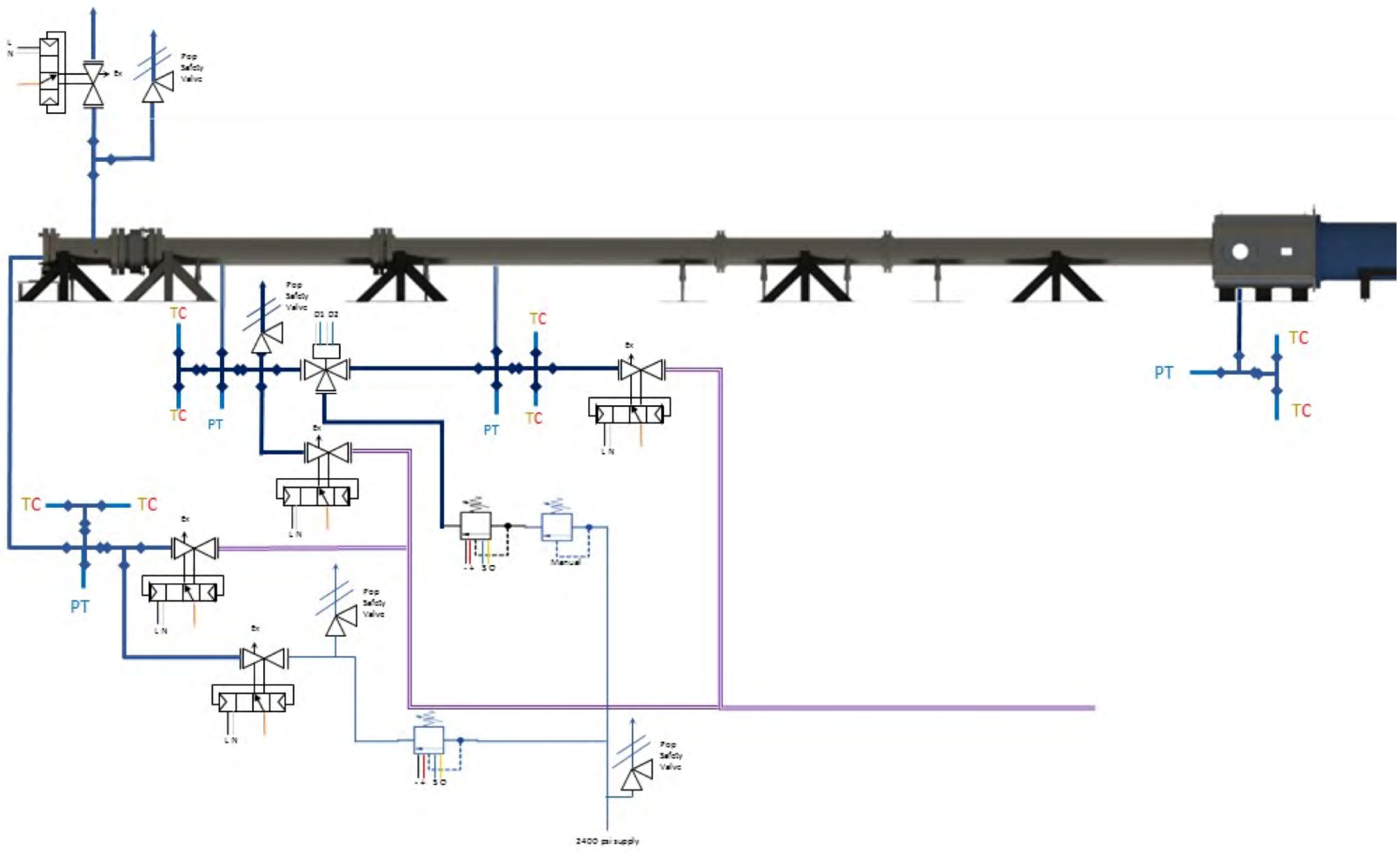

FIG. 30 Flow diagram for HXT with pressure (blue lines), vacuum (purple lines), ball valve placement, digital regulators, and pressure relief valves.

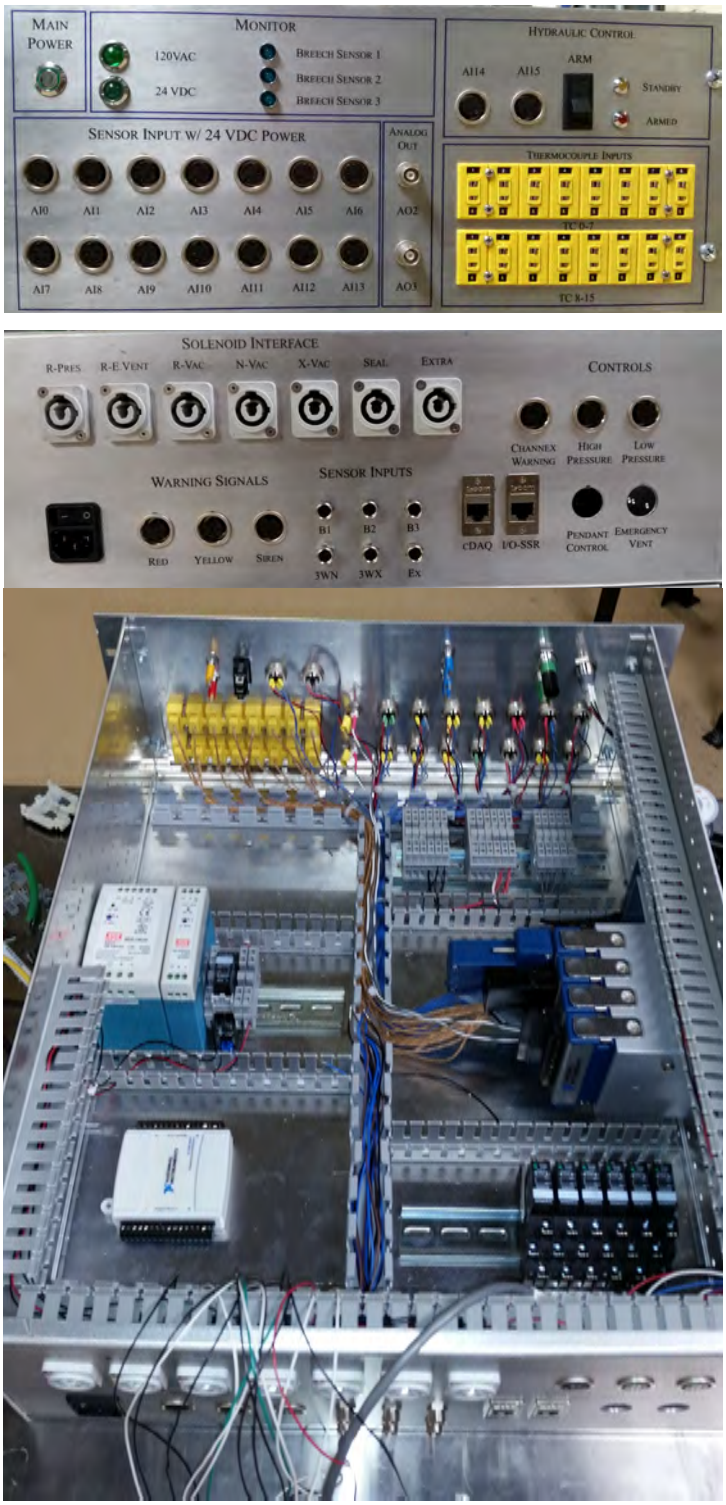

FIG. 31 Tunnel control circuit. (TOP) Front panel. (Middle) back panel of the control and instrumentation hardware interface electronics housing. (Bottom) Internal circuitry.

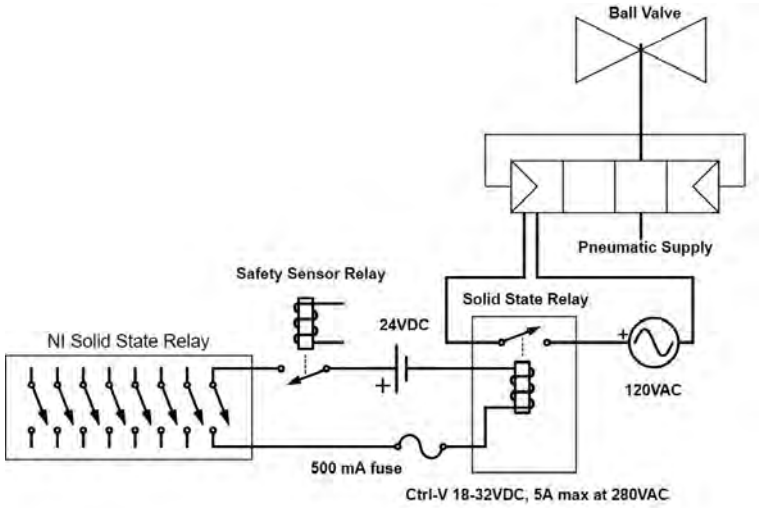

FIG. 32 Schematic representing the current rating amplification when using the ni solid state relays and standard relays in series.

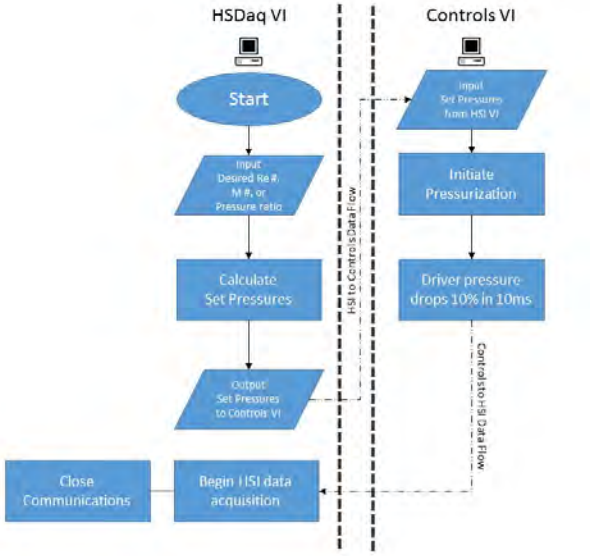

FIG. 33 Data flow diagram of information passed between the Controls and HSDaq VI programs.

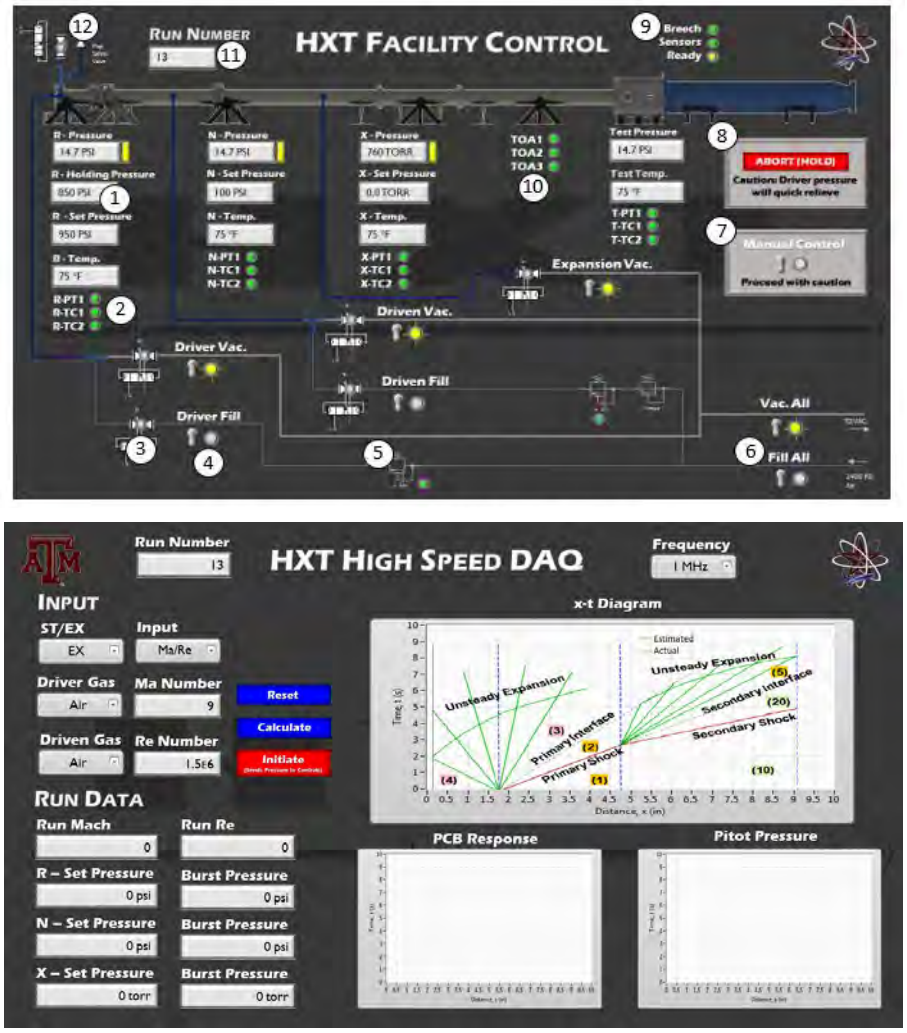

FIG. 34 Controls and HSDaq computer VI monitor interface.

Table 6 Milestones and Timeline

Milestone ↓ Time (months) →	1	3	6	9	12	15	18
Task 1: Finalize HXT Design							
Task 2: Construct/Analyze HXT Facility							
Task 3: Integrate HXT into the NAL							
Task 4: HXT Characterization							

DRIVER
DRIVEN
EXP-ANSION
EXP-ANSION TUNNEL MODE
DIESEL SECTION
DUMP TANK AND AIR RECEIVER

(a)

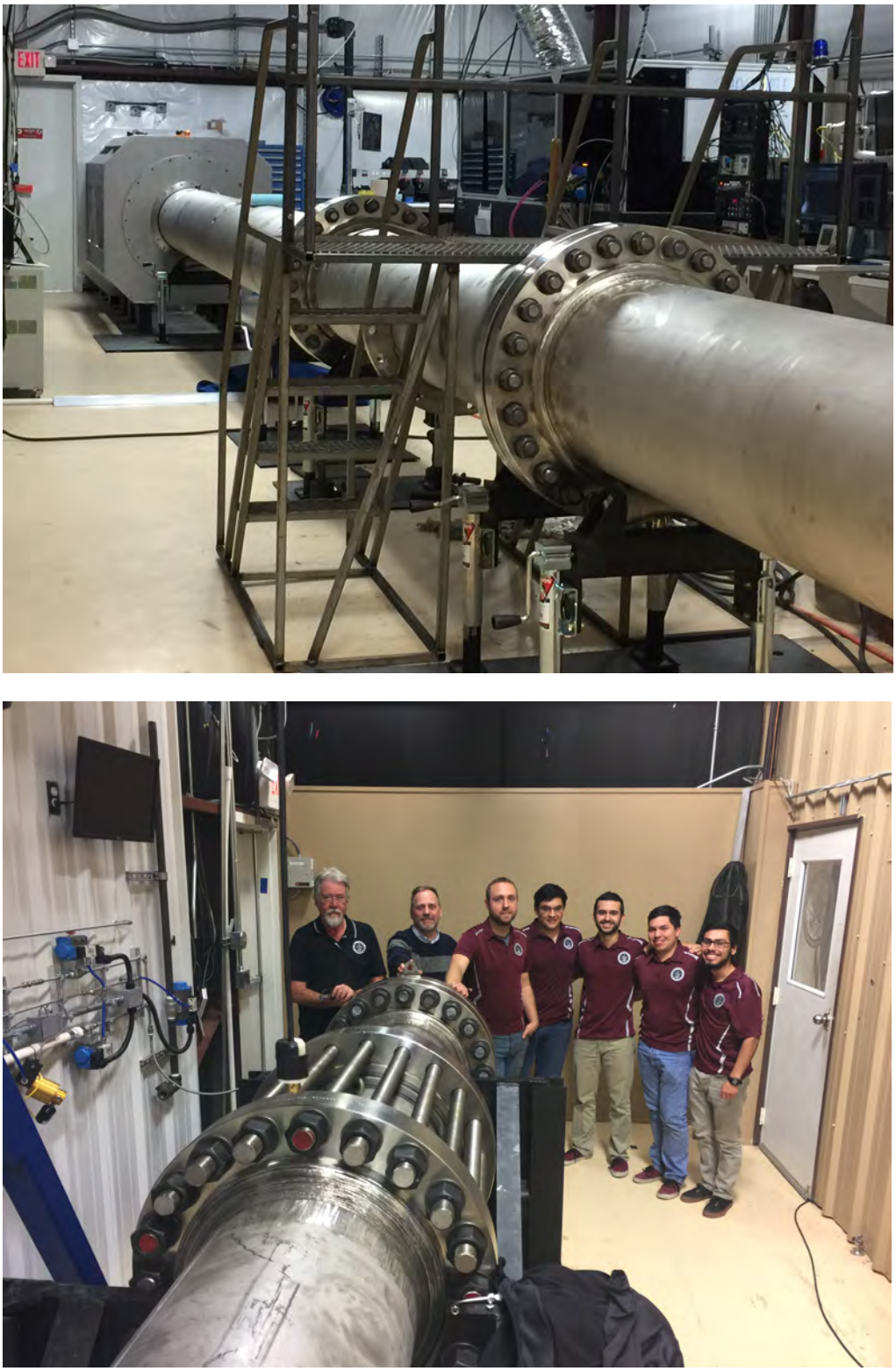

(b)

FIG. 35 HXT facility as built during this project. (a) CAD Drawings in XT mode (upper). (b) Photographs of test section, with laser diagnostics (upper), and the driver section, with some members of the research team (lower, left-to-right: C. Rhodes, R. Bowersox, E. Marcotte, S. Canchola, A. Pages, G. Aguilar, C. Sanchez. Not shown are E. White and S. North).

9. REFERENCES

Albrechcinski, T., Boyer, D., Chadwick, K., and Lordi, J., "Calspan's upgraded 96-in hypersonic shock tunnel: Its development and application in performance of research and testing at higher enthalpies," AIAA Paper 95-0236, 1995.

Ben-Yakar, A. and Hanson, R. K., "Characterization of Expansion Tube Flows for Hypervelocity Combustion Studies," Journal of Propulsion and Power, Vol. 18, No. 4, 1992, pp. 943–952.

Dufrene, A., Sharma, M. and Austin, J., "Design and Characterization of a Hypervelocity Expansion Tube Facility," AIAA-2007-1327, 2007.

Dufrene, A., MacLean, M., Parker, R., Wadhams, T., and Holden, M., "Characterization of the New LENS Expansion Tunnel Facility, AIAA-2010-1564, 2010.

Erdos, J., Bakos, R., Castrogiovanni, A., and Rogers, R., "Dual mode Shock Expansion / Reflected Shock Tunnel," AIAA 1997-0560, 1997.

Graf, G., *Personal Communication*, 2014.

Holden, M., "The LENS Facilities and Experimental Studies to Evaluate the Modeling of Boundary Layer Transition, Shock/Boundary Layer Interaction, Real Gas, Radiation and Plasma Phenomena in Contemporary CFD Codes," RTO-EN-AVT-186, 2010.

Holden, M., MacLean, M., Wadhams, T. and Dufrene, A., "Measurements of Real Gas Effects on Regions of Laminar Shock Wave/Boundary Layer Interaction in Hypervelocity Flows for "Blind' Code Validation Studies," AIAA-2013-2837, 2013.

Hornung, H., "Experimental hypervelocity flow simulation, needs, achievements and limitations. Invited presentation," PICAST 1, Tainan, Taiwan, Dec. 1993.

Hornung, H., "Performance data of the new free-piston shock tunnel at GALCIT," AIAA 1992-3943, 1992.

Hsu, A., Srinivasan, R., Bowersox, R., North, S., ***AIAA J.***, Vol. 47, No. 11, 2009, pp. 2597-2604.

Li, F., Choudhari, M., Change, C-L., White, J., Kimmel. R., Adamczak, D., Borg, M., Stanfield, S., and Smith, M., AIAA Paper 2012-2961, 2012.

Miller, C., "Shock shapes on blunt bodies in hypersonic-hypervelocity helium, air, and CO2 flows, and calibration results in Langley 6-in expansion tube," NASA TN D-7800, 1975.

Mirles, H., Shock Tube Test Time Limitation Due to Turbulent-Wall Boundary Layer," *AIAAJ.*, Vol. 2, No. 1, 1964, pp. 84-93.

Neely, A. J. and Morgan, R. G., "The Superorbital Expansion Tube concept, experiment and analysis," *Aeronautical Journal*, Vol. 973, 1994, pp. 97–105.

Paull, A. and Stalker, R., "Test Flo Disturbances in an Expansion Tube," *JFM*, Vol. 245, 1992, pp. 493-521.

Sánchez-González, R., Srinivasan, R., Bowersox, R., North, S., ***Optical Letters***, Vol. 36, No. 2, 2011.

Sánchez-González, R. Bowersox, R., North, SW., ***Optical Letters,*** Vol. 39, No. 9, 2014, pp. 2771-2774.

Shinn, J. L. and Miller, C. G., "Experimental Perfect Gas Study of Expansion-Tube Flow Characteristics," NASA TP 1317, 1978.

Scott, M., *Development and Modeling of Expansion Tubes*, PhD Dissertation, School of Engineering, University of Queensland, June 2006.

Trimpi, R. L., "A preliminary theoretical study of the expansion tube, a new device for producing high enthalpy short-duration hypersonic gas flows," NASA TR R-133, 1962.

Trimpi, R., "A theoretical investigation of simulation in expansion tubes and tunnels," NASA TR R-243, 1966.

APPENDIX A - REQUIREMENTS DOCUMENTS

This section lists each requirements document in order of manuscript presentation. The requirements are a series of design points needing to be achieved in order for proper and safe operation. These requirements are listed as primary and contain the word 'shall' in bold letters for each point. Derived requirements are additional conditions imposed by the specific nature of the design route taken and the location at the NAL. The following documents will be presented in this Appendix:

- Driver, Driven, Accelerator
- Diaphragm System
- Test Section
- Stands
- Hydraulic System
- Instrumentation and Electronics

Driver, Driven, and Accelerator Pipe Design Requirements

Primary Engineering and Safety Requirements

- Pipe shall be able to achieve the operating conditions equal to or greater than those presented in the ONR proposal
    - 2000 psi max pressure in driver
    - 100 psi max pressure in driven
    - 10^5-10^7/m in Reynolds number range
    - Mach 5-15 with nozzle addition
- Pipe shall allow the installation of a nozzle at a later time as part of the accelerator section
- Pipe shall be reconfigurable as to operate in a shock tunnel mode
- Pipe, flanges, and fittings shall safely maintain pressures and temperatures as set out in the ONR proposal and abide by ASME codes
- Pipe shall have ports capable of filling and vacuuming each section independently
- Pipe shall fit in space allocated at the NAL as to not require extensive construction of additional lab space
- Pipe costs shall lie within the allotted budget set out, potentially increasing pipe size and core flow diameter

Derived Requirements

- Pipe should have multiple ports located along the accelerator for mounting time-of-arrival sensors
- Pipe should expand on the core flow parameters set out in the ONR proposal and investigate improving/expanding upon the predicted operating envelope of the facility

- Accelerator pipe should be dividing into 20/10/20ft segments to allow the replacement of the third segment with the future nozzle
- Pipe should be located along the length of the support structures in a configuration that allows 4 of the 5 stands to be used while in shock tunnel mode
- Pipe should be welded and approved by board certified inspectors according to ASME Section VIII, Division 1

Diaphragm System Design Requirements

Primary Engineering and Safety Requirements

- System shall allow easy access to diaphragms
- System shall align diaphragms in a specific orientation in regard to the bursting pin
- System shall interface appropriately with the driver, driven, and accelerator sections
- System shall be able to withstand operating temperatures and pressures
- System shall be able to transmit any recoil force from the driver to the driven and not yield
- System shall be removable from the facility in case of malfunction, maintenance, or further testing
- System shall seal at all operating pressures and temperatures
- System shall have a backup configuration that works without any use of any part of the diaphragm system except the diaphragm holder

Derived Requirements

- System should allow access to diaphragms by moving the driver back away from the breech
- System should align the diaphragm using dowel pins located in the diaphragm holder and alignment grooves with the backup configuration
- System should interface with the 900-lb flanges that are already welded on the driver and driven sections of the facility
- System should be manufactured with equally rated flanges and wall thicknesses as are used in the design for the rest of the driver, driven, and accelerators
- System should be able to handle at least 3 times the recoil force designated at 404,540 lbf, but preferably 4 times
- System should be removable at the 900-lb interfaces, meaning it shall too have 900-lb flange interfaces
- System should utilize o-rings in order to seal at the necessary interfaces, especially in regard to the diaphragm holder
- System should use spacers as a backup configuration using leftover sections of pipe cut from the 20ft schedule 160 stainless piece
- System should use two separate systems for the driver/driven and driven/accelerator diaphragms since the pressures seen by these two diaphragms vary drastically

- System should use a breech mechanism to seal the high-pressure driver/driven diaphragm since these are known to be able to the expected forces as noted in 2 different papers [4,5]
- System should utilize a slip-disk system for the lower pressure mylar diaphragm to reduce cost and manufacturing time

Test Section Design Requirements

Engineering Requirements

- The Test Section shall hold models capable of being placed wholly in the flow both with and without a nozzle
    - 19-in diameter without a nozzle
    - 36-in diameter with a nozzle
- The Test Section shall have the access to remove and/or replace test models
- The Test Section shall have convenient run-to-run access of the models
- The Test Section shall have model and optics mounting capabilities
- The Test Section shall have laser diagnostic access through multiple lines of sight (LOS)
- The Test Section shall maintain operating pressures without loss to structural integrity of the facility
    - Pressure after 2000 psi R expansion fire: 36.5psia
    - Pressure after 1000psi R/N shock tunnel fire: 72.75psia
- The Test Section shall resist pressures on all access points into the facility
- The Test Section shall include a shock delay line for maximum operating runtime
    - Calculated at approximately 17ft
- The Test Section shall not be larger or longer than the space available at the NAL
- The Test Section shall be simple and cost-effective to manufacture
- The Test Section shall seal completely with the use of o-rings at each access point and on the front face with the 20-in pipe and in the back with the tailpipe

Derived Requirements

- The Test Section should be roughly 4’ in diameter (or slants) or larger to accommodate models and prevent blockage
- The Test Section should have door(s) on each side for multiple access points to the models
- The Test Section should split the door access on each side into two doors to reduce the loads on each individual door, reducing the number of fasteners needing to be removed
- The Test Section should have an upper access panel to allow larger models to be inserted into the facility
- The Test Section should have a lower access panel to allow for window access points to be machined if need be
- The Test Section should be at least 5 ft long to allow plenty of room both in front of and behind the model for sensor equipment and optical mirrors

- The Test Section should be made into an octagonal prism in order to reduce the loads on the walls when the test section acts as a pressure vessel
- The Test Section should minimize the surface area of the additional four walls and make them access points in case window access needs to be machined into those locations
- The access panels and doors should have approximately twice as many fasteners as theoretically needed and the exact number needed to maintain proper squeeze on the o-rings
- The Test Section and Tailpipe should not exceed a length of 28ft and width of 7ft to accommodate the space available at the NAL
- The Tailpipe should be approximately 20ft in length to conform to standard pipe lengths available for purchase in industry
- The Tailpipe should have a diameter of roughly 40-in to accommodate residual expansion of the flow field through the test section at maximum flow area

Support Stands Design Requirements

Engineering Requirements

- Structural support system shall be able to handle 408k lbf of instantaneous load
- Structural support system shall be able to support facility weight
- Structural support system shall provide a nominal facility height
- Structural support system shall be easy to operate and maintain
- Each structural support shall be aligned to specification
    - Horizontal alignment offset shall not exceed ± 1 deg.
    - Center line of pipe between supports shall not exceed 0.25 in.
- Each structural support shall be able to interface with existing location layout

Derived Requirements

- Each structure should have a safety factor of 4x design load
- Failure criterion should be defined as the yield stress
- Primary and Secondary stands should have available space allocated for vertical load supports
- Material should be weldable and machineable.
    - Material should be ATSM-A36-Steel
- All structural supports should interface with 20 in. OD pipe
- Primary supports should interface with 20 in. – 900 flanges
- Secondary supports should interface with 20 in. – 150 flanges
- Supports should provide a centered and level mounting interface
    - Steel plate base
- Supports should provide a nominal pipe centerline of 36 in from the base plate
- Roller supports should facilitate installation
    - Crank jacks
- Roller supports should be rated for two time the weight of the facility

- Roller supports should minimize friction in the horizontal direction
- Supports should minimize stress concentrations throughout the structure

Instrumentation and Electronics Design Requirements

Engineering Requirements

- The Controls **shall** monitor real-time temperature in 4 locations:
    - 1 in the Driver
    - 1 in the Driven
    - 1 in the Expansion
    - 1 in the Hydraulics (return line)
- The Controls shall monitor real-time pressure in 4 locations:
    - 1 in the Driver
    - 1 in the Driven
    - 1 in the Expansion
    - 1 in the Hydraulics (fill line)
- The temperature range of the tunnel shall be between 70°F – 400°F
- The temperature range of the hydraulic system shall be between 70°F – 180°F
- The Controls shall remotely set the pressures to the Driver, Driven, and Expansion:
    - Driver: 0 – 2100 psia
    - Driven: 0 – 150 psia
    - Expansion: 0 – 760 torr
- The Controls shall remotely open and close the Driver and Driven fill lines
- The Controls shall monitor the open and close status of the breach
- The Controls shall require the breach to report "closed-in status before allowing pressurization
- The Controls shall incorporate a remotely controlled emergency vent line for the Driver section
- The system shall include an operational manual, circuitry diagrams, and operational algorithms

Derived Requirements

Pressure

- The Driver, Driven, and Expansion pressures should be controlled via digital pressure regulators with the following requirements:
    - Driver pressure range: 20 – 2,500 psia
    - Driven pressure range: 0 – 200 psia
    - Expansion pressure range: 0 – 760 torr
- There should be a protective *manual* pressure regulator before the Driven *digital* pressure regulator (see diagram)
- An additional pressure transducer should be placed in the Nozzle Exit or Test Section to fully define the state of the HXT facility

- The pressure transducers should
    - Range between zero to twice the hydraulic pressure
    - Be protected or rated against pressure spikes
    - Be shielded against EMF and routed to avoid high EMF areas
    - Be sealed against dust and fluids
- Pressure input should be an analog to digital converter (ADC) input with the following requirements:
    - At least 12-bit resolution
    - Enough channels for pressure regulators *and* pressure transducers

Temperature

- The temperatures should be monitored via K-type thermocouples
- There should be an additional thermocouple in the Nozzle Exit or Test Section to fully define the state of the HXT facility
- There should be one redundant thermocouple for every thermocouple
- The thermocouple input should be a dedicated thermocouple module with the following requirements:
    - At least 12-bit resolution
    - Enough channels for thermocouples and redundant thermocouples

Remote Controls and Relays

- The breach open/close monitoring should:
    - Utilize magnetic proximity sensors
    - Have at least 2 redundant proximity sensors (3 total)
- All pressure lines should be open or closed with ball valves
- Remotely actuated ball valves should be used wherever possible (especially if manual actuation compromises safety)
- Solid state relays should be used to control and monitor the ball valves and proximity sensors, respectively, with the following requirements
    - Enough channels for Driver fill and vacuum, Driven fill and vacuum, Expansion vacuum, Driven vent, and proximity sensors
    - Enough current output to actuate any ball valves
    - Compatible switching voltage for circuit requirements
- The pressure inputs (regulators and transducers) should be consolidated on a single module with at least 12 bit resolution and enough channels
- The pressure regulation output **should** be controlled via a digital-to-analog converter (DAC) module with enough channels for the two digital pressure regulators (see diagram)

Computers

- The Controls **should** utilize computers currently owned by the NAL
- The following programs **should** be installed on the Controls computer:

    - NI LabVIEW
    - NI DAQmx
    - NI MAX
    - Microsoft Office Suite
- The Controls computer **should** have the following specifications:
    - Minimum 16 GB of RAM
    - Quad core CPU
    - Minimum 500 GB Hard Drive Disk, SATA 6.0 GB/s, 7200 RPM
    - Windows 7 or later
    - VGA or DisplayPort ports for compatibility with currently owned NAL monitors

APPENDIX B - TECHNICAL DRAWINGS

This section provides technical drawings for each of the components designed and manufactured for the facility.

- Driver, Driven, and Expansion Pipe Drawings
  - Engineering Drawings
    - Figure B-1: Driver(R) Sectional Drawing
    - Figure B-2: Driven(N) Sectional Drawing
    - Figure B-3: Accelerator 1(A1) Sectional Drawing
    - Figure B-4: Accelerator 1(A2) Sectional Drawing
    - Figure B-5: Accelerator 1(A3) Sectional Drawing
  - Welder-Approved Drawings
    - Figure B-6: Driver(R) Sectional Drawing 1
    - Figure B-7: Driver(R) Sectional Drawing 2
    - Figure B-8: Driven(N) Sectional Drawing 1
    - Figure B-9: Driven(N) Sectional Drawing 2
    - Figure B-10: Accelerator 1(A1) Sectional Drawing 1
    - Figure B-11: Accelerator 1(A1) Sectional Drawing 2
    - Figure B-12: Accelerator 1(A2) Sectional Drawing 1
    - Figure B-13: Accelerator 1(A2) Sectional Drawing 2
    - Figure B-14: Accelerator 1(A3) Sectional Drawing 1
    - Figure B-15: Accelerator 1(A3) Sectional Drawing 2
    - Figure B-16: Hole Alignment Drawing
    - Figure B-17: R/N/A Overall Drawing
  - Component Drawings
    - Figure B-18: 20-in 900-lb RTJ Blind
    - Figure B-19: 20-in 900-lbRTJ Slip-on Flange
    - Figure B-20: 20-in 300-lb RTJ Slip-on Flange
- Test Section Drawings
    - Figure B-21: Bottom Access (BA)
    - Figure B-22: Back Main (BM)
    - Figure B-23: Back Main (BM)-2
    - Figure B-24: Door Side (DS)
    - Figure B-25: Front Main (FM)
    - Figure B-26: Slant Side (SS)
    - Figure B-27: Top Access (TA)
- Primary Stand Drawings
    - Figure B-28: 2-in Cradle Plate-900-lb Mount
    - Figure B-29: Primary Baseplate
- Secondary Stand Drawings

Engineering Drawings

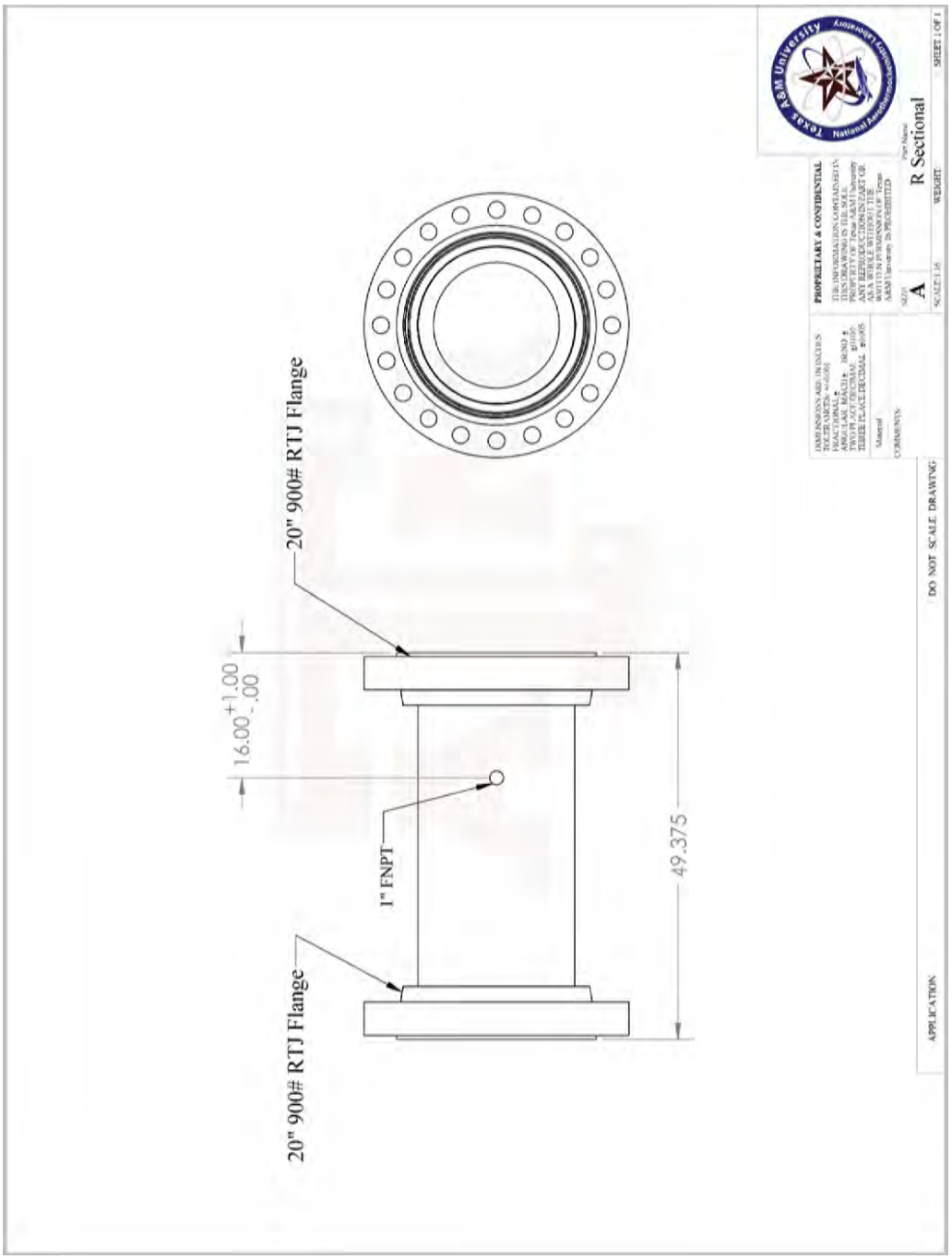

FIGURE B-1. DRIVER SECTION DRAWING SUBMITTED TO CIRCLE H MANUFACTURING FOR ASME CERTIFIED HIGH PRESSURE WELDING.

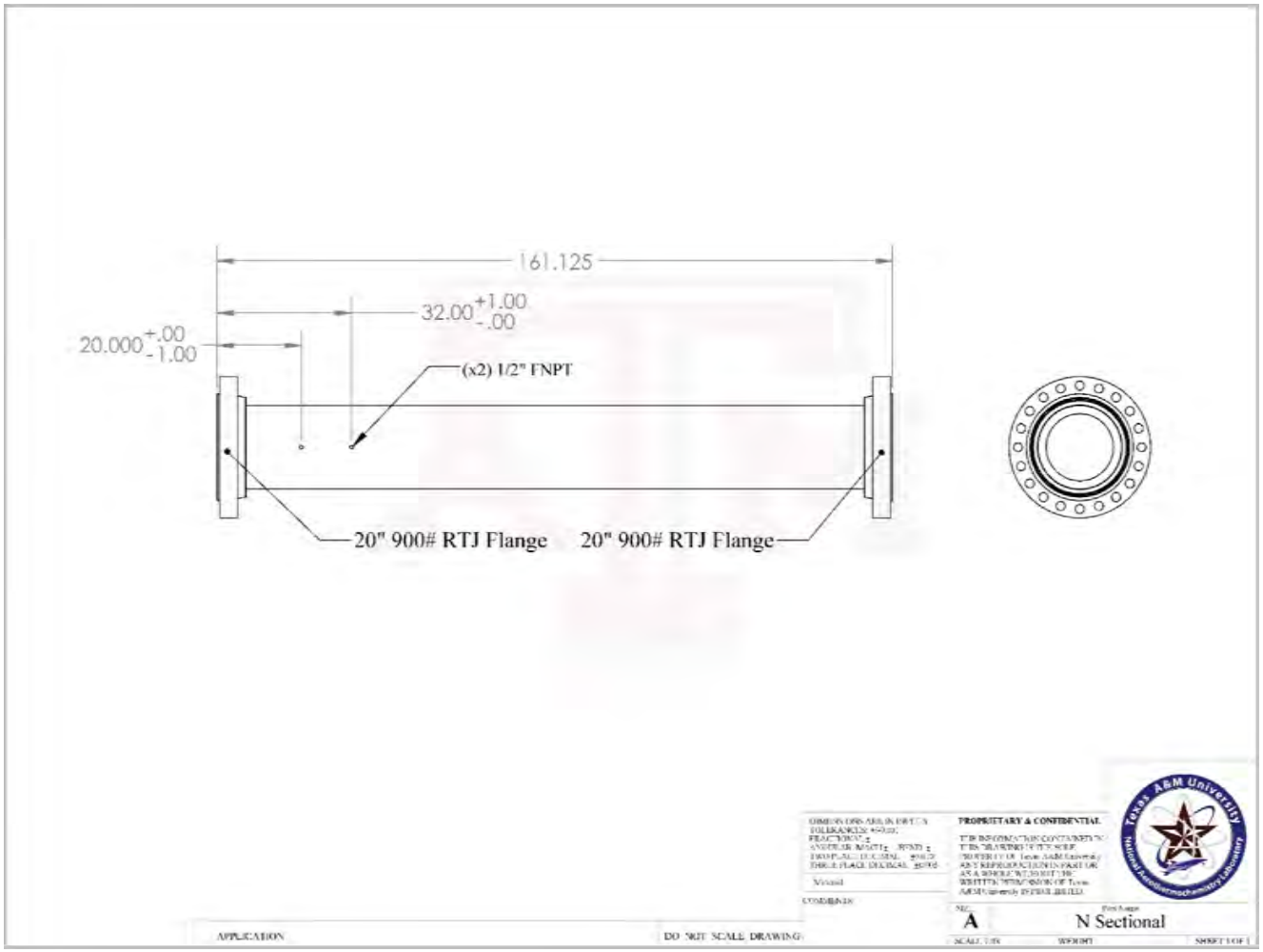

FIGURE B-2. DRIVEN SECTION DRAWING SUBMITTED TO CIRCLE H MANUFACTURING FOR ASME CERTIFIED HIGH PRESSURE WELDING.

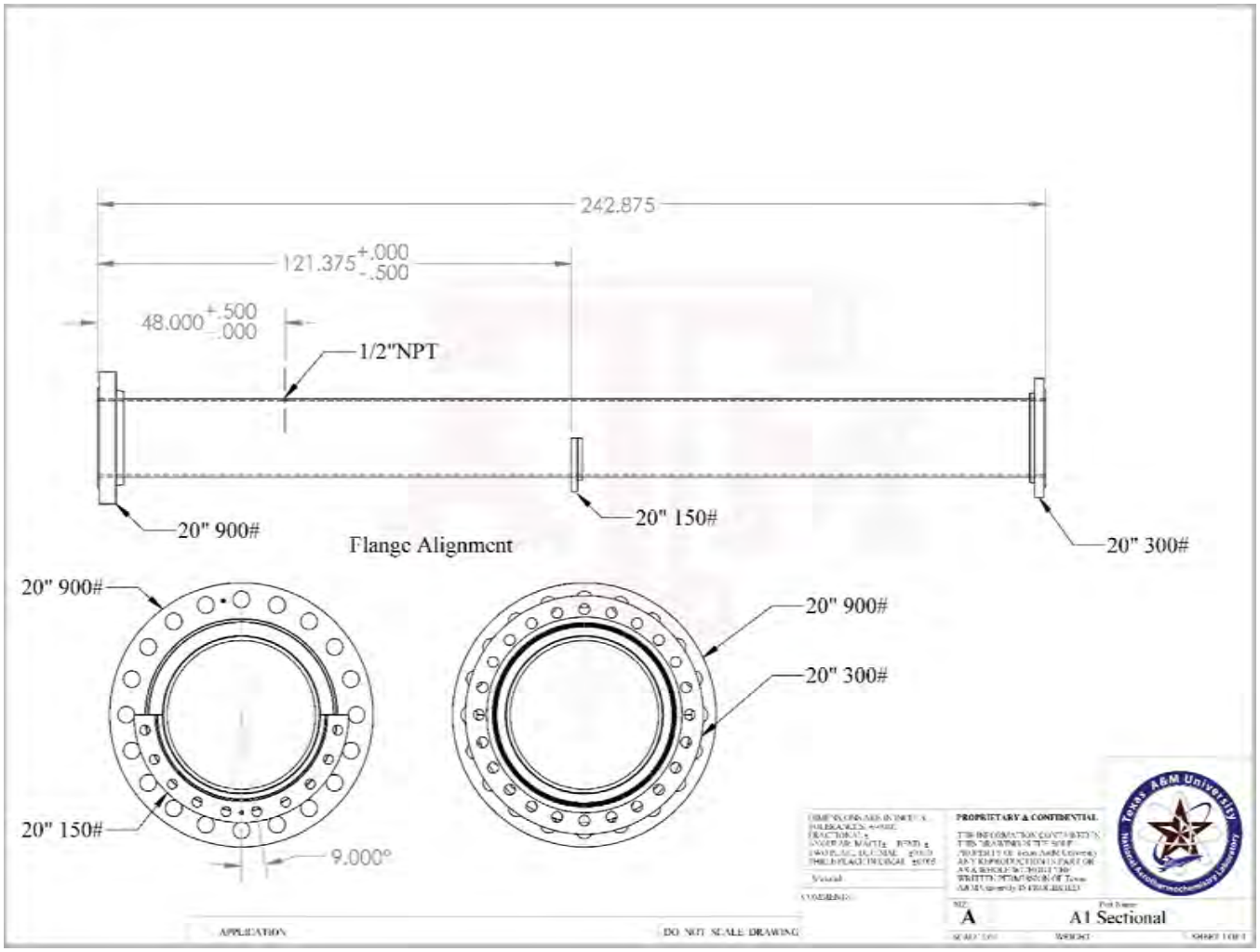

FIGURE B-3. FIRST ACCELERATOR SECTION DRAWING SUBMITTED TO CIRCLE H MANUFACTURING FOR ASME CERTIFIED HIGH PRESSURE WELDING.

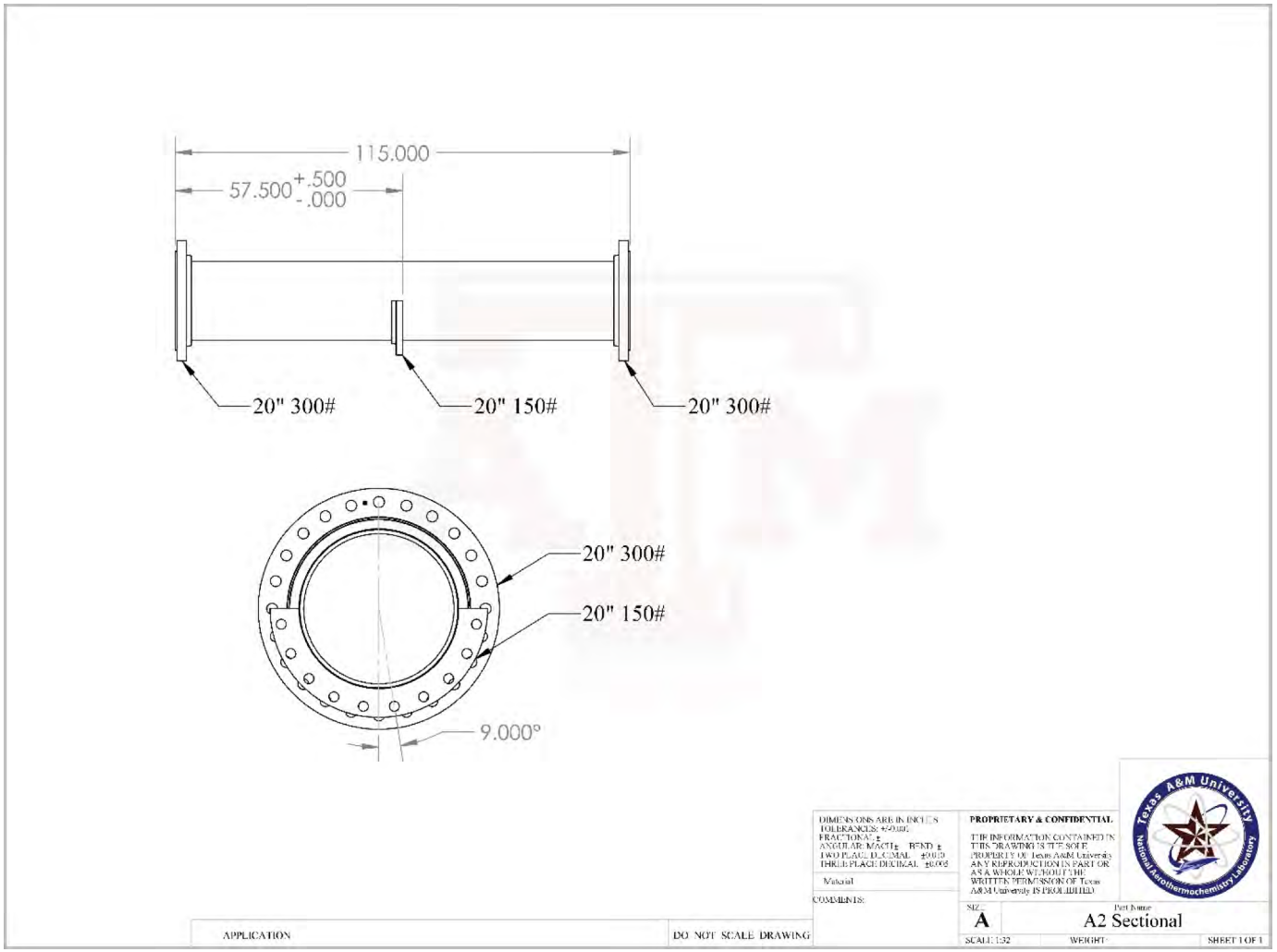

FIGURE B-4. SECOND ACCELERATOR SECTION DRAWING SUBMITTED TO CIRCLE H MANUFACTURING FOR ASME CERTIFIED HIGH PRESSURE WELDING.

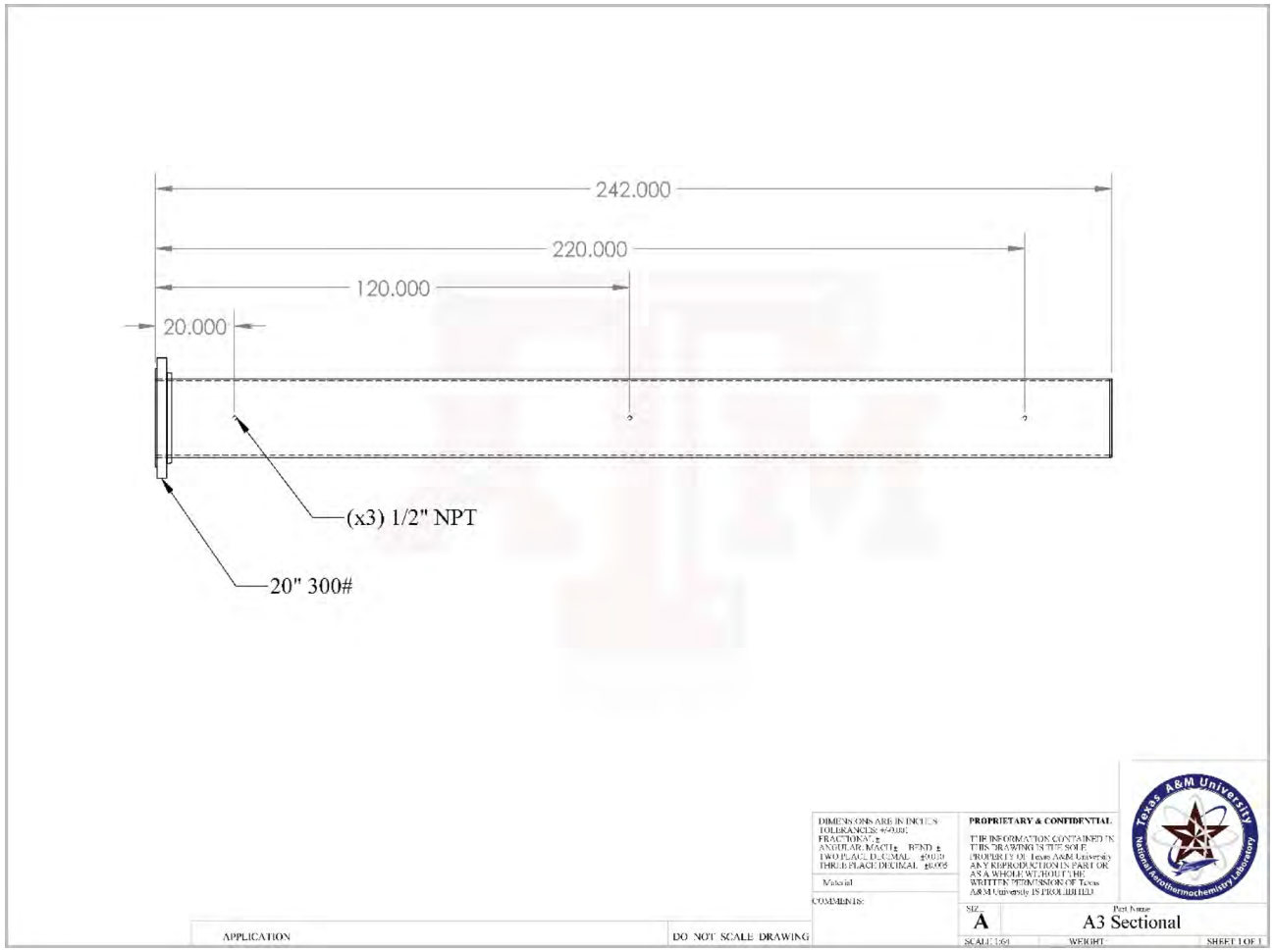

FIGURE B-5. THIRD ACCELERATOR SECTION DRAWING SUBMITTED TO CIRCLE H MANUFACTURING FOR ASME CERTIFIED HIGH PRESSURE WELDING.

Welder-Approved Drawings

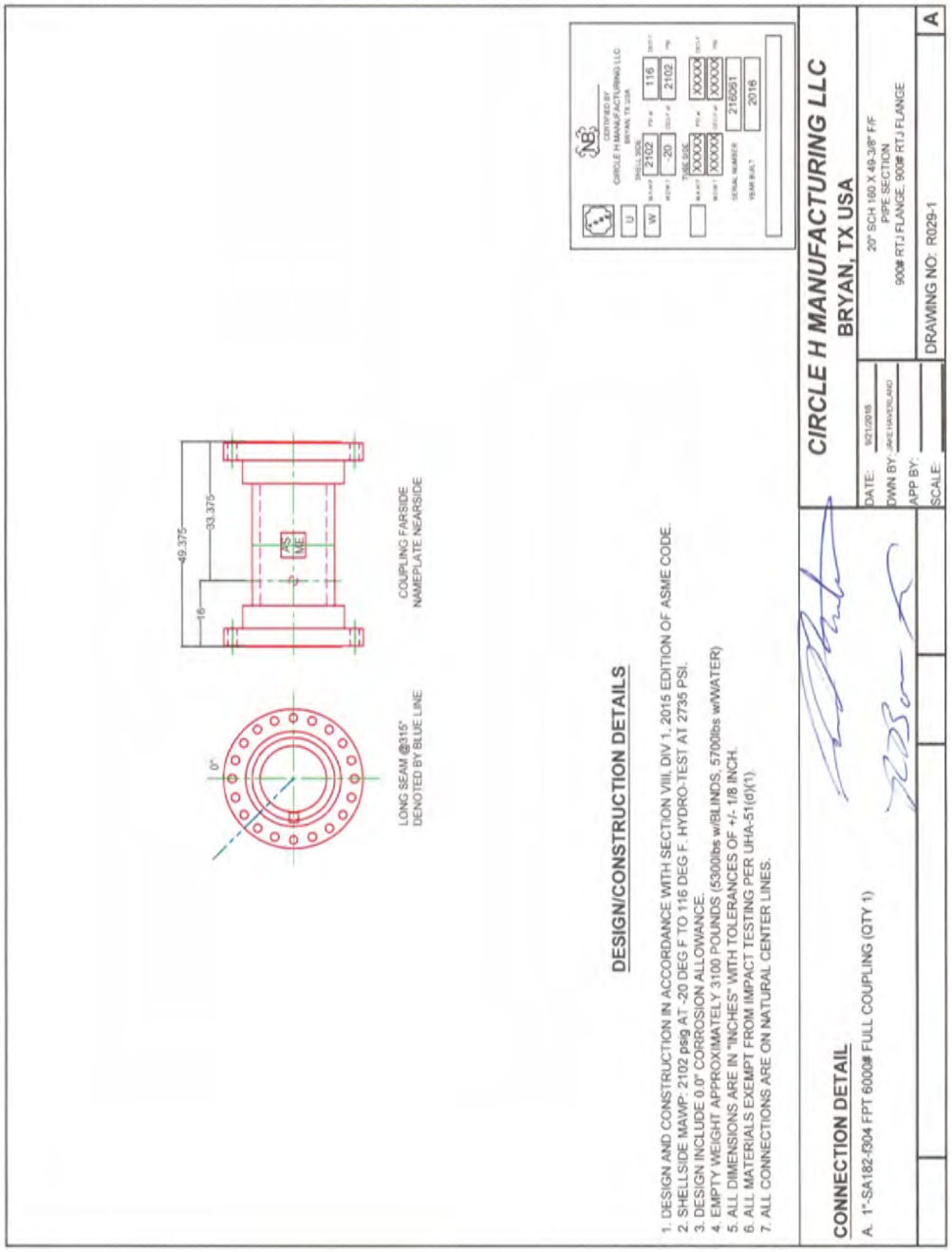

FIGURE B-6. CIRCLE H MANUFACTURING DRAWING OF THE DRIVER AS CERTIFIED WITH APPROVAL SIGNATUIRES FROM THE RESPONSIBLE ENGINEERS.

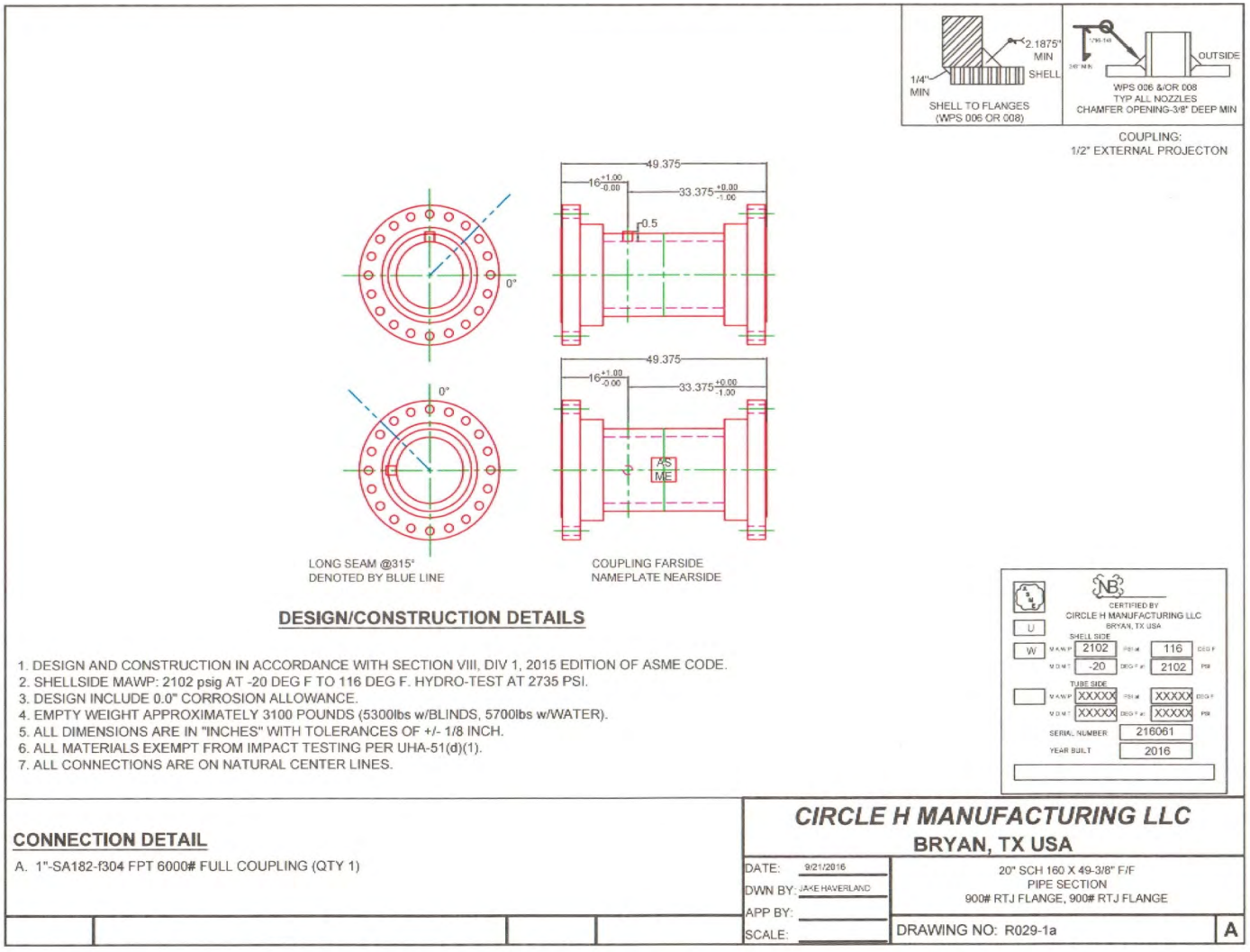

FIGURE B-7. CIRCLE H MANUFACTURING DRAWING OF THE DRIVER AS CERTIFIED AND APPROVED.

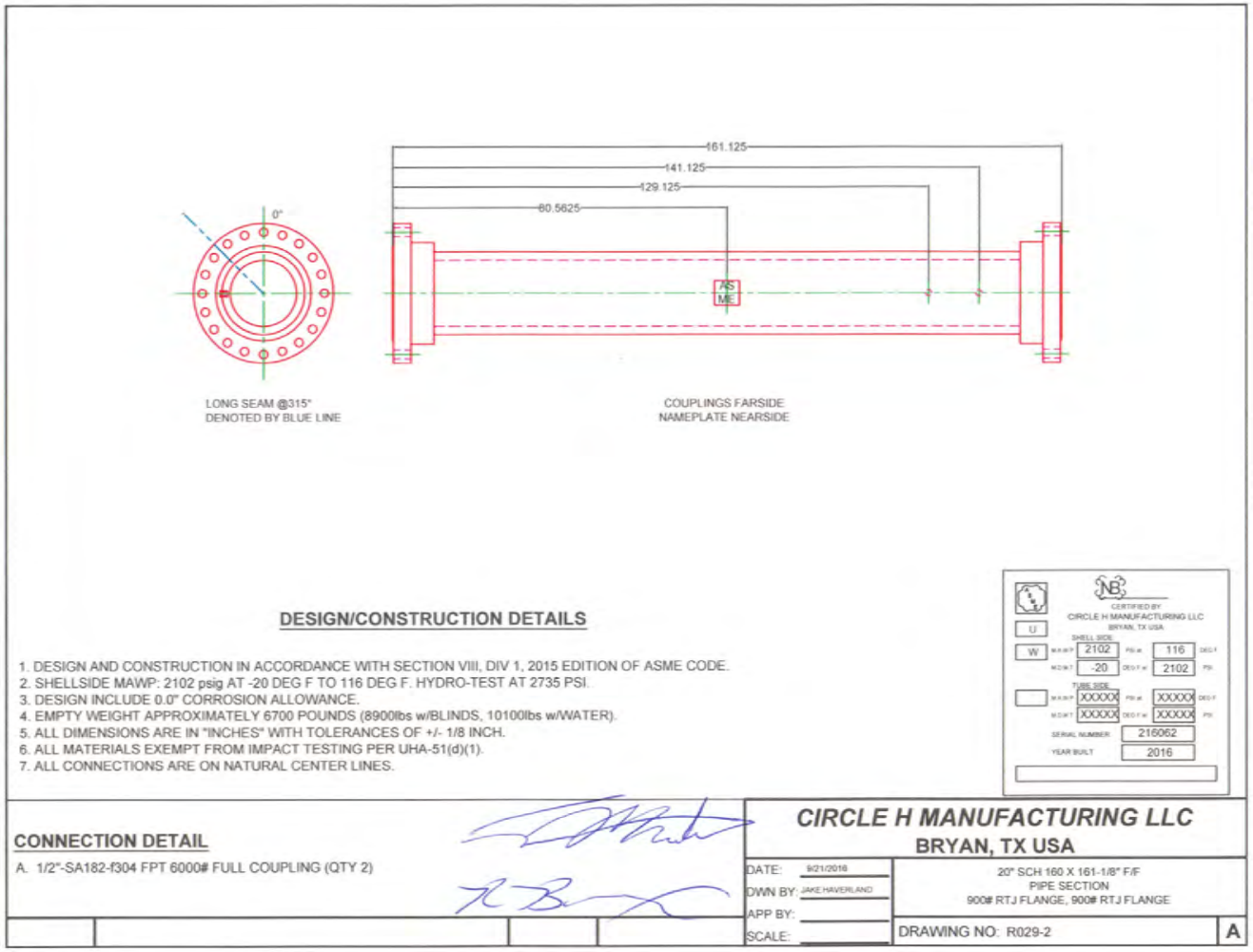

FIGURE B-8. CIRCLE H MANUFACTURING DRAWING OF THE DRIVEN AS CERTIFIED WITH APPROVAL SIGNATURES OF THE RESPONSIBLE ENGINEERS.

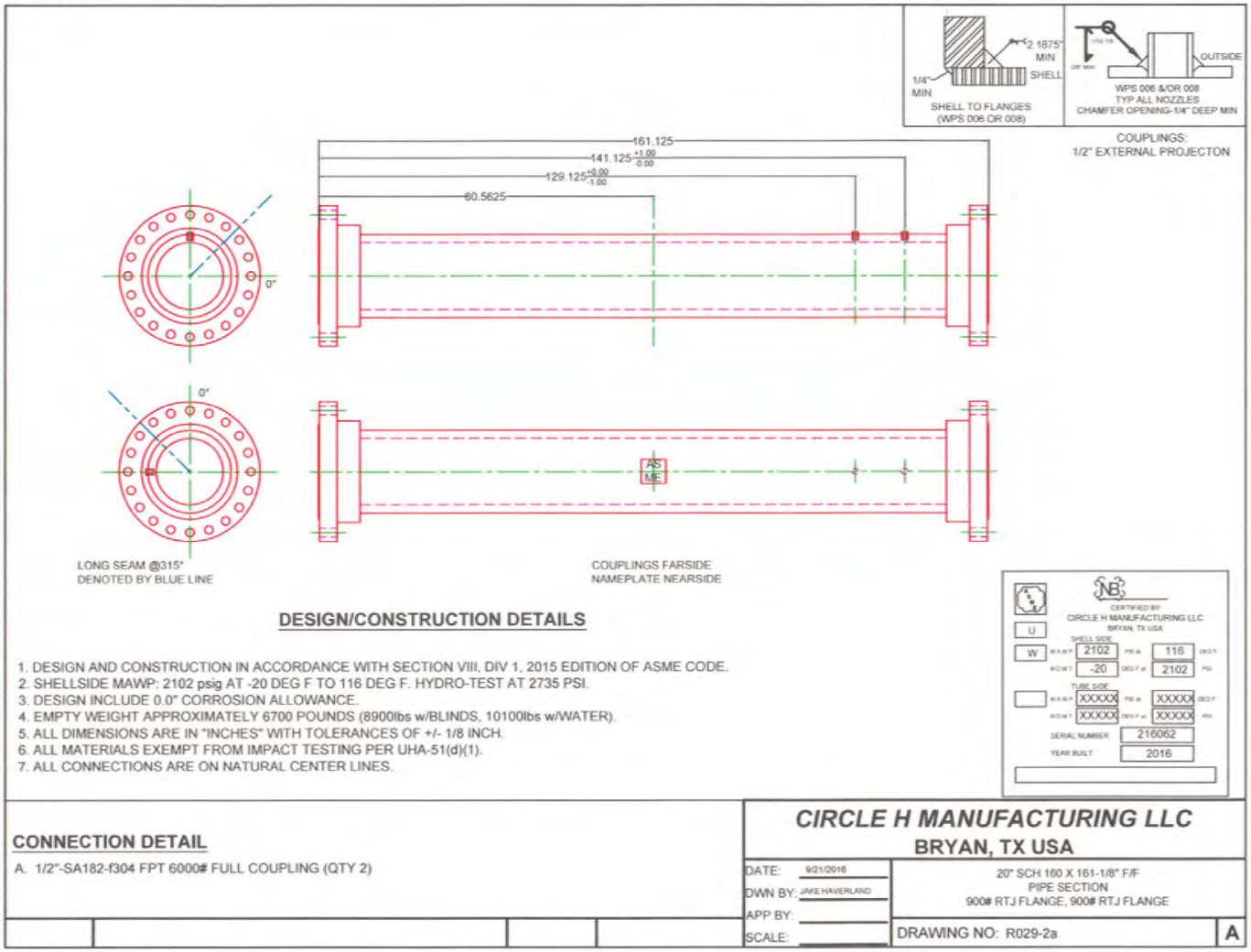

FIGURE B-9. CIRCLE H MANUFACTURING DRAWING OF THE DRIVEN AS CERTIFIED AND APPROVED.

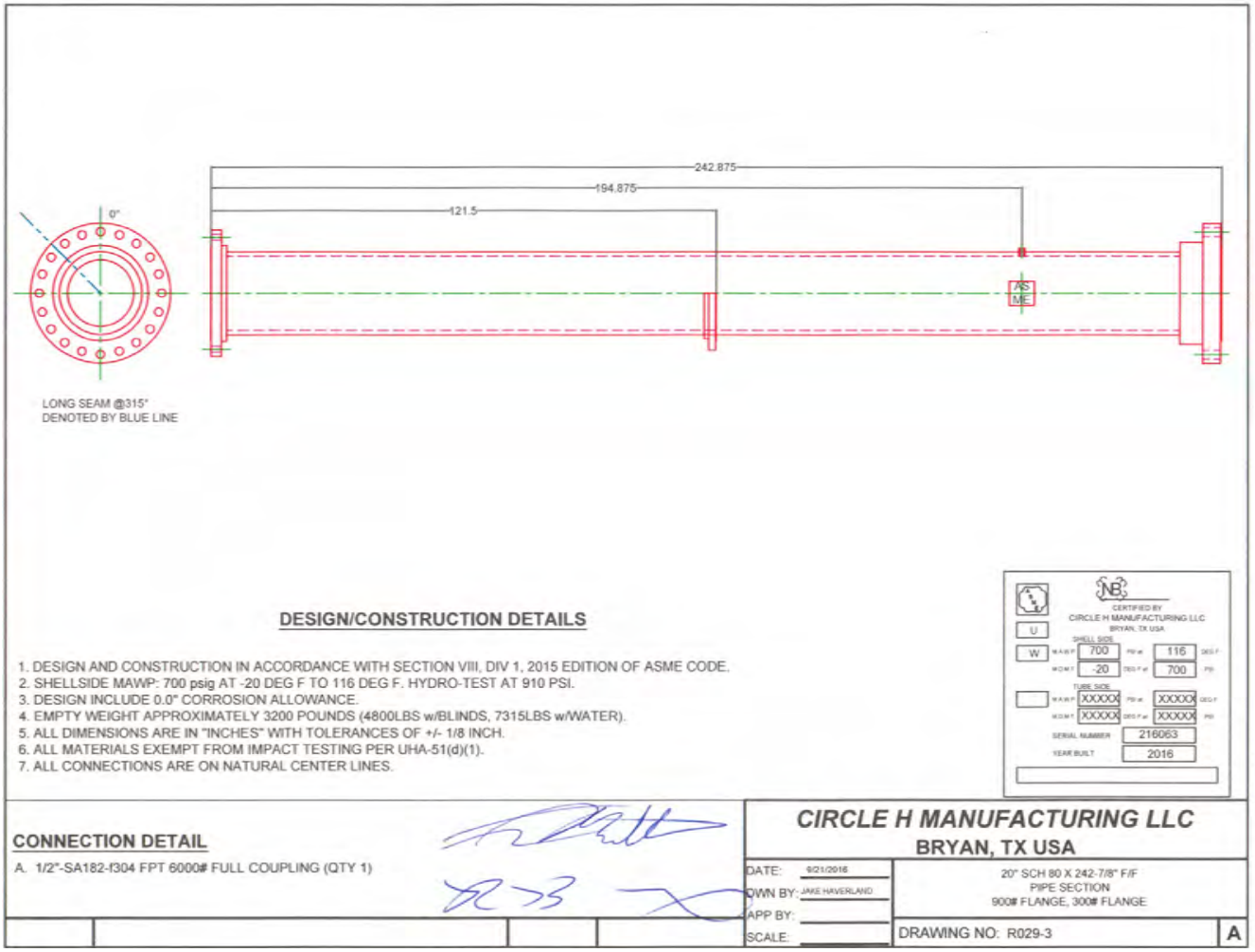

FIGURE B-10. CIRCLE H MANUFACTURING DRAWING OF THE FIRST ACCELERATOR SEGMENT AS CERTIFIED WITH APPROVAL SIGNATURES OF THE RESPONSIBLE ENGINEERS.

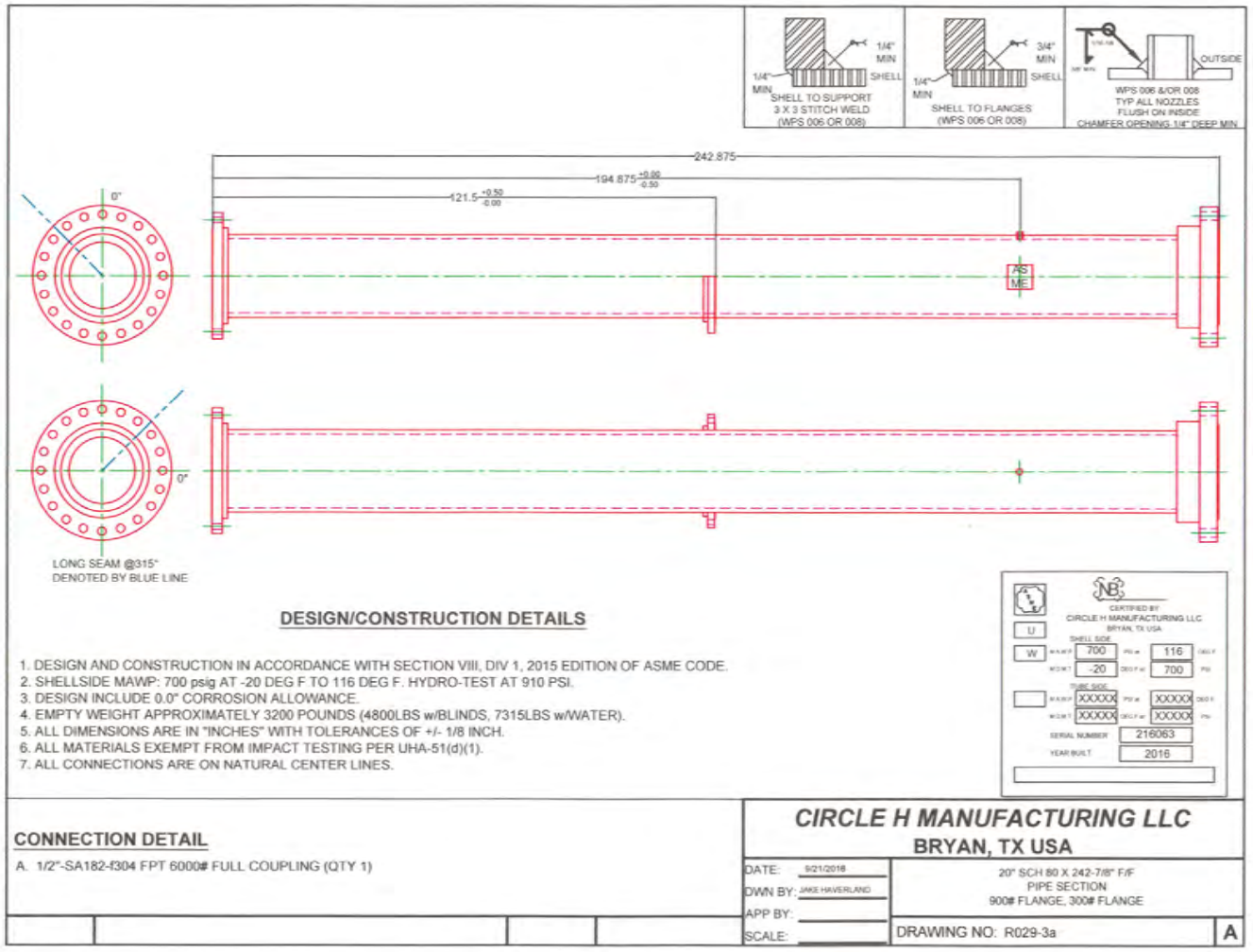

FIGURE B-11. CIRCLE H MANUFACTURING DRAWING OF THE FIRST ACCELERATOR SEGMENT AS CERTIFIED AND APPROVED.

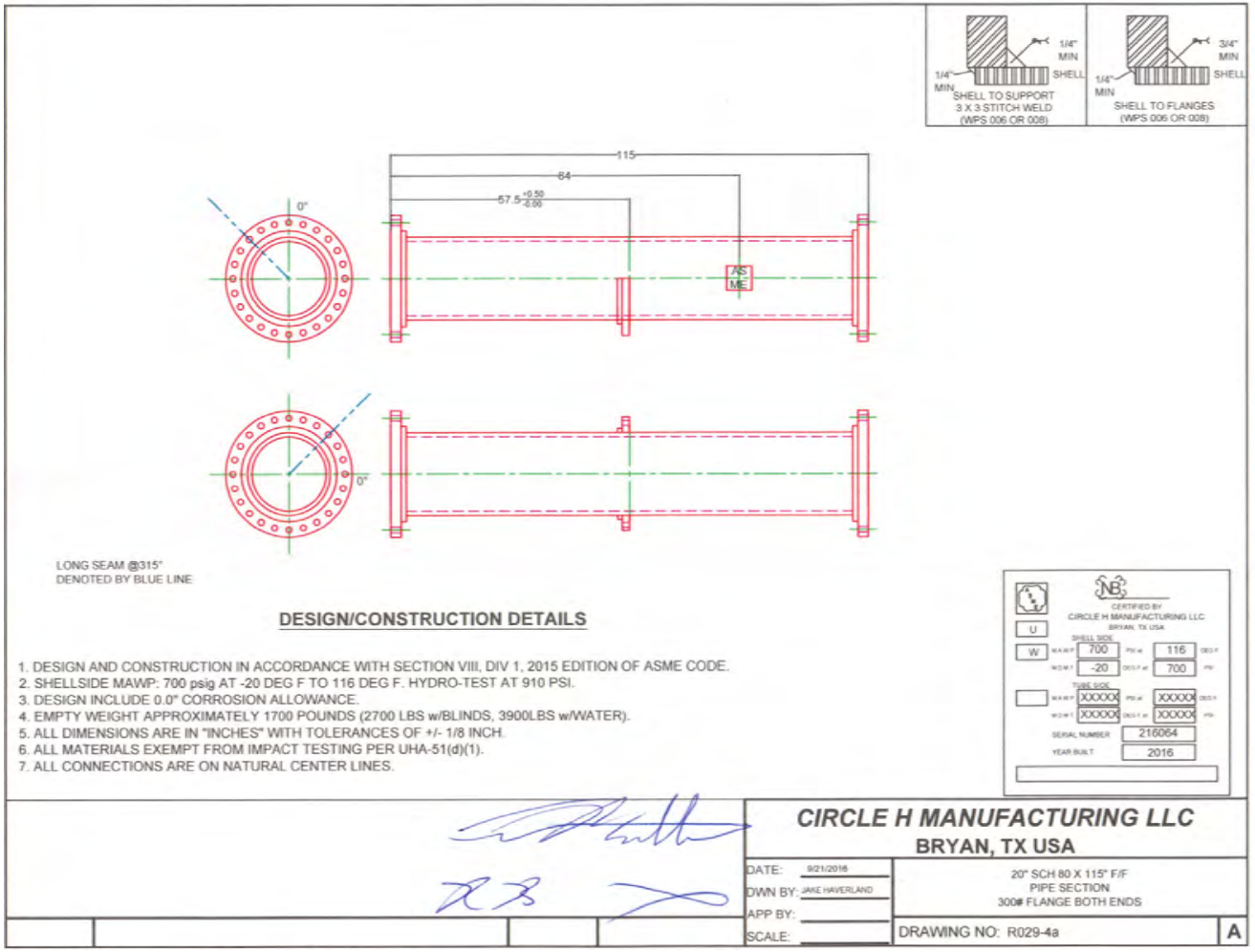

FIGURE B-12. CIRCLE H MANUFACTURING DRAWING OF THE DRIVEN AS CERTIFIED WITH APPROVAL SIGNATURES OF THE RESPONSIBLE ENGINEERS.

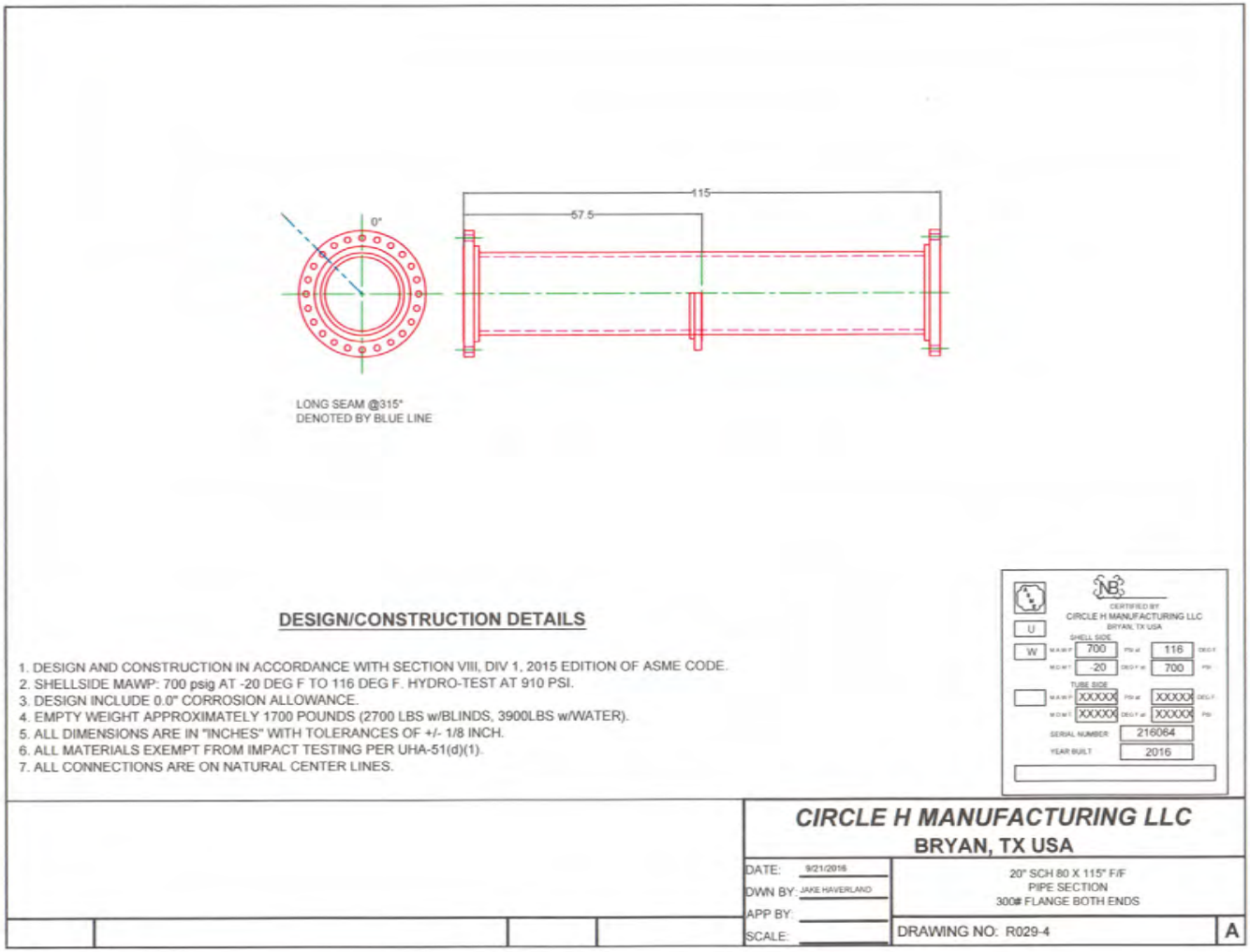

FIGURE B-13. CIRCLE H MANUFACTURING DRAWING OF THE DRIVEN AS CERTIFIED AND APPROVED.

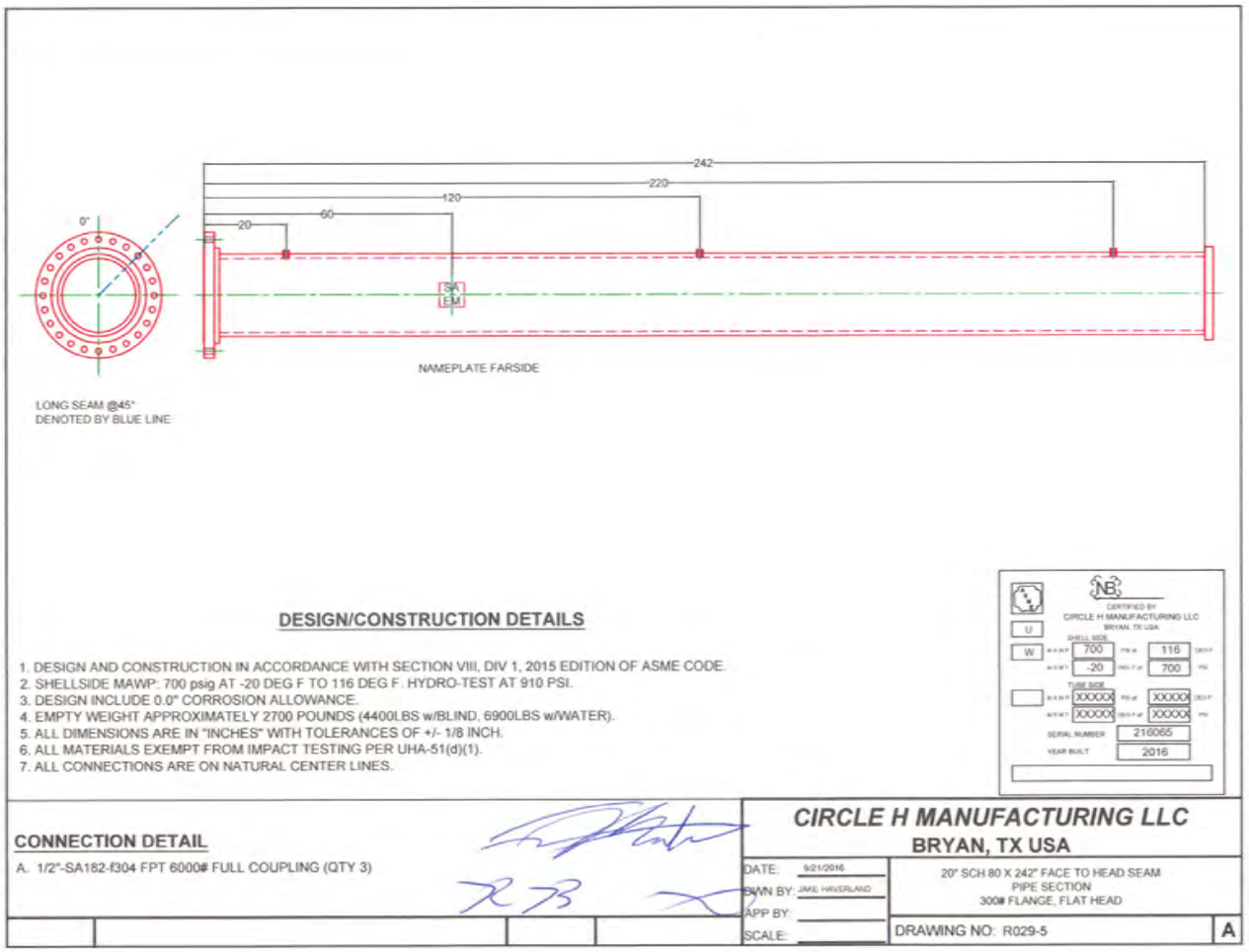

FIGURE B-14. CIRCLE H MANUFACTURING DRAWING OF THE DRIVEN AS CERTIFIED WITH APPROVAL SIGNATURES OF THE RESPONSIBLE ENGINEERS.

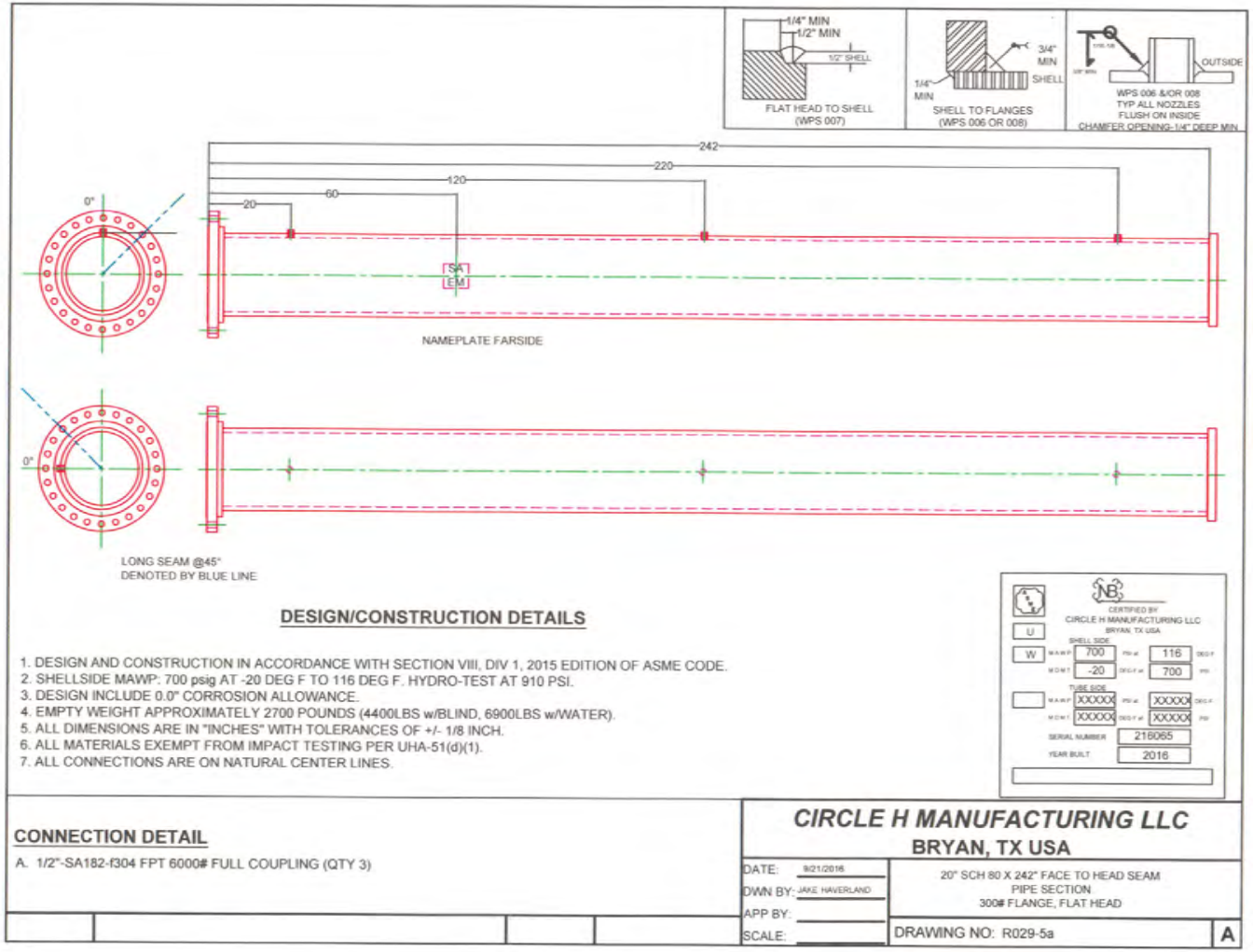

FIGURE B-15. CIRCLE H MANUFACTURING DRAWING OF THE DRIVEN A.S CERTIFIED AND APPROVED.

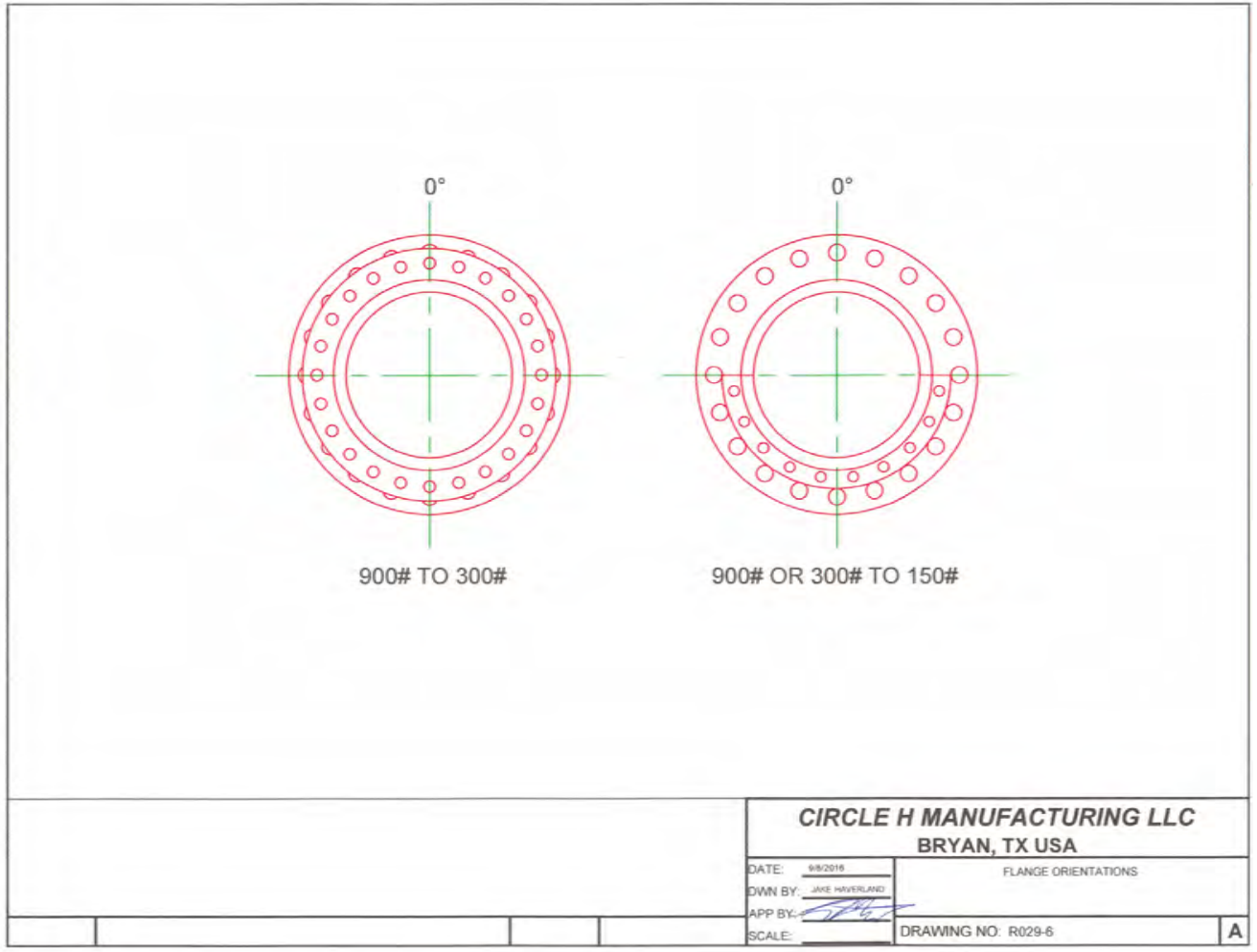

FIGURE B-16. CIRCLE H MANUFACTURING DRAWING DETAILING THE HOLE ALIGNMENT OF THE FLANGES RELATIVE TO ONE ANOTHER.

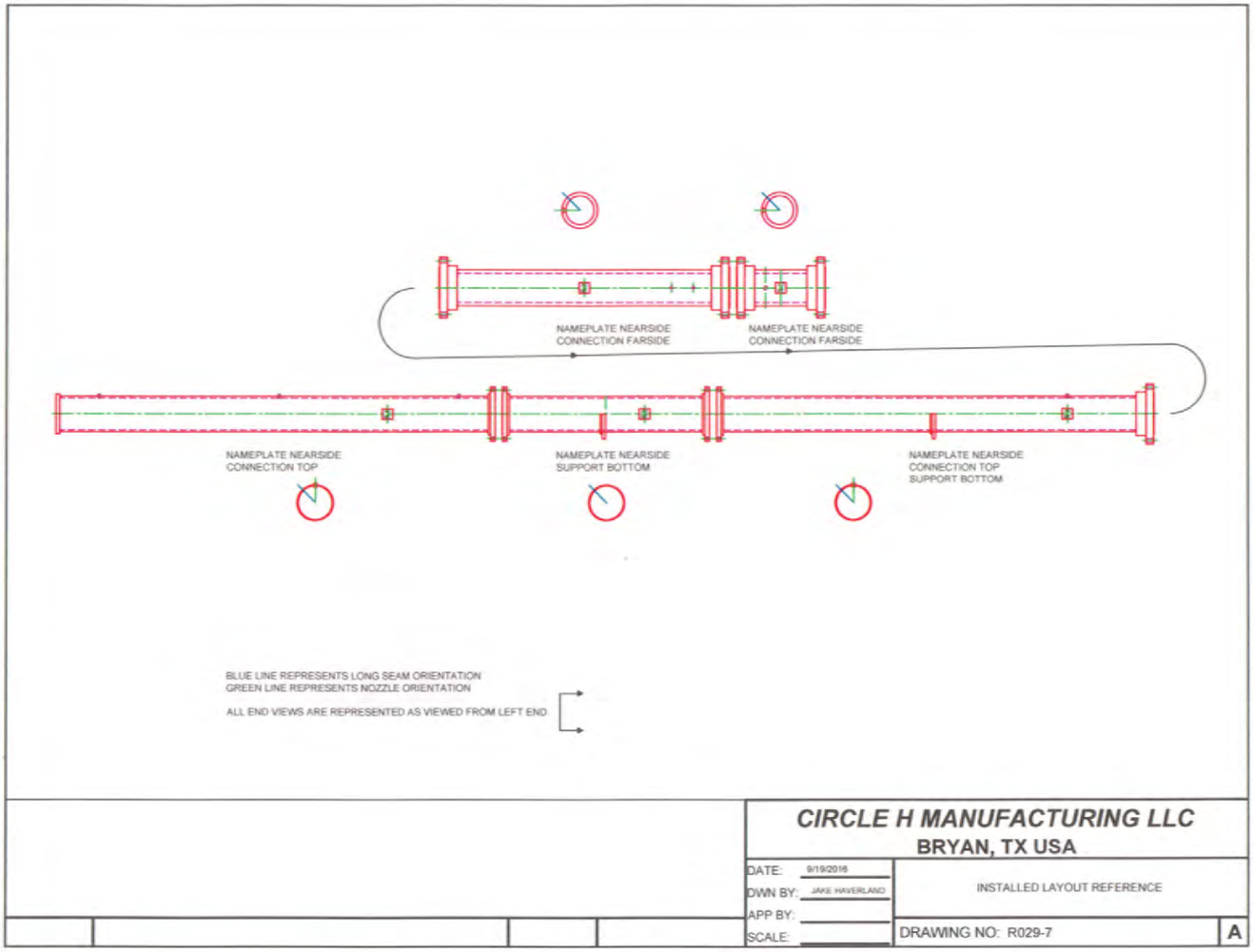

FIGURE B-17. CIRCLE H MANUFACTURING DRAWING OF THE ENTIRE PIPE SECTION ASSEMBLY WITH ORIENTATION OF THE NAME PLATES AND INTERFACING FLANGES.

Tube Components

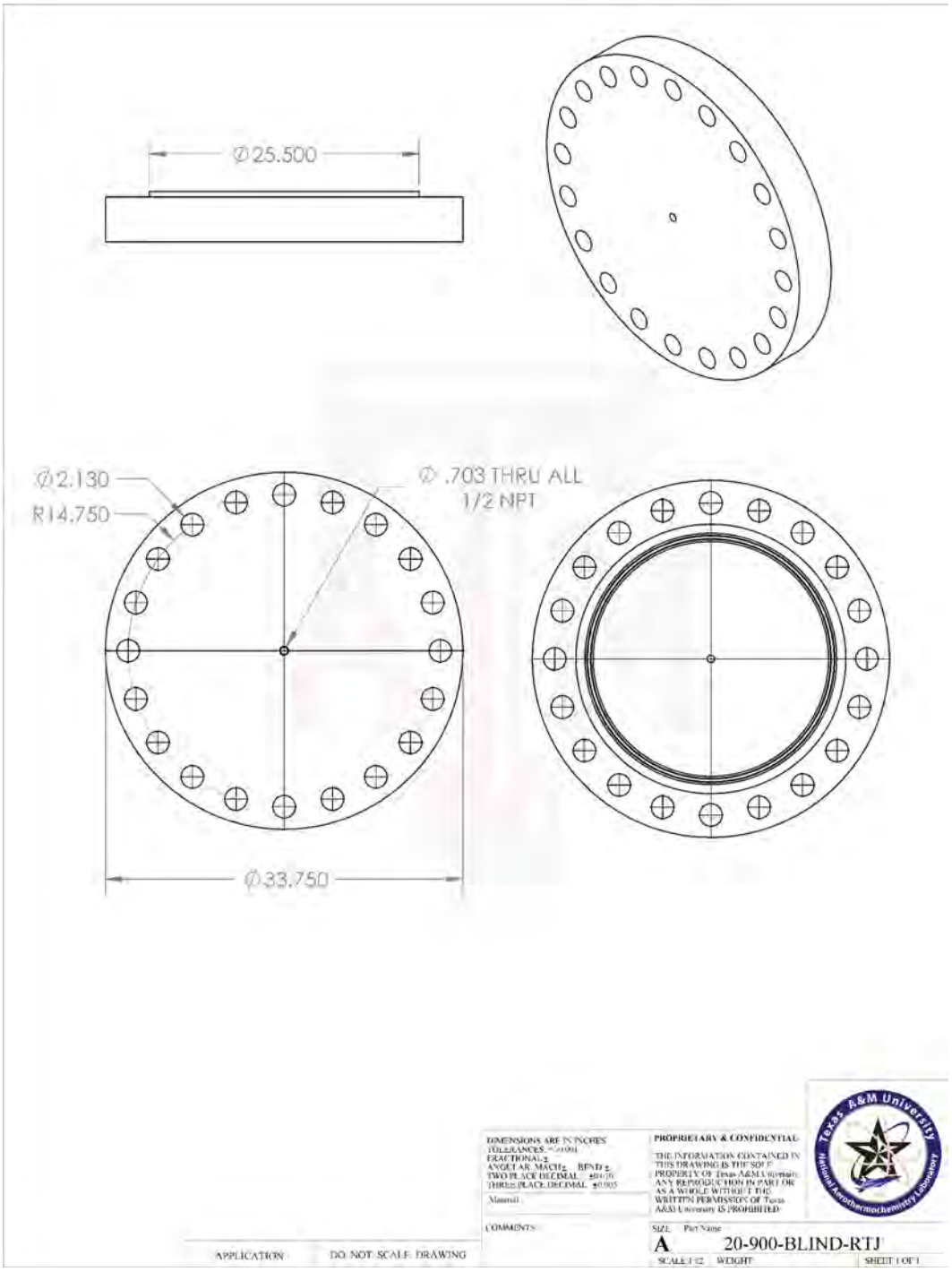

FIGURE B-18. DIMENSIONAL DRAWING FOR A 20-IN CLASS 900 RTJ BLIND.

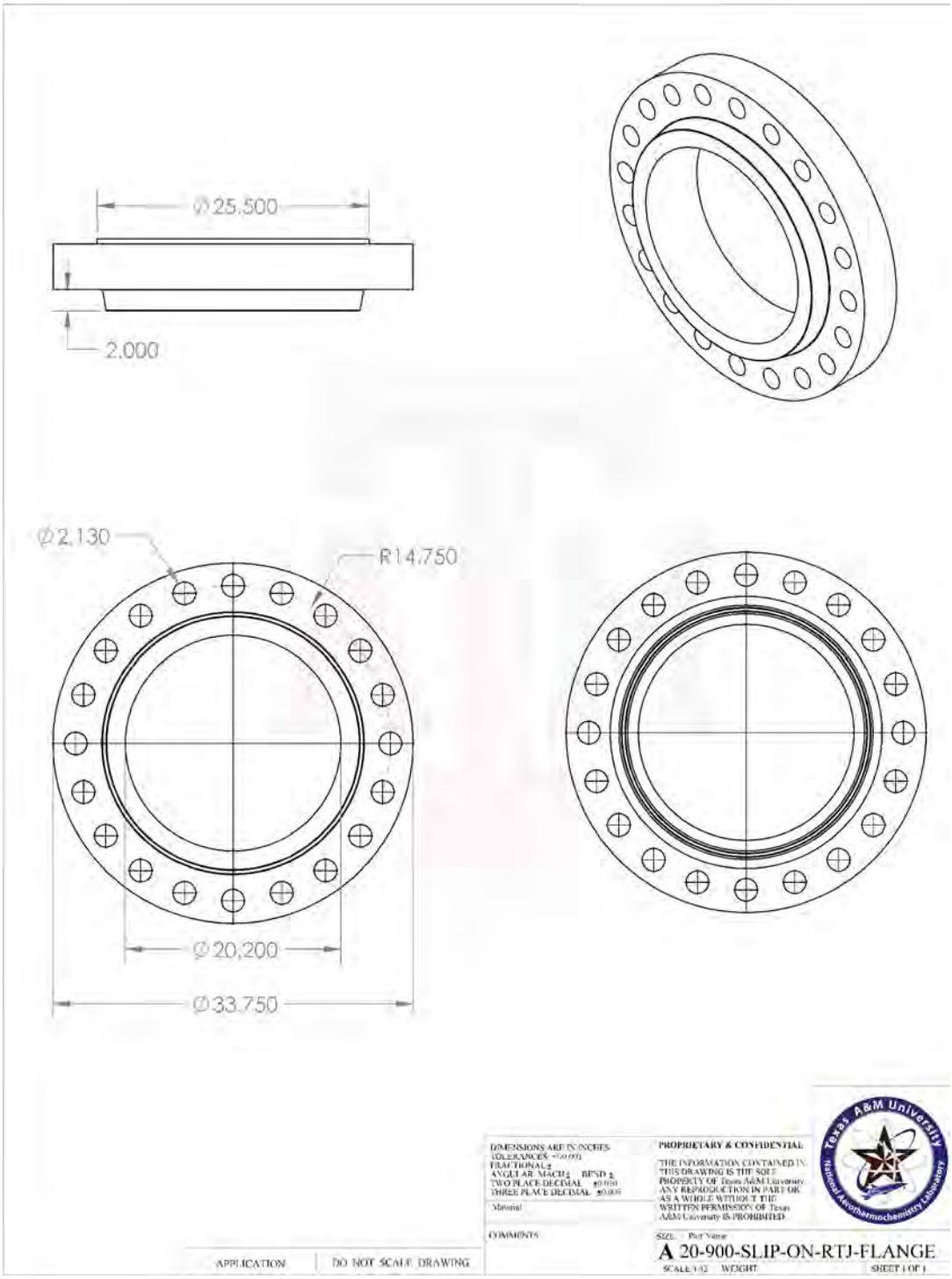

FIGURE B-19. DIMENSIONAL DRAWING FOR A 20-IN CLASS 900 RTJ SLIP-ON FLANGE.

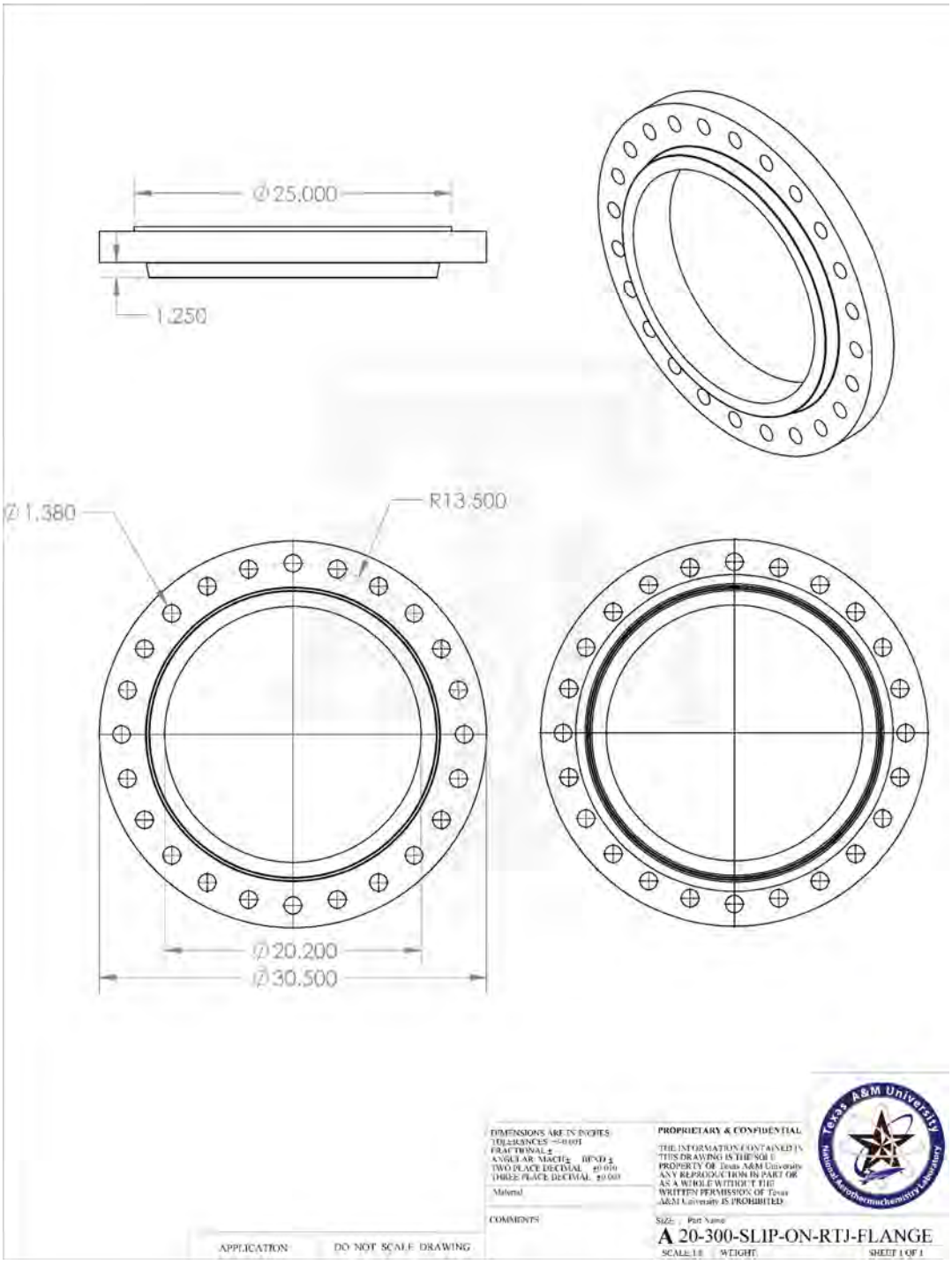

FIGURE B-20. DIMENSIONAL DRAWING FOR A 20-IN CLASS 300 RTJ SLIP-ON FLANGE.

Test Section

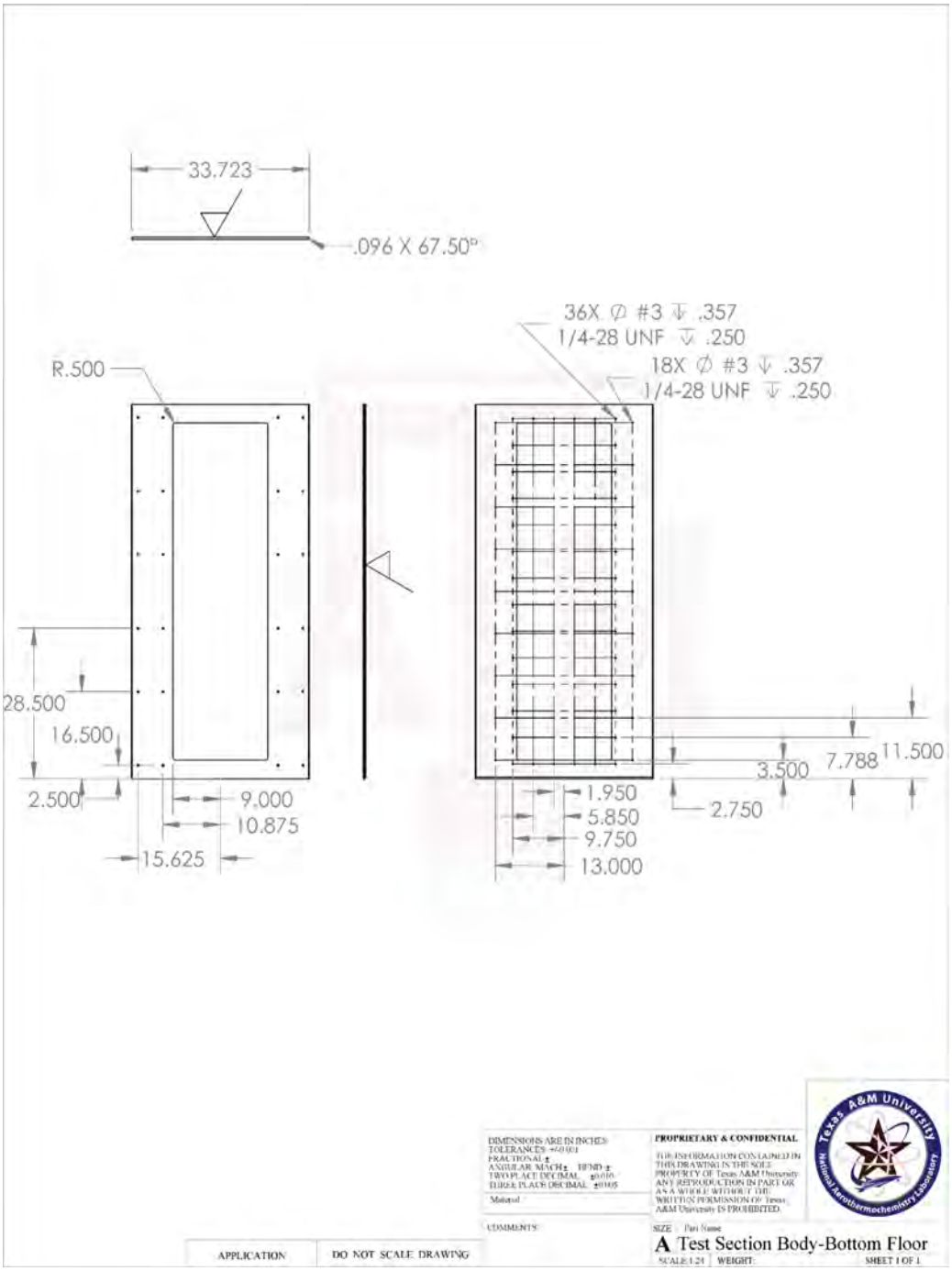

FIGURE B-21. DIMENSIONAL DRAWING FOR THE FLOOR ACCESS PLATE OF THE TEST SECTION SKELETON.

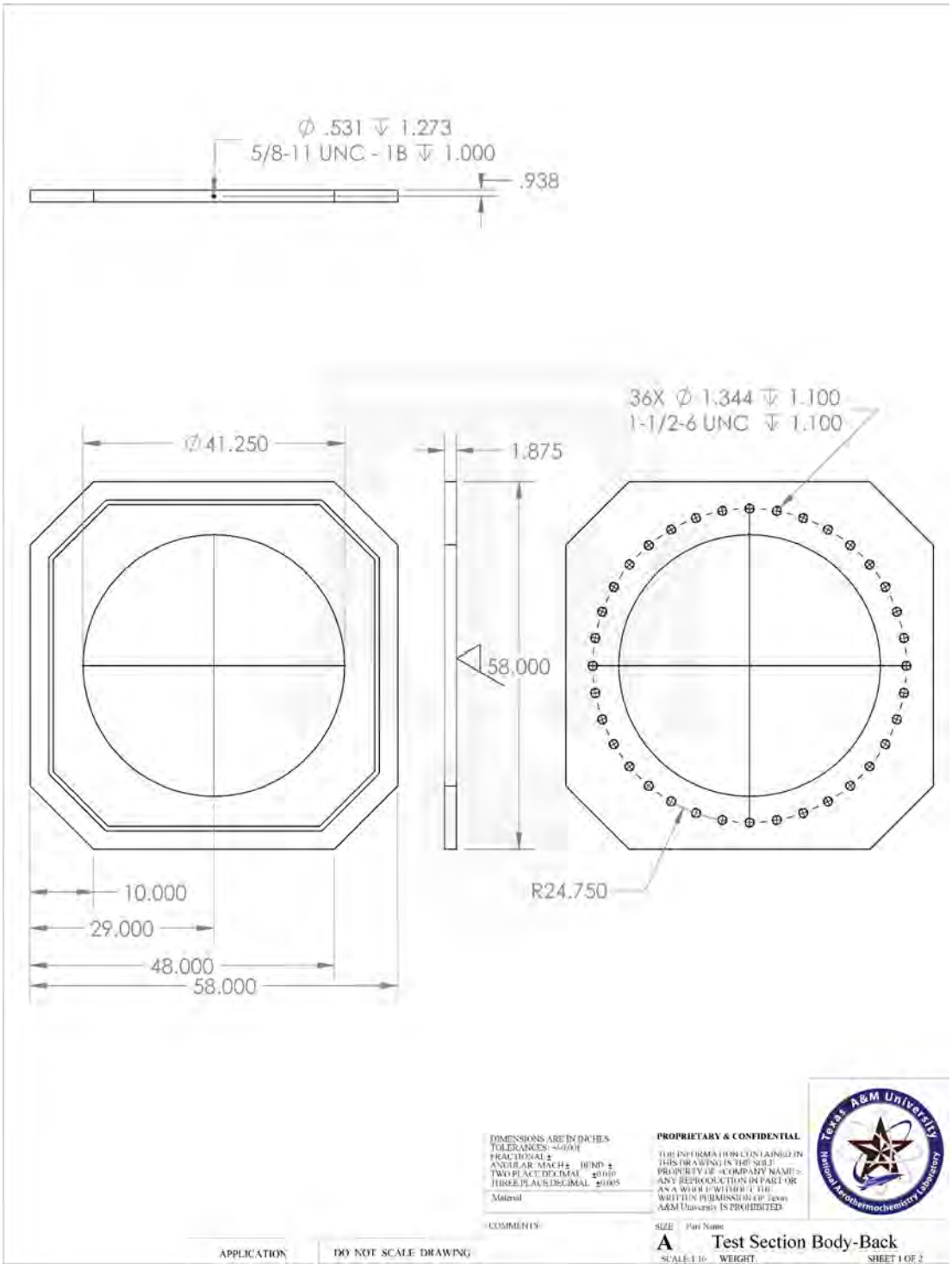

FIGURE B-22. DIMENSIONAL DRAWING FOR THE BACK PLATE OF THE TEST SECTION SKELETON WITHOUT DIMENSIONS OF THE ALIGNMENT GROOVE.

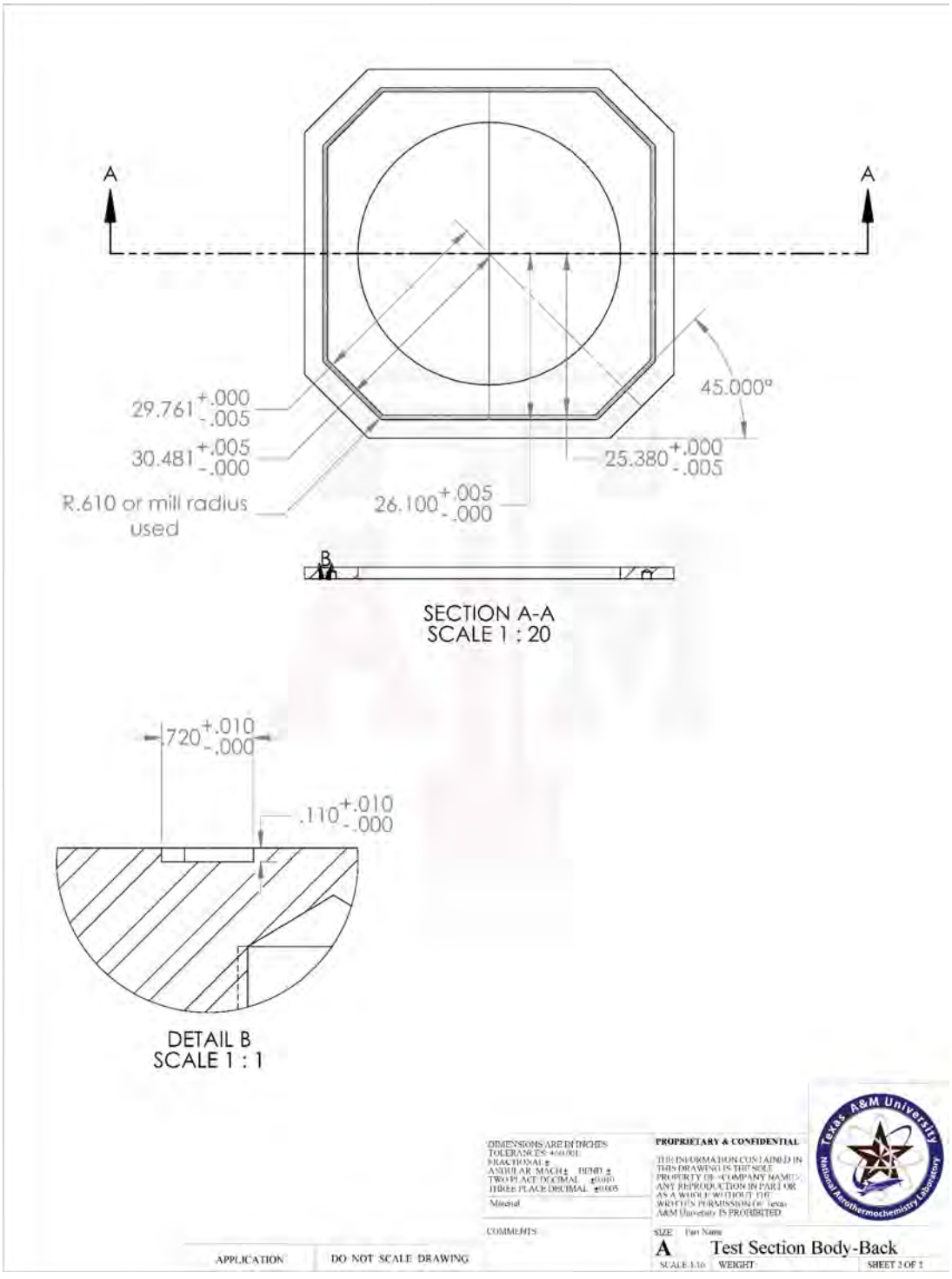

FIGURE B-23. DIMENSIONAL DRAWING FOR THE BACK PLATE OF THE TEST SECTION SKELETON WITH DIMENSIONS FOR THE ALIGNMENT GROOVE.

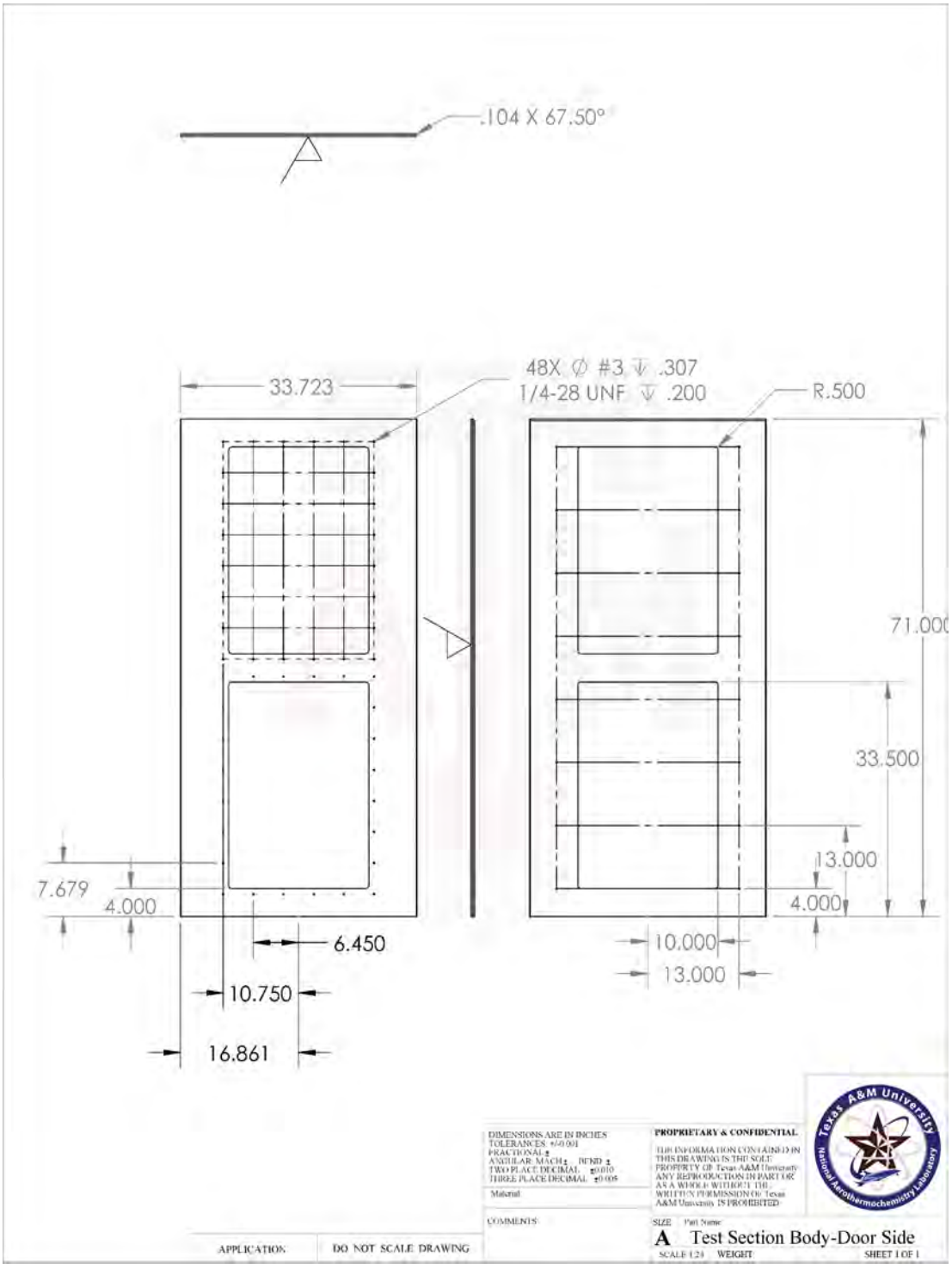

FIGURE B-24. DIMENSIONAL DRAWING FOR THE DOOR PLATES OF THE TEST SECTION SKELETON.

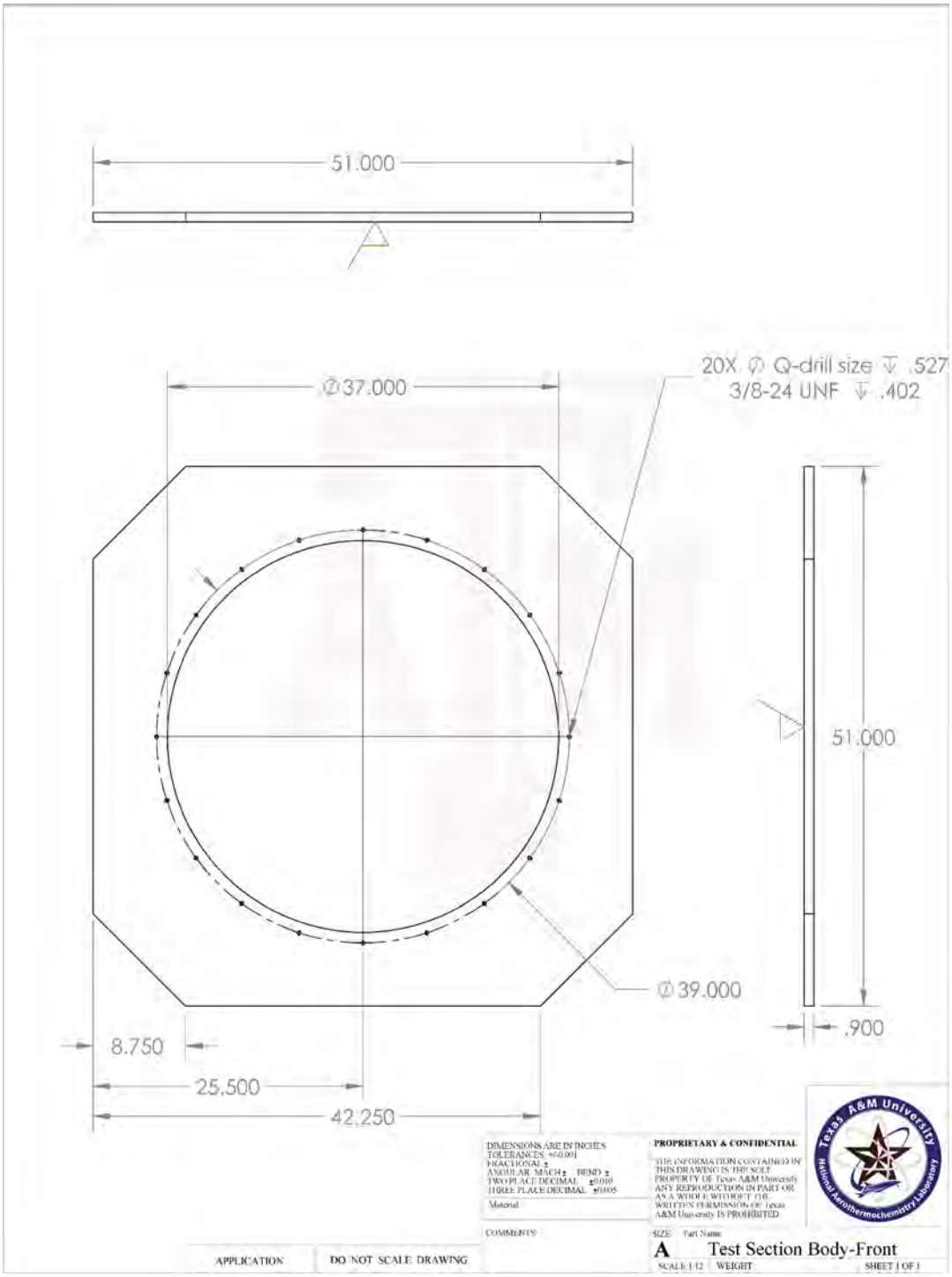

FIGURE B-25. DIMENSIONAL DRAWING FOR THE FRONT PLATE OF THE TEST SECTION SKELETON.

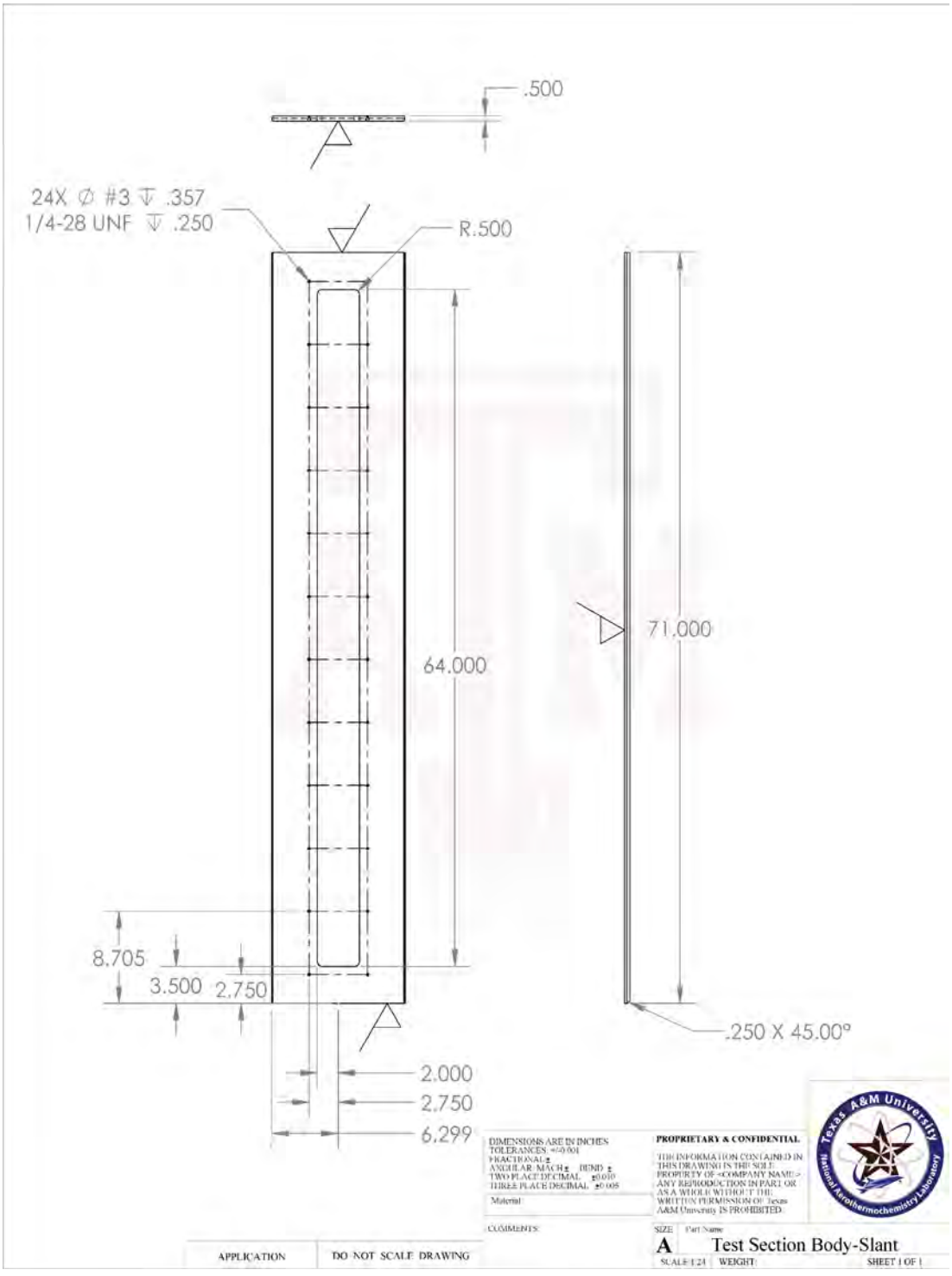

FIGURE B-26. DIMENSIONAL DRAWING FOR THE DIAGONAL PLATES OF THE TEST SECTION SKELETON.

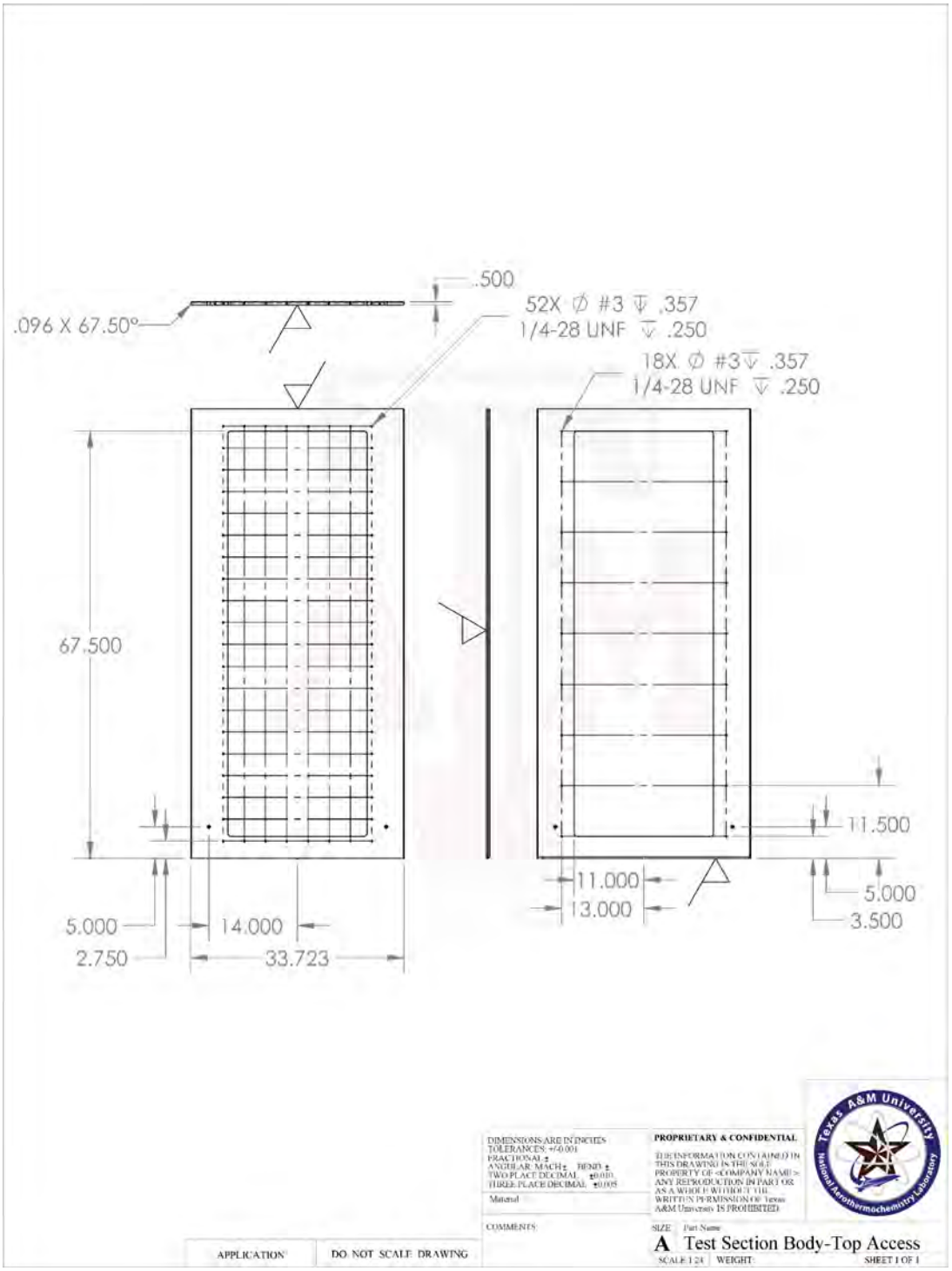

FIGURE B-27. DIMENSIONAL DRAWING FOR THE ROOF PLATE OF THE TEST SECTION SKELETON.

Primary Support Stands

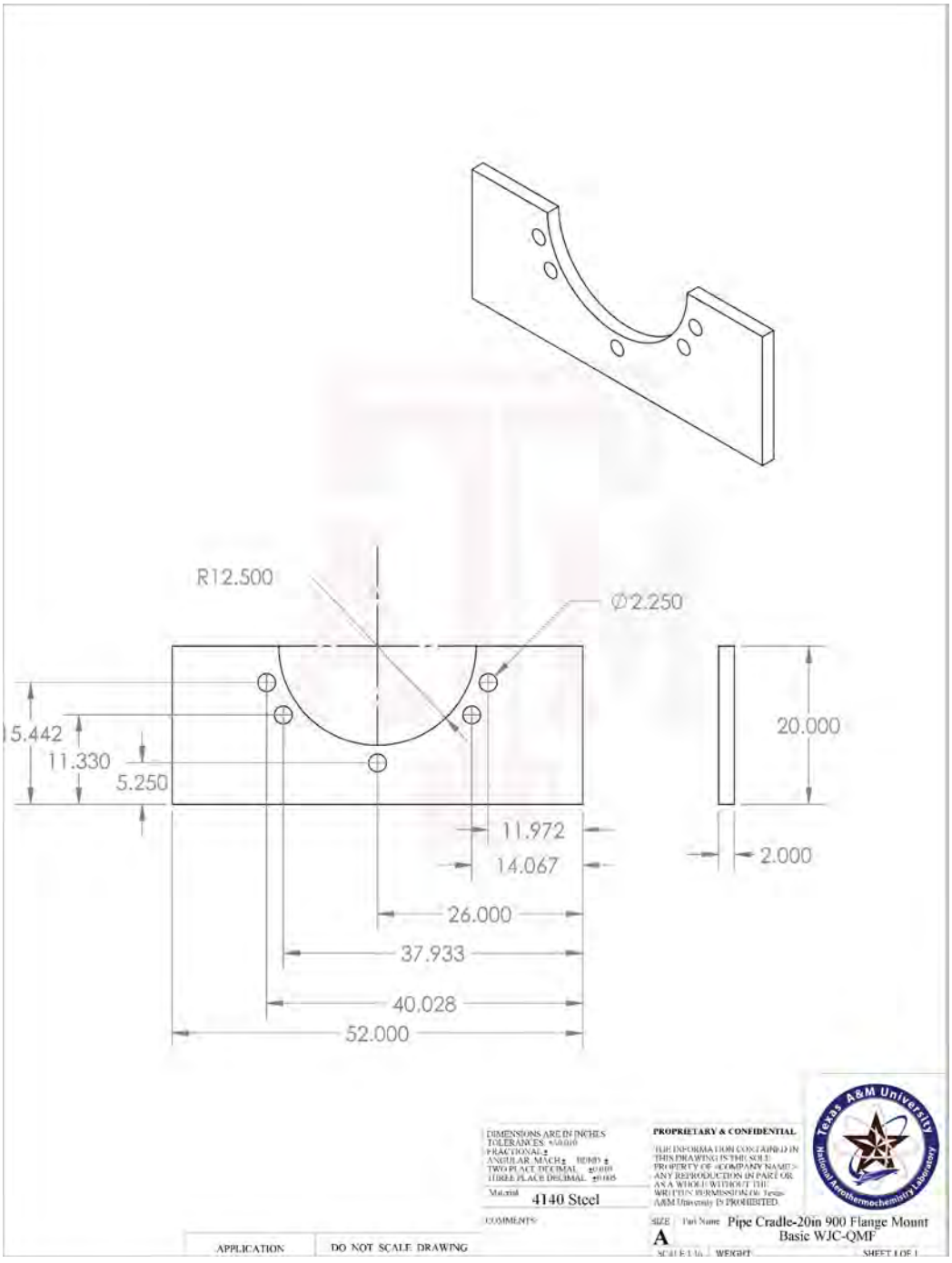

FIGURE B-28. DIMENSIONAL DRAWING FOR PIPE CRADLE PLATE TO HOLD THE 20-IN 900-LB FLANGES AND 20-IN SCHEDULE 160 PIPE.

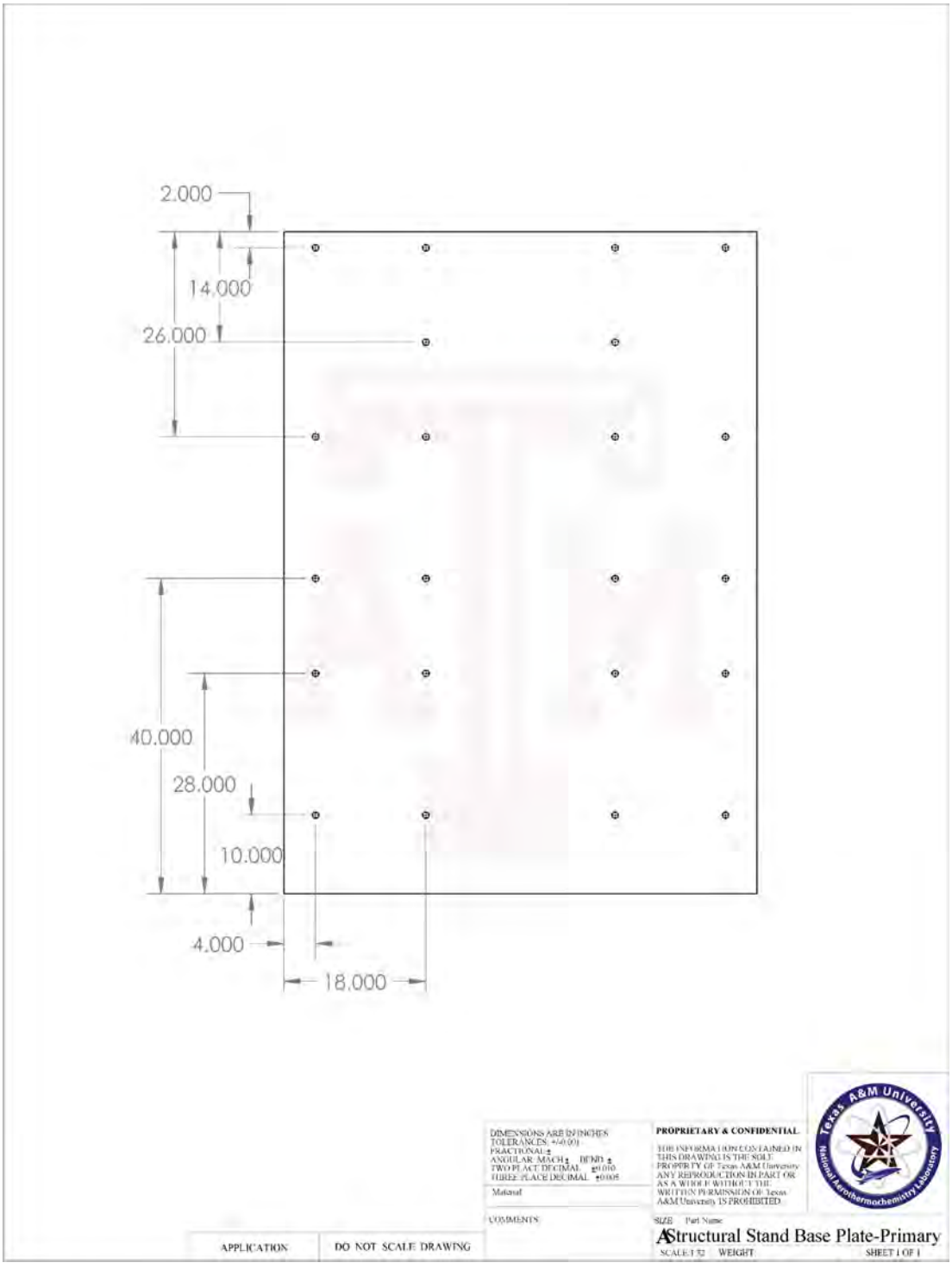

FIGURE B-29. DIMENSIONAL DRAWING FOR PRIMARY STAND BASEPLATE WITH ¾-IN FREE CLEAR HOLES THAT ARE TORCHED INTO THE PLATE.

Secondary Support Stands

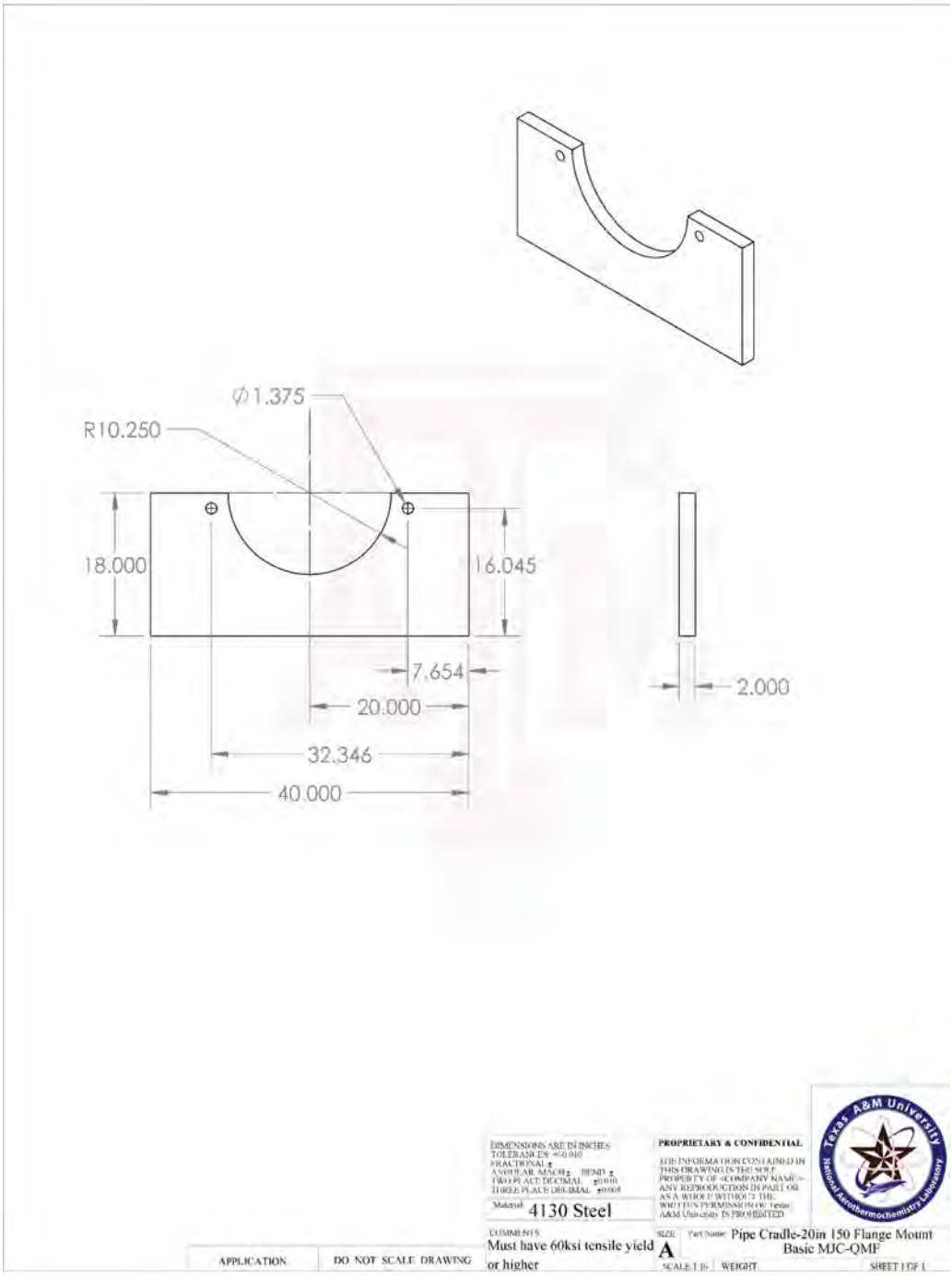

FIGURE B-30. DIMENSIONAL DRAWING FOR PIPE CRADLE PLATE TO HOLD THE 20-IN 150-LB FLANGES AND 20-IN SCHEDULE 80 PIPE.

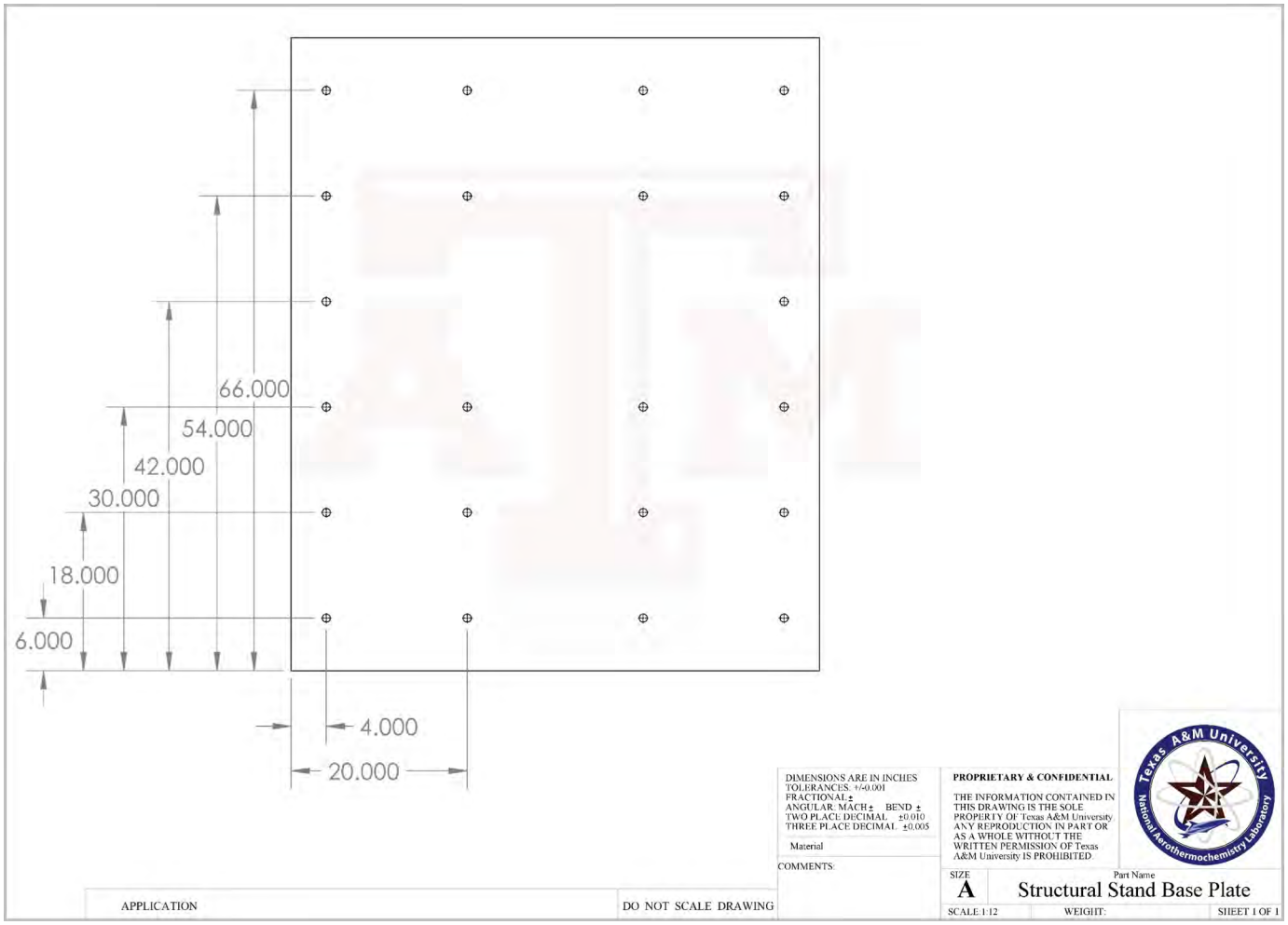

FIGURE B-31. DIMENSIONAL DRAWING FOR SECONDARY STAND BASEPLATE WITH ¾-IN FREE CLEAR HOLES THAT ARE TORCHED INTO THE PLATE.

APPENDIX C – AIR RECEIVER

An air receiver adds volume to increase the operational envelope of the facility in ST mode. The tube volumes are summarized in Table C.1. In expansion tunnel mode, as detailed in Section 2.2, the facility operates with a maximum driver pressure of 2000-psia and a driven pressure not to exceed 110-psia. Shock tunnel mode differs in that the ST-driver is the sum of both the XT-driver and XT-driven pipe lengths. Because this combined volume of 211 gallons would quadruple the mass if operated at 2000-psia, the operating pressure of the shock tunnel mode was reduced to 500-psia. The resulting pressure are summarized in Table C.2. The addition of an air receiver allows the shock tunnel mode to increase its driver pressure to approximately 1000-psia, thus doubling the operational Reynolds number.

TABLE C.1 Volume for each section of the facility

Section	Dimensions [in]	Volume [in^3]	Volume [gallons]
Driver	60[L]x16.064[d]	12,160	53
Driven	180[L]x16.064[d]	36,480	158
Accelerator	600[L]x19.00[d]	170,100	295
Test Section	2,447.875 in^2 [CSA]	171,400	742
Tailpipe	252[L]x41.25[d]	336,800	1458
	Total w/o Receiver	**726,900**	**3,147**
Air Receiver	220[L]x60[d]	582,100	2520
	Total with Receiver	**1,309,000**	**5,667**

[L]: length, [d]: diameter, [CSA]: cross-sectional area of the prism.

TABLE C.1 Mass (kg) present in each section

	Driver	Driven	Acc.	Test Sect.	Tailpipe	EoOP [psia]
XT	32.25	5.32	~0.00	~0.00	~0.00	38
ST	32.25	N/A	2.26	2.27	4.47	43
ST-AR	32.25	N/A	2.26	2.27	4.47	24

Driver pressure = 2000-psia, driven pressure = 110-psia for XT mode; driver pressure = 500-psia, driven of 50-psia for ST mode. The end-of-operation pressure (EoOP) is calculated using the entire volume of facility.